A LITERATURE REVIEW OF THE STRUCTURAL INTEGRITY OF ANALOG CANISTERS

Prepared for

U.S. Nuclear Regulatory Commission
Contract NRC–02–07–006

Prepared by

T. Wilt[1]
A. Chowdhury[1]
T. Ahn[2]

[1]Center for Nuclear Waste Regulatory Analyses
San Antonio, Texas

[2]U.S. Nuclear Regulatory Commission
Office of Nuclear Material Safety and Safeguards
Division of High-Level Waste Repository Safety
Washington, DC

October 2010

CONTENTS

CONTENTS (continued)

FIGURES

FIGURES (continued)

TABLES

ACKNOWLEDGMENTS

This report was prepared to document work performed by the Center for Nuclear Waste Regulatory Analyses (CNWRA®) for the U.S. Nuclear Regulatory Commission (NRC) under Contract No. NRC–02–02–012. The activities reported here were performed on behalf of the NRC Office of Nuclear Material Safety and Safeguards, Division of High-Level Waste Repository Safety. This report is an independent product of the CNWRA and does not necessarily reflect the view or regulatory position of the NRC. The NRC staff views expressed herein are preliminary and do not constitute a final judgment or determination of the matters addressed or of the acceptability of a license application for a geologic repository at Yucca Mountain.

The authors thank F. Ferrante for technical review, B. Sagar for programmatic review, and L. Mulverhill for skillful editorial review. The authors also appreciate A. Ramos for providing word processing support in the preparation of this document.

QUALITY OF DATA, ANALYSES, AND CODE DEVELOPMENT

DATA: No CNWRA-generated original data are contained in this report. Sources for other data should be consulted for determining the level of quality for those data.

ANALYSES AND CODES: No CNWRA computer analysis results are used in this report.

EXECUTIVE SUMMARY

This report is the result of a literature review pertaining to evaluating the structural behavior of the U.S. Department of Energy (DOE) standardized spent nuclear fuel canister, Idaho Spent Fuel Project canisters, multi-canister overpacks, and high-level waste canisters. These canisters can be considered analogous to the transportation, aging, and disposal (TAD) canister (DOE, 2006) concept DOE has proposed. Information from these analog canister systems can help inform U.S. Nuclear Regulatory Commission staff's review of potential TAD canister performance characteristics. The primary objective was to investigate different types of canisters and their structural robustness when subjected to a drop event at a number of drop orientations and heights. The process used to develop structurally robust DOE canister designs includes (i) using limited small- or full-scale testing to evaluate the proposed canister design, (ii) using visual inspection and pressure testing of dropped canisters to verify structural integrity, and (iii) comparing small- and full-scale test results with the corresponding three-dimensional finite element analyses that provide detailed stress–strain distributions to further examine canister structural integrity.

In 1999, the National Spent Nuclear Fuel Program began developing and testing standardized spent nuclear fuel canisters. A standardized spent nuclear fuel canister would provide a uniform design for confining the spent nuclear fuel (which includes ease of handling); provide a single canister for transportation, storage, and compatibility with disposal at a repository; and remain sealed throughout each phase. Testing results showed that the canister design performed as expected with the canister body maintaining its structural integrity with respect to containment. Structural performance of the canisters was evaluated using observed damage to the containment boundary and pressure tests to verify the canister remained leaktight. A key component of the DOE standardized canister is a skirt attached at each end to limit the effects of drop impacts. In all but one drop orientation, the skirt did function as intended. The only case in which the skirt was not effective was for the case of a horizontal drop; however, in this case, the impact energy was distributed over the entire length of the canister with no significant damage to the containment boundary. Deformations obtained from the three-dimensional finite element analyses matched those observed in the full-scale tests. Additionally, the finite element results provided maximum effective plastic true strains at the surface and midsurface (midthickness), which were especially important because they indicated whether any surface damage would propagate through the containment boundary and result in a breach. The maximum equivalent plastic true strains were below the true strain at failure.

The Idaho Project Spent Nuclear Fuel canister was based upon the standardized spent nuclear fuel canister with modifications limited to fabrication details (i.e., wall thickness, attachment of the dished head and skirt). In all cases, the maximum plastic true strain at the canister surface and midsurface (midthickness) of the containment pressure boundary was below the elongation value, indicating no failure was likely to occur.

Conceptual canister designs for the disposal of calcine waste were also presented. Designs similar to the standardized canister were used with one notable exception: a 1.676-m [5.5-ft]-diameter, 5.5-m [18-ft]-long canister having a flat bottom, which is similar to the proposed TAD canister. The material chosen for these conceptual canisters was 316L stainless steel. The proposed canisters were subjected to a number of drop simulations. The parameters used

in this study to evaluate the proposed designs were maximum equivalent plastic true strains and maximum deformation. Note that the flat bottom canister with a wall thickness of 25.4 mm [1 in] and a bottom head thickness of 89 mm [3.5 in] was determined to have acceptable deformations.

High-level waste canisters constructed of either Titanium Grade 2 or 304L stainless steel were subjected to full-scale drop tests. The structural behavior was measured in terms of deformations, ductility, and resistance to tearing. For the titanium canister, when subjected to a drop on the corner of the fill nozzle, significant damage around the nozzle was evident in which failure due to tearing (possible high shear stress) was observed. A similar test of a stainless steel canister with the same orientation did not exhibit the tearing failure. The difference in ductility of titanium, which is less than stainless steel, was attributed to the failure. For bottom drop tests, no failure of the containment boundary was observed, even though these canisters do not have skirts as the standardized canisters have.

An extensive presentation of results and discussion with regard to full-scale testing and three-dimensional finite element simulations of canister drop events has been documented. As part of this review, finite element analysis has accurately analyzed canister behavior such that for other loading scenarios, full-scale testing may not be required. Knowledge gained from the full-scale testing and the corresponding finite element analysis of the canisters presented in this report should prove useful when evaluating the proposed TAD canister.

Reference

DOE. DOE/RW–0585, “Preliminary Transportation, Aging, and Disposal Canister System Performance Specification Rev. B.” Las Vegas, Nevada: DOE, Office of Civilian Radioactive Waste Management. 2006.

1 INTRODUCTION

1.1 Background

The U.S. Department of Energy (DOE) has proposed a number of canister systems over the years for transportation, storage, and disposal of commercial spent fuel at the potential repository at Yucca Mountain. A single-purpose canister would be used only for transportation, or storage, or disposal, as appropriate. A dual-purpose canister would serve both transport and storage. A multipurpose canister could serve all three functions: transportation, storage, and disposal. In 1994, DOE decided to design and develop a multipurpose canister that would meet the U.S. Nuclear Regulatory Commission (NRC) standards for transportation, storage (10 CFR Parts 71 and 72), and disposal (10 CFR Part 63) (DOE, 1994a,b). Westinghouse Electric Corporation initially evaluated the multipurpose canister with regard to commercial spent fuel. That study primarily concluded that most of the commercial spent fuel at that time was not sufficiently characterized (e.g., fuel dimensions, composition) to be placed into the multipurpose canister. It was noted, however, that there were advantages to having standardized canisters with respect to handling and improved human factors, which should be considered in future DOE spent nuclear fuel program planning (Knecht, 1994).

A goal of the multipurpose canister design is to provide storage at a reasonable cost, high strength, criticality control, radiation shielding, and efficiency (DOE, 1994a,b). In addition, advantages of using standardized packages are reduced handling, possible reduced radiation exposure, and possible reduced risk of radionuclide release and airborne contamination (DOE, 1994a,b; Lopez and Abbott, 1994; International Atomic Energy Agency, 2000). The multipurpose design would enable spent fuel assemblies to be loaded into a canister and permanently sealed at the loading site. The permanently sealed canister could then be transported, stored, and disposed using an appropriate overpack.

In 1995, DOE terminated its design of the multipurpose canister and instead developed a market-driven strategy in which the private sector would pursue further work. Recognition of the advantages of the multipurpose canister system has led to the development of commercial applications of this design approach, such as the multipurpose canisters of Holtec International and the Universal Multipurpose System (UMS™) of NAC International.

DOE has recently announced that it proposes a predominantly clean canister approach to commercial spent fuel handling operations (DOE, 2006) at the potential Yucca Mountain Repository. The transportation, aging, and disposal canister concept is intended to eliminate the need to perform extensive handling of bare spent nuclear fuel or repackaging operations at the Yucca Mountain facility prior to disposal, because 90 percent of bare spent fuel will be loaded into canisters and permanently sealed at the originating sites. Under the approach announced by DOE, the transportation, aging, and disposal canister is a single component in the complete waste disposal system: a transportation overpack, as licensed under 10 CFR Part 71, will be used for transport to the geologic repository; a storage overpack, as licensed under 10 CFR Part 72, will be used for interim storage; and a disposal overpack, as licensed under 10 CFR Part 63, will be used for permanent disposal at the repository.

1.2 Objectives and Scope

This report investigates, through a literature review, the structural robustness of existing canisters that may be an analog for the canister to be used at the potential repository when subject to a drop event. DOE spent nuclear fuel and DOE high-level waste canisters are sealed prior to transportation and remain sealed throughout handling, storage, and disposal. Because of this, the structural behavior of these canisters is studied to determine whether these are suitable analogs for the proposed transportation, aging, and disposal canister design.

Documentation pertaining to spent nuclear fuel canisters currently in use will be reviewed, and full-scale test information regarding spent nuclear fuel canisters will be evaluated. The full-scale tests involve free drops and puncture tests as specified in 10 CFR 71.73. Finite element analyses simulating the full-scale tests will be evaluated to determine their accuracy in effectively modeling the observed behavior of the full-scale tests.

This report is organized into nine chapters. Chapter 1 provides the background and scope of this report. Chapter 2 examines preliminary work pertaining to small-scale testing of proposed DOE spent nuclear fuel canisters and the corresponding finite element analyses of the tests. Chapter 3 examines the full-scale testing of the standardized commercial spent fuel canisters.

Chapter 4 briefly discusses the finite element analysis of the standardized canister and addresses the appropriate modeling of the surface friction coefficient and the rate-dependent material data. Chapter 5 will look at the Idaho spent fuel canister design, which is a modified version of the standardized spent nuclear fuel canister. Chapter 6 considers the structural behavior of the multi-canister overpacks, and Chapter 7 discusses full-scale testing and preliminary finite element modeling of high-level waste canisters.

Chapter 8 will also discuss fabrication issues such as canister welding and the effects of flaws in the canister construction. Finally, Chapter 9 summarizes information collected as a result of the literature review.

2 PRELIMINARY STUDY OF DOE SPENT NUCLEAR FUEL CANISTERS

The standardized DOE spent nuclear fuel canister has to be flexible enough to handle all spent nuclear fuel for a variety of storage and transportation systems. The canister must also be standardized so that it will be compatible with disposal requirements at the repository. To fulfill these criteria, the canisters must be capable of withstanding mechanical loads during handling operations and provide confinement in the event of an accidental drop. The design of a structurally robust canister will rely on experimental tests as well as numerical analysis. For example, finite element analysis can be used to predict a canister's structural response (e.g., plastic deformation, geometry changes) for a number of drop heights and orientations. These analyses permit the selection of a preliminary canister design and the development of test canisters. This preliminary design would then be validated by limited experimental drop tests (either small or full scale) of the representative canisters, and subsequent pressure testing of the canisters can also be used to demonstrate that the containment boundary is maintained. Comparing the results of the finite element solution to those of the corresponding full-scale test verifies the ability to accurately model the deformation behavior of the canister. Thus, the finite element analysis and experimental testing can become a coupled process.

2.1 Preliminary Numerical and Experimental Structural Evaluation of a DOE Spent Nuclear Fuel Canister

Due to the dynamic nature of an impact, canister design involves deformations that are significantly in the inelastic range, and the inelastic deformation is highly localized primarily at the point of impact. Allowing plastic deformation to occur is acceptable as long as containment is not compromised due to rupture. Inelastic deformation allows both a significant amount of kinetic energy due to impact to be absorbed by the canister and an efficient design. A design that was restricted such that the complete canister behaved elastically would lead to a significant amount of conservatism and, thus, to a costly design (Blandford, et al., 2003). Important aspects to consider for inelastic design (using finite element analysis, for example) are maximum deformation limits, inelastic material properties, possible strain-rate effects, and maximum strength limits (Blandford, et al., 2003).

Snow, et al. (1999) evaluated a specific proposed canister design (Figures 2-1 and 2-2) that would continue to contain spent nuclear fuel after a drop event and suffer only minor damage with no breach. The proposed canister was subjected to a drop of 9 m [30 ft] and struck a flat, unyielding surface. The canister design was evaluated through small- and full-scale experimental testing and finite element analysis. In this test program, the impact surface consisted of a 51-mm [2-in]-thick carbon steel plate placed on a 203-mm [8-in]-thick concrete pad. The concrete pad had steel rails on two sides, and the concrete pad was placed such that it spanned the rails. It was noted, however, that this arrangement could not be considered truly rigid (Snow, et al., 1999).

Because of the high strain rate and large deformations that the canister will undergo due to impact, the selected material required sufficient ductility. In addition, because the canister may

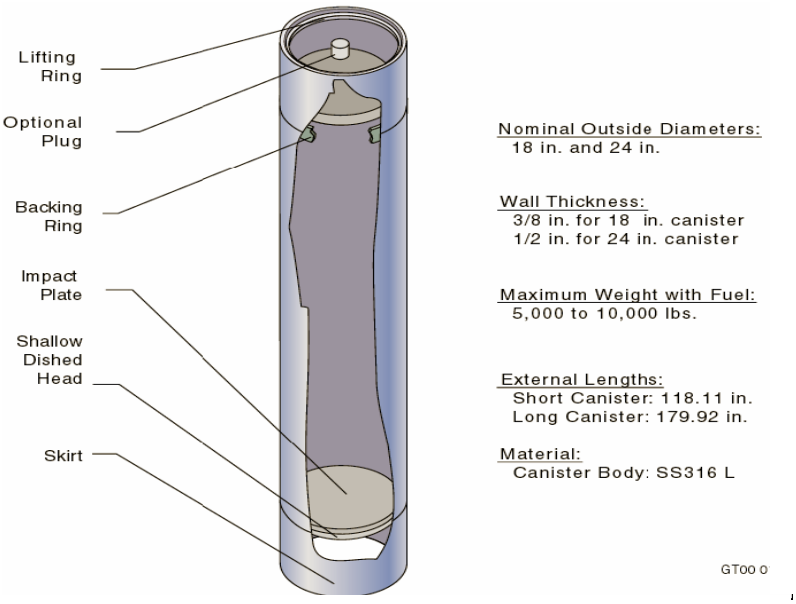

Figure 2-1. DOE Standardized Spent Nuclear Fuel Canister (Morton, et al., 2006, Used With Permission of the American Nuclear Society, Copyright 2006) [25.4 mm = 1 in] [1 kg = 2.21 lb]

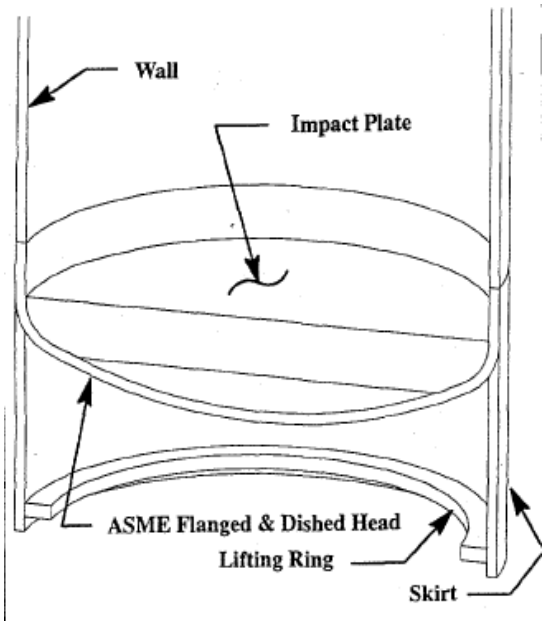

Figure 2-2. Spent Nuclear Fuel Canister End Details (Snow, et al., 1999, Used With Permission of the American Society of Mechanical Engineers, Copyright 1999)

be subjected to a corrosive environment, corrosion resistance was also considered. The DOE spent nuclear fuel canister used in Snow, et al. (1999) was constructed of 304L stainless steel.

Initially, 304L stainless steel was used in early conceptual designs; this was subsequently switched to 316L to improve the canister's resistance to corrosion and hydrogen embrittlement (Snow, et al., 1999; DOE, 1999a,b). While the results in Snow, et al. (1999) used 304L stainless steel {σ_u = 500 mPa [73 Ksi] elongation = 45 percent}, its similarity in material strength and ductility allows these results to be applicable to the actual 316L stainless steel {σ_u = 485 mPa [70 Ksi] elongation = 40 percent} material to be used in the standardized canister.

2.2 Small-Scale and Finite Element Simulation of Drop Tests

As different preliminary designs of the spent nuclear fuel canisters were investigated (Snow, et al., 1999), a number of finite element analyses were performed on small-scale canisters to investigate the structural behavior of the various end conditions of the canister. One of the requirements was that the design of the canister end be constructed of standard pressure vessel heads and the canister body constructed of standard pipe (e.g., ASTM SA–312 pipe) sections. Both of these requirements would result in ease of fabrication and cost savings. Figure 2-3 shows the end conditions under consideration. Note, however, that the end design with a hemispherical head and no skirt will not allow the canister to stand vertically on its own.

The finite element models of the four canisters with the different head configurations were analyzed using ABAQUS/Explicit. The model canisters were 457 mm [18 in] in diameter with wall thicknesses of 6.35, 9.52, and 12.7 mm [0.25, 0.375, and 0.5 in] and length of 3 or 4.5 m [10 or 15 ft]. The canisters had drop orientations of 0, 6, 15, and 30° off vertical with a drop height of 4.5 to 9 m [15 to 30 ft].

The results of the finite element analysis showed that the reversed, hemispherical, and hemispherical with a skirt had significant inelastic deformations (Snow, et al., 1999). The hemispherical heads also exhibited structural instability in the form of snap through buckling (i.e., they deformed to a reversed hemispherical shape). The end condition of the shallow head with the skirt had the best deformation response because the skirt absorbed the impact kinetic energy without damaging the canister body (Snow, et al., 1999). This response was noted for all wall thicknesses, drop orientations, and drop heights. Therefore, a standard American Society of Mechanical Engineers flanged and dished head (American Society of Mechanical Engineers International, 2001) was recommended to be used at each end.

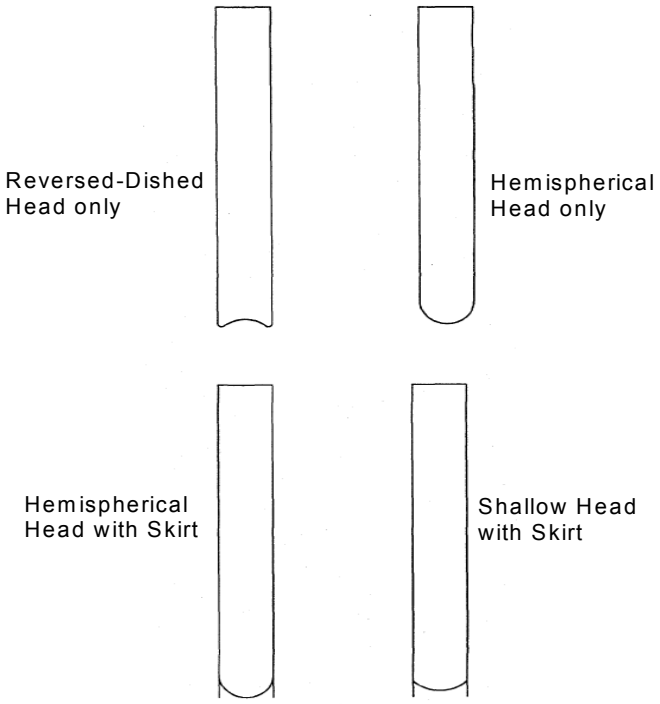

Figure 2-3. Different End Designs of Preliminary Canister Design (Snow, et al., 1999, Used With Permission of the American Society of Mechanical Engineers, Copyright 1999)

Based upon these finite element results, seven small-scale canister test specimens were fabricated. Six of the canisters were constructed using a thin wall tube having a diameter of 127 mm [5 in] and a length of 914 mm [36 in]; the seventh canister was constructed of the same thin wall tube with a 457-mm [18-in] diameter and a length of 1,524 mm [60 in]. The canister body was constructed using a tube with a welded longitudinal seam instead of seamless tubing. These tubes had a flat plate welded to each end of the canister and a second thick plate welded 76 mm [3 in] from the end to support the internal contents, which were represented by lengths of #4 rebar {12.7-mm [0.5-in]-diameter carbon steel rods}. Of the six canisters, five had a weight of 52 kg [115 lb], and the sixth had a weight of 34 kg [111 lb]. The 127-mm [5-in]-diameter canisters were oriented at 15° off vertical and dropped from heights of 3, 4.6, 6.1, and 9 m [10, 15, 20, and 30 ft] onto a rigid surface (Snow, et al., 1999).

The results of the seven small-scale tests confirmed that the inelastic deformations were limited to the end of the canister. The experimentally measured deformation behavior was compared with that predicted by the finite element analysis, and Snow, et al. (1999) found that the finite element models matched the experimental observations quite well, validating the finite element modeling and accuracy of the predicted deformation response. From these finite element analyses, the amount of plastic strain in the test canisters was determined. As can be expected, the maximum equivalent plastic true strain increased with the drop height

(Snow, et al., 1999). For the highest drop height, the maximum equivalent plastic true strain was calculated to be 86 percent at the surface and 26 percent at the midsurface (thickness) on the containment boundary. The midsurface strains are important because they indicated whether any surface crack would propagate through the thickness. Subsequent pressure testing of the canisters showed that the pressure boundary was maintained (Snow, et al., 1999). With respect to the welds, the canister was oriented with the longitudinal seam on the impact side of the canister, and it was observed that for all the drop events, the welds deformed similarly to the base metal of the canister.

Based on the numerical results and the small-scale tests, the skirt welded around the end of the canister was determined to absorb a significant amount of kinetic energy by plastic deformation, leaving the main body of the canister undamaged (Snow, et al., 1999). This end design was selected for use in the subsequent experiments on the full-scale canisters.

The seventh small-scale test used a canister with a 457-mm [18-in] diameter, a wall thickness of 4.78 mm [0.188 in], and length of 1,524 mm [60 in]. The impact end was constructed using the shallow dished head with a 178-mm [7-in]-long skirt and an interior impact plate (Snow, et al., 1999). The contents of the canister were simulated by #4 rebar and a 304L stainless steel internal support structure, having a total weight of 4,535 kg [10,000 lb]. The canister was oriented 32° off vertical and dropped from a height of 9 m [30 ft]. As predicted, the inelastic deformation was limited to the skirt at the end of the canister. The skirt buckled and curled inward but did not damage the dished head (Snow, et al., 1999). The finite element analysis produced a 13 percent maximum equivalent plastic surface true strain and a 3 percent midsurface (thickness) equivalent plastic true strain in the canister pressure boundary. On the other hand, the skirt had 48 percent maximum equivalent plastic true strain on the surface and 13 percent maximum equivalent plastic true strain at the midsurface (thickness). This marked increase in plastic strain demonstrated that the skirt absorbs the majority of the drop energy.

The results appeared to exhibit a deformation response that depended on the coefficient of friction used for the canister impact surface interface. A value of 0.5 produced incorrect deformation in the skirt, while a value of 0.1 produced a skirt deformation close to that observed in the test canister. The effect of the friction coefficient is detailed in Section 4.2.

2.2.1 Full-Scale and Finite Element Simulated Drop Tests of 457- and 610-mm [18- and 24-in] Canisters

With the preliminary work completed, full-scale experimental tests were performed on two canisters. One canister was 457 mm [18 in] in diameter, the second was 610 mm [24 in] in diameter, and both of the canisters were 4.6 m [15 ft] in length. The 457-mm [18-in] canister was oriented at 6° off vertical, while the 610-mm [24-in]-diameter canister was oriented at 9° off vertical. Note that these orientation angles were selected such that the canisters' center of gravity was approximately over the location where the skirt contacted the rigid surface. The test drop height for both canisters was 9 m [30 ft].

A 406-mm [16-in]-diameter pipe was placed inside the 457-mm [18-in]-diameter canister, and the pipe was filled with rebar and concrete. The outside of the pipe was also surrounded by rebar such that the canister had a maximum weight of 2,580 kg [5,690 lb]. The 610-mm

[24-in]-diameter canister contained a 508-mm [20-in]-diameter pipe, which was also filled with rebar and concrete for a total weight of 4,440 kg [9,790 lb] (Snow, et al., 1999).

Explicit finite element analyses were performed using ABAQUS/Explicit to model the proposed canister designs and perform the impact analysis. The finite element model of the canister utilized geometric symmetry of the canister such that only one half of the canister was modeled (Figure 2-4). The impact surface was modeled using a rigid surface as defined in ABAQUS, and the coefficient of friction at the impact interface was selected as 0.3. To account for the dynamic high strain-rate effect, the yield stress and stress–strain data of the 304L stainless steel was increased by 20 percent (Snow, et al., 1999). The accuracy of this assumption is further discussed in Section 4.3.

Figure 2-5(a) shows the deformed 457-mm [18-in] canister after the full-scale test. The full-scale test results show that the significant amount of deformation was limited to the skirt, demonstrating that the skirt serves its intended purpose as an energy absorption device. The canister was pressure tested at 175 kPa [25 psig] and held for 1 hour with no drop in pressure, which confirmed that the canister pressure boundary remains intact. Figure 2-5(b) shows that the finite element results captured the same deformation behavior of the full-scale test. Because no strain data was measured from the full-scale test, the results of the finite element analysis were used to study the strain distribution in the canister. The finite element analysis calculated low strain magnitudes in the canister pressure boundary components (i.e., lower and upper head and canister body) with a maximum surface true strain of 3 percent and a 1 percent midsurface true strain. Postdrop tensile testing of a material sample taken from the 457-mm [18-in] canister body showed a minimum ultimate plastic true strain of 66 percent (Snow, et al., 1999). Because the strains of the canister pressure boundary components were less than 66 percent, no rupture was predicted. On the other hand, the skirt had a maximum surface true strain of 67 percent and a midsurface true strain of 18 percent.

As part of the drop tests, the same 457-mm [18-in] canister was dropped a second time from 30 feet, but with a horizontal orientation. The canister deformation (flattening) was distributed over a 2.4-m [8-ft]-long by 152-mm [6-in]-wide area. The 2.4 m [8 ft] of flattening corresponds to the length of the impact surface's steel plate. This canister also satisfied the 172 kPa [25 psig] pressure test (Snow, et al., 1999). This demonstrates that the 457-mm [18-in] canister maintained its pressure boundary after two successive drop events.

A 610-mm [24-in] canister was also subjected to a vertical drop similar to the previous test. The plastic deformation was confined to the end skirt as shown in Figure 2-5(c). Subsequent pressure testing was used to verify the structural integrity of the canister pressure boundary. The canister was pressurized to 172 kPa [25 psig] and held for 1 hour, indicating that the canister containment boundary was maintained. The deformation predicted by the finite element analysis compares quite well with the full-scale test as shown in Figure 2-5(d). Again, because no strain measurements were recorded from the test, the output from the finite element model was used to investigate the strain distribution in the canister. The plastic straining in the

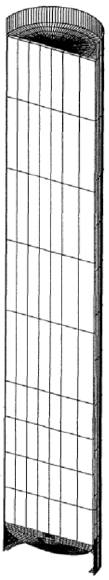

Figure 2-4. Representative Finite Element Model of 610-mm [24-in] Canister (Snow, et al., 1999, Used With Permission of the American Society of Mechanical Engineers, Copyright 1999)

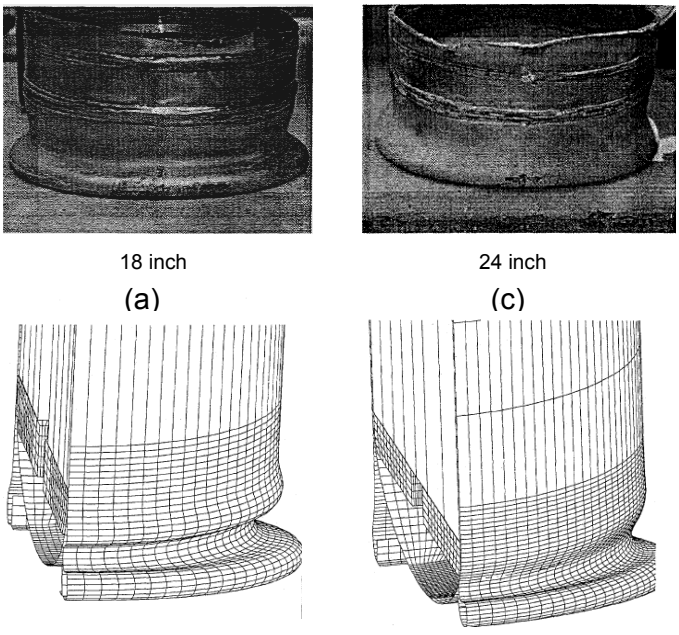

Figure 2-5. Comparison of Full-Scale Test Results and Finite Element Analysis (Snow, et al., 1999, Used With Permission of the American Society of Mechanical Engineers, Copyright 1999)

canister pressure boundary components was low: 4 percent on the canister surface and 1 percent at the midsurface. On the other hand, the skirt had a maximum plastic true strain of 80 percent at the surface and 16 percent at the midsurface. Postdrop testing of a sample of the material from the 610-mm [24-in] canister produced a minimum ultimate plastic true rupture strain of 76 percent (Snow, et al., 1999). Therefore, the strains in the canister pressure boundary components were below the test rupture strain, indicating no failure.

However, the finite element models predicted a greater crush depth than the actual experiment because in the experiment, the steel plate fixed on the ground rebounded with the canister. Thus, some of the impact kinetic energy was transferred to the plate as elastic energy and to the concrete base and soil (Snow, et al., 1999). The finite element simulation conservatively modeled the impact surface as perfectly rigid such that the canister directly absorbed all of the impact energy. A second set of finite element analyses was performed in which the rigid surface was modeled as a surface supported by an elastic foundation. The results of these analyses produced deformations closer to those observed in the tests. However, the foundation spring stiffnesses used in the elastic foundation were chosen arbitrarily (Snow, et al., 1999).

From the finite element analysis, a coefficient of friction of 0.3 compared best with the finite element deformation response produced in the full-scale test. Snow, et al. (1999) observed that the coefficient of friction appeared to affect the deformation the finite element method predicted. Recall that this effect was also observed in the small-scale tests. With this validation of the finite element analyses, additional canister orientations (other than the two full-scale tests) were investigated to evaluate the effect of the coefficient of friction. Snow, et al. (1999) reported that orientations between 0 and 45° with a higher coefficient of friction produced more accurate deformations, unlike the orientations of 6 and 9° off vertical in which a smaller coefficient of friction was required. However, Snow, et al. (1999) did add the caveat that these effects were simply observations and were strictly preliminary. Additional discussion of this effect will be addressed later in this report.

3 THE DOE STANDARDIZED SPENT NUCLEAR FUEL CANISTER

In the late 1990s, the National Spent Nuclear Fuel Program developed a standardized design for the spent nuclear fuel canisters. The motivation behind this standardization was the desire to have a single canister that could handle different types of fuel and internal components having different geometries and simplified handling operations at user storage sites, transportation, and emplacement at the final repository. The canister design should also be robust enough to withstand an accidental drop while containing the spent nuclear fuel and provide a common basis for canisters, making them compatible with any proposed lifting fixtures and handling requirements (Morton, et al., 2000).

The preliminary work of Snow, et al. (1999) established a workable canister design based upon small- and full-scale testing and finite element analysis. Finite element analysis was used to investigate proposed designs before the limited small- and full-scale tests were performed. Subsequently, full-scale drop tests determined the canister structural integrity and validated the finite element analysis. Fabrication, full-scale testing, and finite element modeling of the standardized canister will be discussed next.

3.1 Fabrication of the Standardized Spent Nuclear Fuel Canisters

The standardized canisters had either a 457- or 610-mm [18- or 24-in] diameter with lengths of 3 and 4.6 m [10 and 15 ft]. The canister body is constructed from longitudinally welded SA–312 pipe made of 316L stainless steel. The pipe selected for the drop tests was longitudinally welded as opposed to using seamless pipe. This was because the weld could possibly increase the likelihood of containment failure when subjected to a drop test (Blandford, et al., 2003), and the canister was oriented such that the weld would be on the side that makes impact. The welds were made using welders who were qualified as per American Society of Mechanical Engineers Boiler and Pressure Vessel Code, Section IX, and the materials used are specified in Section III (Blandford, et al., 2003). The pipe wall thickness is 9.5 and 12.7 mm [0.375 and 0.5 in] for the 457- and 610-mm [18- and 24-in] canisters, respectively (DOE, 1999a). The heads of the canister are American Society of Mechanical Engineers flanged and dished heads made of 316L stainless steel (Figure 2-1) as specified in the Boiler and Pressure Vessel Code, Section III, Division 1, Subsection ND (American Society of Mechanical Engineers International, 2001), with a wall thickness of either 9.5 or 12.7 mm [0.375 or 0.5 in]. The interior impact plates located at each end have a thickness of 51 mm [2 in] and are made of A–36 carbon steel plate. The skirts at each end are 203 mm [8 in] long and are made of 316L stainless steel (Snow, et al., 2005, 2000).

3.2 Drop Testing and Modeling of Standardized Canisters

The objective of drop testing canisters is to show that for any drop orientation, containment is preserved. It is also important to assess the amount of canister deformation to determine whether the canister can fit into other containers (e.g., a waste package). The full-scale tests presented in Snow, et al. (2000) provided additional data on the structural behavior of the standardized canister design. The additional experimental data further demonstrated that finite element analysis accurately simulated drop tests. In addition, the number of experimental tests

was expanded from previous studies to include drop tests at additional orientations, and puncture tests were conducted to further evaluate the canister's structural integrity.

3.3 Scope of Experimental Drop Test Program

The experimental tests used in this study are based on the proposed standardized DOE spent nuclear fuel canister design discussed in Chapter 2. In Snow, et al. (2000) and Morton and Snow (2000), the 457-mm [18-in]-diameter canister was selected. Table 3-1 summarizes nine full-scale tests. Canister drop orientations (angle) investigated were 0, 6, 45, 80, and 90° off vertical. All of these canisters were tested at a drop height of 9 m [30 ft] and had a length of 4.6 m [15 ft], except Canisters 06 and 07, which had a length of 3 m [10 ft]. These experimental tests were conducted at Sandia National Laboratories facilities, which had an impact surface consisting of a flat 102-mm [4-in]-thick steel plate embedded in a reinforced concrete base that has an approximate weight of 9.1×10^5 kg [2×10^6 lb]. This surface was assumed to be unyielding (Snow, et al., 2000).

Canisters 01, 02, 04, and 05 were dropped at an orientation of 0, 6, 45, and 80° off vertical, respectively. The case of 6° off center positioned the canister such that its center of gravity was located directly over the point of impact. The test orientation of 80° off center was considered to be the worst case for a slapdown event because the skirt does not absorb a significant amount of energy in this orientation (Snow, et al., 2000). Canisters 03, 06, and 07 were vertical drops with the canister in a horizontal orientation (90° off vertical).

Canister 08 represents a drop onto a repository waste package. This canister, with an initial orientation of perfectly vertical, was dropped from a height of 0.61 m [2 ft] onto a vertical 51-mm [2-in]-thick plate representing the edge of a waste package. Once the canister contacts the vertical plate, it will rotate (tip over) and strike a second vertical 51-mm [2-in]-thick plate. Canister 09 was tested for puncture resistance when dropped from a height of 1 m [40 in] onto a 152-mm [6-in]-diameter steel bar (Snow, et al., 2000).

Figure 3-1 shows the different internal configurations used in each test canister. Canisters 01 to 05 had the spoked-wheel basket that was filled with rebar (carbon steel bar) inside of a protective sleeve. The spoked-wheel basket was chosen because the spokes would result in concentrated forces over a small area of the canister body. The weight of these five canisters was approximately 2,721 kg [6,000 lb]. Canister 06 used simulated high-integrity cans (Holmes, 1999; Spears, 1999) represented by stainless steel pipe and filled with rebar for a total weight of 1,724 kg [3,802 lb], which was limited by the amount of rebar that could fit into the cans. Canister 07 used simulated Shippingport fuel internal components represented by two 187-mm [7.375-in]-square tubes loaded with rebar for a total weight of 1,359 kg [2,997 lb] {approximately 181 kg [400 lb] above the actual weight of two Shippingport fuel bundles} (Morton and Snow, 2000). Canisters 08 and 09 had the spoked-wheel basket but with no internal sleeve.

Table 3-1. Test Matrix for Nine Standardized Spent Nuclear Fuel Canisters*				
Canister No.	Length (m) [ft]	Impact Angle (degrees)	Total Weight (kg) [lb]	Drop Height (m) [ft]
01	4.6 [15]	0	2,737 [6,035]	9 [30]
02	4.6 [15]	6	2,698 [5,949]	9 [30]
03	4.6 [15]	90	2,719 [5,995]	9 [30]
04	4.6 [15]	45	2,719 [5,995]	9 [30]
05	4.6 [15]	80	2,706 [5,967]	9 [30]
06	3.00 [10]	90	1,725 [3,804]	9 [30]
07	3.00 [10]	90	1,360 [3,000]	9 [30]
08	4.6 [15]	0	2,709 [5,973]	0.61 [2]
09	4.6 [15]	90	2,760 [6,086]	1 [3.28]

*Morton, D.K., S.D. Snow, T.E. Rahl, and A.G. Ware. "Containment and Analysis Capability Insights Gained from Drop Testing Representative Spent Nuclear Fuel Containers." 16th International Conference on Structural Mechanics in Reactor Technology. Washington, DC: Structural Mechanics in Reactor Technology. 2001. Used with permission of Structural Mechanics in Reactor Technology, Copyright 2001.

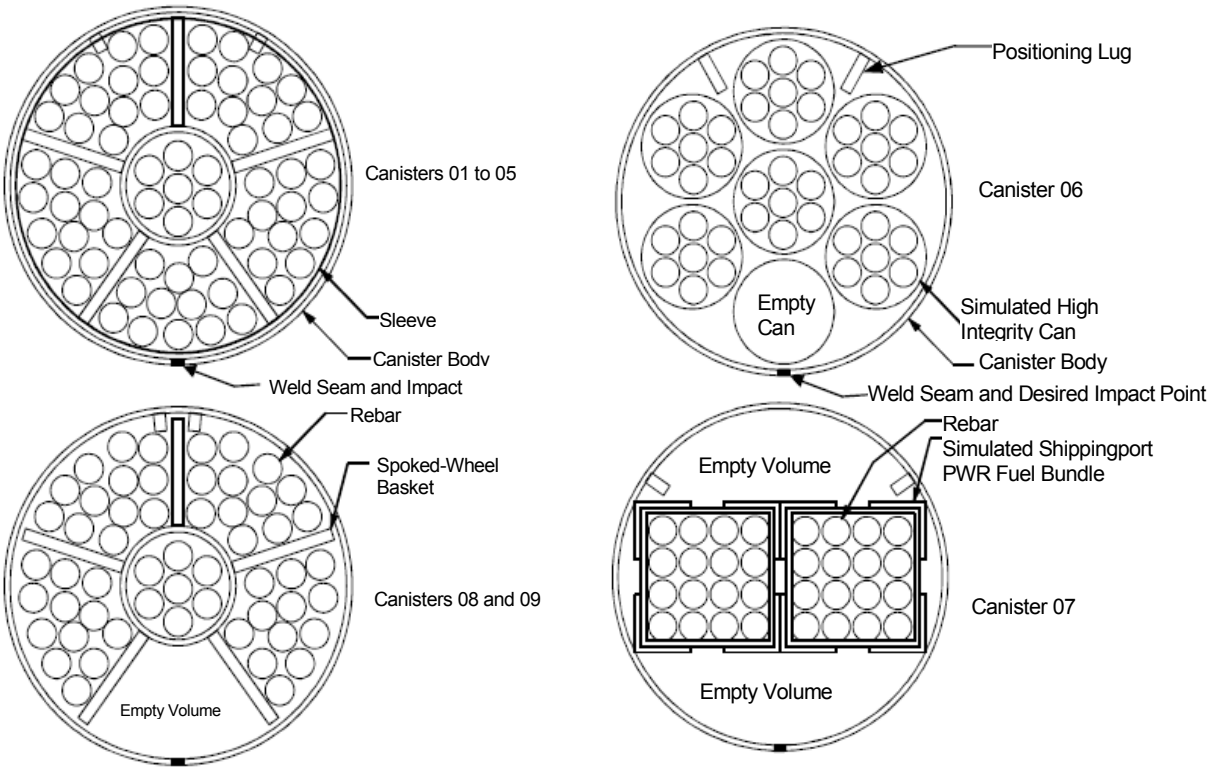

Figure 3-1. Internal Configurations for Spent Nuclear Fuel Canisters (Morton, et al., 2001, Used With Permission of Structural Mechanics in Reactor Technology, Copyright 2001)

Because Canisters 08 and 09 were involved in a puncture event, the internal sleeve was removed, resulting in further concentrated loads on the containment boundary. Both of these canisters had a weight of 2,721 kg [6,000 lb].

The test canisters had a number of welds that did not receive any postweld heat treatment (Morton, et al., 2000b). The pipe used for the canister containment boundary and skirt was longitudinally welded. Seamless pipe could have been used, but these tests aimed to demonstrate that the type of welds used were sufficient. The pipe orientation was such that the side with the weld would contact the impact surface and would experience the most stress (and plastic deformation), demonstrating that the containment boundary would not be breached.

3.4 Experimental Drop Test Results and Validation of Finite Element Modeling

Figures 3-2 to 3-5 (Canister 01) show select deformation results from the full-scale and finite element analysis results. Figure 3-2(a,b) is the 0° off-vertical orientation. Note the similarity in the deformation of the skirt in the test and that predicted by the finite element analysis. Note that the skirt sidewall just above the end in the finite element analysis bulges inward [Figure 3-2(b)] instead of outward as in the test [Figure 3-2(a)]. This difference can be explained by the fact that in this region, the skirt buckles, and the shape orientation depends on any imperfections in the actual test cylinder. Morton, et al. (2001) attribute the differences to possible residual stresses from the welds and the fact that the skirt may not be completely round. On the other hand, the finite element model does not account for these imperfections; thus, the buckling could occur either outward or inward (Snow, et al., 2000). Figure 3-3(a,b) (Canister 04) is for an orientation of 45° off vertical and, again, as intended, the skirt absorbs the impact force and exhibits significant plastic deformation. Figure 3-4(a,b) (Canister 05) corresponds to the case of 80° off vertical. The skirt again deforms, while the canister body remains intact. Note that in the finite element results, there was a bulge in the dished head on the side of impact [Figure 3-4(b)], and similar deformation was said to have occurred in the test canister (Snow, et al., 2000; Morton, et al., 2001). Finally, Figure 3-5(a,b) (Canister 09) shows the results of the horizontal drop onto a 152-mm [6-in]-diameter post with similar deformation in both the test results and the finite element analysis.

3.5 Finite-Element-Predicted Maximum Equivalent Plastic True Strains

3.5.1 The 457-mm [18-in]-Diameter Standardized Canister

Section 3.4 showed the good correlation between experiment test results and finite element estimated deformations; therefore, in this section, Snow, et al. (2000) used the strains available from the previous finite element analyses to further evaluate the canister's structural response. Table 3-2 presents the maximum equivalent plastic true strains from the finite element analysis for each canister test. As shown, plastic strains predicted from the finite element analysis showed a maximum equivalent plastic true strain of 62 percent on the pressure boundary (Canister 07). However, Snow, et al. (2000) noted that this may be caused by conservative

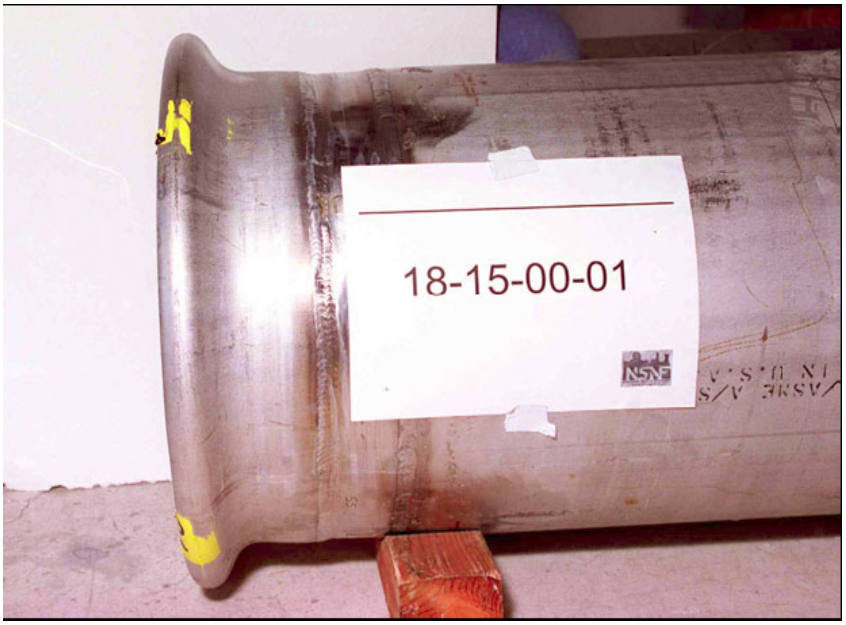

(a)

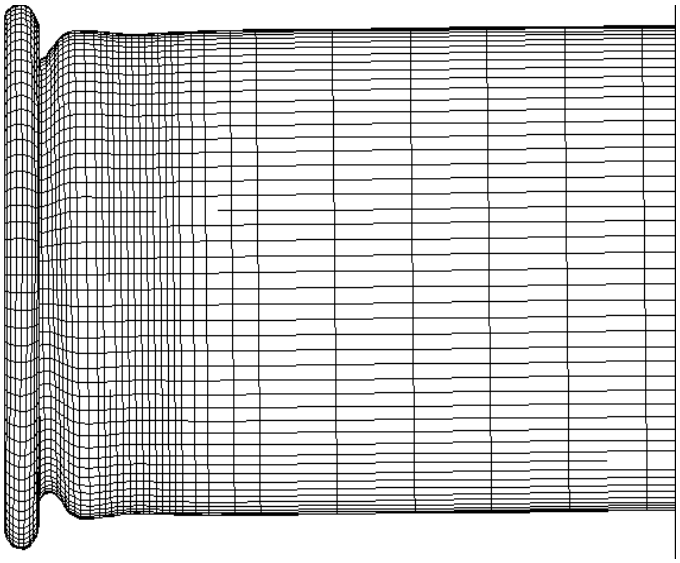

(b)

Figure 3-2. DOE Standardized Spent Nuclear Fuel Canister 01: Vertical End Drop, 9 m [30 ft] (Morton, et al., 2001, Used With Permission of Structural Mechanics in Reactor Technology, Copyright 2001)

(a)

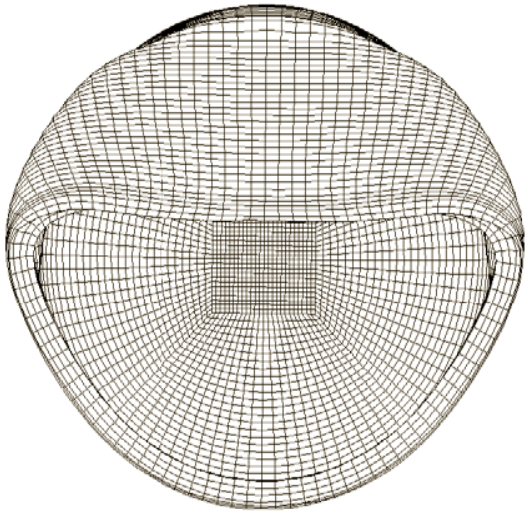

(b)

Figure 3-3. DOE Standardized Spent Nuclear Fuel Canister 04: Vertical Drop, 45° Off Vertical, 9 m [30 ft] Drop Height (Morton, et al., 2001, Used With Permission of Structural Mechanics in Reactor Technology, Copyright 2001)

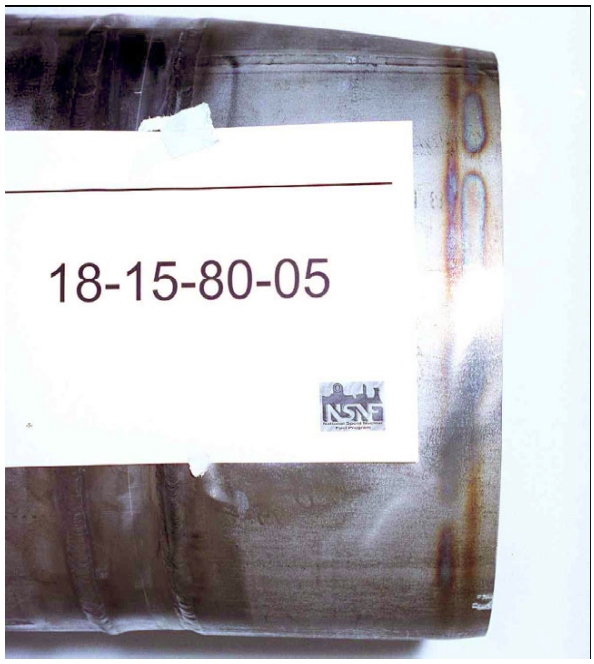

(a)

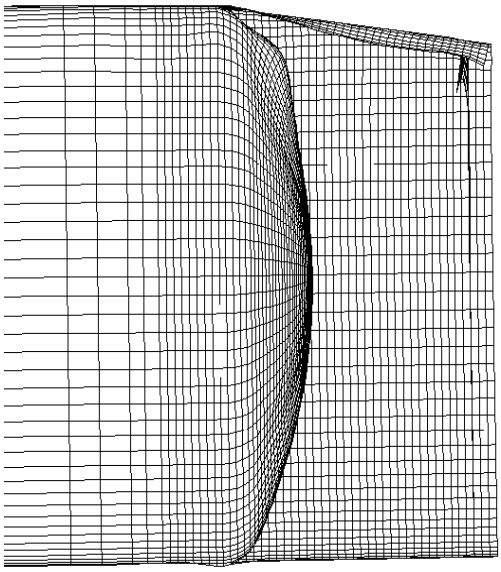

(b)

Figure 3-4. DOE Standardized Spent Nuclear Fuel Canister Case 05: Vertical Drop, 80° Off Vertical, 9 m [30 ft] Drop Height (Morton, et al., 2001, Used With Permission of Structural Mechanics in Reactor Technology, Copyright 2001)

(a)

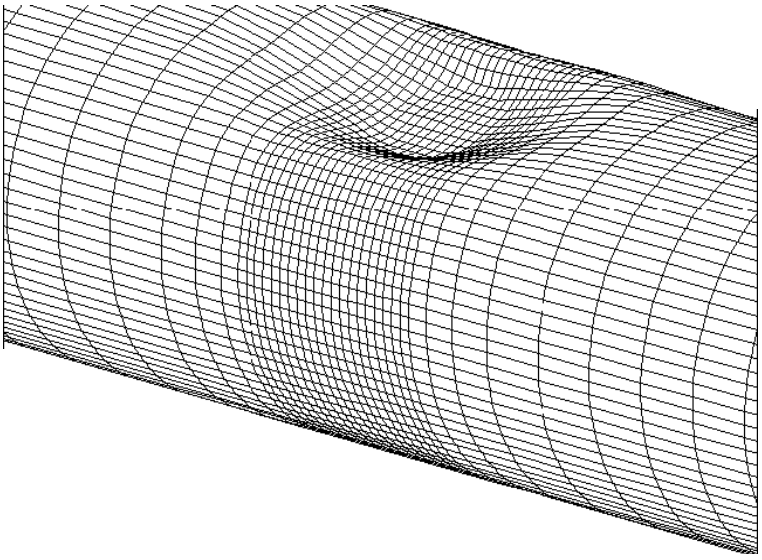

(b)

Figure 3-5. DOE Standardized Spent Nuclear Fuel Canister 09: Vertical Drop, 90° Off Vertical Puncture Test (Morton, et al., 2001, Used With Permission of Structural Mechanics in Reactor Technology, Copyright 2001)

Table 3-2. Test Matrix of Maximum Equivalent Plastic True Strains*							
Test Canister	Impact Angle	Maximum Equivalent Plastic True Strains (%)					
		Containment Material			Skirts and Lifting Rings		
		Outside	Midplane	Inside	Outside	Midplane	Inside
01	0	7	3	6	91	17	75
02	6	9	3	10	107	21	94
03	90	40	15	26	10	10	10
04	45	33	9	36	52	33	84
05	80	57	19	42	24	20	19
06	90	44	17	31	21	10	18
07	90	62†	22†	42†	11	10	10
08	0	20‡	7‡	18‡	38‡	38‡	38‡
09	90	39	14	40	—	—	—

*Morton, D.K., S.D. Snow, T.E. Rahl, and A.G. Ware. "Containment and Analysis Capability Insights Gained From Drop Testing Representative Spent Nuclear Fuel Containers." 16th International Conference on Structural Mechanics in Reactor Technology. Washington, DC: Structural Mechanics in Reactor Technology. 2001. Used with permission of Structural Mechanics in Reactor Technology, Copyright 2001.

†Maximum strains due to conservative modeling of internals as discussed in text. Actual maximum straining estimated to be below that reported for Canister 06.

‡Reported maximum containment material strains due to impact with second vertical plate. Maximum skirt and lifting ring strains due to impact with first vertical plate.

modeling of the canister internals. Specifically, in the full-scale test, the Shippingport pressurized water reactor fuel bundles were simulated using square tubing with the rebar located inside. The fuel bundles (rebar) deformed (bent) significantly due to the impact.

However, the finite element analysis used solid steel sections that contacted the canister head without bending; thus, all of the energy was transferred to the canister head (Snow, et al., 2000).

The maximum amount of equivalent plastic true strain in the skirt was for Canister 02 with a 6° off-vertical orientation. At this orientation, the center of gravity of the canister was in line with the corner of impact, thereby creating the most deformation in the skirt. As expected for other orientations (i.e., 45, 80, and 90° off vertical), the skirt absorbed lesser amounts of impact energy. Canister 05 had a maximum equivalent plastic surface true strain of 57 percent, which occurred in the canister upper head. This result is consistent because Canister 05 has the largest amount of slapdown in which the top head will contact the rigid surface with the most energy. A maximum midplane (thickness) true strain of 19 percent and a maximum inside surface strain of 42 percent occurred for Canister 05. The maximum surface, midplane, and inner surface plastic strains did not always occur at the same location in the finite element model of the canister; however, the maximum values reported (Morton and Snow, 2000) were of interest. Because all of the midsurface strains were less than the ultimate, no damage would propagate through the thickness. A conservative value of 48 percent ultimate true strain was selected based upon tensile testing of the 316L stainless steel (Snow, et al., 2000).

As discussed previously, there appeared to be a significant friction parameter dependence on the finite element deformation behavior for the near-vertical and off-vertical orientations. Snow,

et al. (2000) did note that this apparent dependence on friction was preliminary, and such effects may be the result of other unknown factors. This effect is further discussed in Chapter 4.

3.5.2 The 610-mm [24-in]-Diameter Standardized Canister

Based on the successful verification and validation of the finite element analysis for the 457-mm [18-in]-diameter standardized canister, finite element analysis of a 610-mm [24-in]-diameter standardized canister was performed to evaluate its structural response. Comparisons of the 457- and 610-mm [18- and 24-in]-diameter analyses also provided insights as to the need for additional finite element or full-scale testing if the structural behavior changed significantly (Blandford, 2003). This section describes the evaluation of the 610-mm [24-in]-diameter canister using the maximum equivalent plastic true strains obtained from the finite element analyses.

Table 3-3 shows the drop events that were studied. These drop heights and orientations were consistent with those performed for the 457-mm [18-in]-diameter canister and were expected to envelope any of the drop events that may occur. The last two cases are for repository events as specified in the Waste Acceptance System Requirements Document (DOE, 2002). Thus, a total of eight different analyses were performed. The 610-mm [24-in]-diameter canister had a length of 4.6 m [15 ft] and a total weight of 4,535 kg [10,000 lb]. The internal configuration as modeled had the spoked-wheel basket and internal sleeve.

Table 3-4 summarizes the maximum equivalent plastic true strains obtained for each of the drop events. The critical case orientation was determined based on the maximum strains in the canister containment boundary components (Blandford, 2003). The maximum plastic true strain for Canister 05 was 57 percent on the outside surface, which occurred at the top head. The maximum midplane true strain was 23 percent. Recall that a value of 48-percent strain was considered to be a conservative estimate of the ultimate strain. Therefore, the maximum strain value of 23 percent at the midplane indicates that the containment boundary would not rupture (Blandford, 2003). The maximum equivalent plastic true strain in the skirt was 95 percent at an orientation of 45° and was located at the lower skirt lifting ring (Blandford, 2003). Although this strain is larger than the rupture strain, the skirt is designed to absorb the impact energy and undergo a large amount of plastic deformation to prevent damage to the containment boundary.

3.5.3 The 457- and 610-mm [18- and 24-in] Canister Comparison

Lastly, Table 3-5 compares the 457- and 610-mm [18- and 24-in]-diameter canisters. Blandford (2003) cautions that the values for the 610-mm [24-in] canister may not correspond to those listed in Table 3-4, because the values for the 610-mm [24-in]-diameter canister were located at the same position as those of the 457-mm [18-in] canister. The values shown in Table 3-4 were the true maximums for the 610-mm [24-in]-diameter case. Overall, Table 3-5 shows that with respect to the canister containment boundary, the 610-mm [24-in]-diameter canister had lower strains than did the 457-mm [18-in]-diameter canister. For the case of Canister 05, which is the

Table 3-3. Standardized Canister Model Designations*		
Canister Model Identification	**Drop Orientation (Degrees Off Vertical)**	**Description**
24-15-00-01	0	Vertical Drop From 9 m [30 ft]
24-15-07-02	7	Center of Gravity-Over-Corner Drop From 9 m [30 ft]
24-15-90-03	90	Horizontal Drop From 9 m [30 ft]
24-15-45-04	45	45° Drop From 9 m [30 ft]
24-15-70-05	70	Worse Orientation Drop From 9 m [30 ft]
24-15-PP-09	90	Puncture, Horizontal Drop on Rigid Post From 1 m [40 in]
24-15-00-RV	0	Repository Vertical Drop From 7 m [23 ft]
24-15-65-RW	65	Repository Worse Orientation Drop From 0.61 m [2 ft]
18-15-00-RV	0	Repository Vertical Drop From 7 m [23 ft]
18-15-80-RW	80	Repository Worse Orientation Drop From 0.61 m [2 ft]

*Blandford, R.K. "Structural Response Evaluation of the 24-Inch Diameter DOE Standardized Spent Nuclear Fuel Canister." EDF–NSNF–026. Idaho Falls, Idaho: Idaho National Engineering and Environmental Laboratory. 2003.

Table 3-4. Maximum Equivalent Plastic True Strains: 610-mm [24-in]-Diameter, 4.6-m [15-ft]-Long, 2,721-kg [6,000-lb] Canister*						
Canister Model	**Maximum Equivalent Plastic True Strains (%)†**					
	Containment Boundary Components			**Skirts and Lifting Rings**		
	Outside	**Middle**	**Inside**	**Outside**	**Middle**	**Inside**
24-15-00-01	6	.6	4	45	16	54
24-15-07-02	.7	.1	.6	76	31	60
24-15-90-03	34	16	22	7‡	3‡	5‡
24-15-45-04	48	22	42	95	33	117
24-15-70-05	57	23	48	74	41	58
24-15-PP-09	16	15	17	§	§	§
24-15-00-RV	6	6	4	44	14	53
24-15-65-RW	23	15	16	24	23	23

*Blandford, R.K. "Structural Response Evaluation of the 24-Inch Diameter DOE Standardized Spent Nuclear Fuel Canister." EDF–NSNF–026. Idaho Falls, Idaho: Idaho National Engineering and Environmental Laboratory. 2003.
†Canisters 03, 04, 05, 09, and RW were dropped from slightly higher distances than specified in the drop event definitions to account for significant (>5%) artificial energy used in the solution routine.
‡Maximum strains in skirt only. Maximum strain in lower lifting ring was 8 percent.
§Skirts and rings not strained until canister falls off the post onto the flat surface below.

Table 3-5. Comparison of Maximum Equivalent Plastic True Strains for 457- and 610-mm [18- and 24-in]-Diameter, 4.6-m [15-ft]-Long Canisters*						
Canister Model	Maximum Equivalent Plastic True Strains (%)					
	Containment Boundary Components			Skirts and Lifting Rings		
	Outside	Middle	Inside	Outside	Middle	Inside
24-15-00-01	6	0.6	4	45	16	54
18-15-00-01	7	3	6	91	17	75
24-15-07-02	0.7	0.1	0.6	76	31	60
18-15-06-02	9	3	10	107	21	94
24-15-90-03	34	16	22	8	8	8
18-15-90-03	40	15	26	10	10	10
24-15-45-04	18	9	15	95	33	117
18-15-45-04	33	9	36	52	33	84
24-15-70-05	57	23	48	30	15	15
18-15-80-05	57	19	42	24	20	19
24-15-PP-09	16	15	17	NA	NA	NA
18-15-PP-09	39	14	40	NA	NA	NA
24-15-00-RV	6	0.5	4	44	14	53
18-15-00-RV	10	3	6	40	16	48
24-15-65-RW	23	15	16	22	21	21
18-15-80-RW	24	11	13	9	8	8

*Blandford, R.K. "Structural Response Evaluation of the 24-Inch Diameter DOE Standardized Spent Nuclear Fuel Canister." EDF–NSNF–026. Idaho Falls, Idaho: Idaho National Engineering and Environmental Laboratory. 2003.

orientation for slapdown to occur, note that the strains for the two canisters are practically the same. With respect to the skirt strains for drop orientations other than 45°, there is comparable surface strain for the 457- and 610-mm [18- and 24-in]-diameter canisters. For a drop orientation equal to 45°, the skirt maximum strains were greater for the 610-mm [24-in] canister, which indicates greater flexibility in the skirt (Blandford, 2003). Maximum equivalent plastic midplane true strains at the containment boundary were 19 and 23 percent for the 457- and 610-mm [18- and 24-in]-diameter canisters, respectively, which indicated that neither canister would likely rupture.

4 NUMERICAL MODELING OF CANISTER DROP TESTS

Finite element analysis can be a powerful tool to investigate the deformation response of a structure when subject to static and dynamic loads. This is especially true when the deformations produce nonlinear material response. Because the canister is allowed to enter the nonlinear (plastic) range, care must be taken to obtain realistic and accurate solutions. As discussed in the previous two chapters, finite element solutions can accurately predict the deformed shape of the spent nuclear fuel canister when compared to experiments.

4.1 General Comments on Finite Element Analysis

Völzke, et al. (2004) present finite element guidelines as set forth by Bundesanstalt für Materialforschung und -prüfung. As stated, a number of points should be considered when using finite element analysis: (i) verification and validation, (ii) benchmarking, (iii) parameter study, (iv) conservative design calculation, and (v) quality assurance.

The chosen finite element code is benchmarked by comparing solutions from different codes as applied to the same model. Glass, et al. (1984) established a set of two-dimensional, casklike problems subjected to dynamic loading. These problems were analyzed by independent analyses using a number of different codes. Results showed that for the explicit codes, the standard deviations were less than 15 percent of the means. As part of the future work, experiments were proposed for validation (Glass, et al., 1984).

Validation and verification are established by comparing finite element solutions with actual test data. As discussed in Snow, et al. (1999), small- and full-scale tests of the canisters were used to verify and validate the modeling aspects of the finite element analysis. Once the finite element model was validated, the model was used to predict canister behavior subject to other drop orientations.

A parameter study using a simple elastic analysis can be used to check items such as boundary conditions and loads of the finite element model. For an elastic analysis, some hand calculations may be used to verify the numerical solutions. For nonlinear material behavior, a single element model can be used to check whether the proper material behavior is recovered, which assures that the material model parameters are entered correctly. Sufficient mesh refinement may be determined based on reasonableness of expected deformation (e.g., Snow, et al., 2000); the stress and strain distribution (e.g., Snow and Morton, 2003); or through a mesh refinement study (e.g., Hollenbeck and Tu, 1999).

Particular items of the finite element analysis addressed in this report are the effects of the coefficient of friction between the canister and the unyielding impact surface and the strain-rate dependence of the canister materials.

4.2 Friction Coefficient Effect on Finite Element Analysis of Drop Tests

As reported by Snow, et al. (1999) for the near-vertical and near-horizontal drops, the numerical results appeared to be mostly independent of the coefficient of friction. It was noted, however, that for the short 457-mm [18-in] canister, the friction coefficient did appear to have a significant effect. A coefficient of friction value of 0.1 produced the best correlation of the deformed shape between the experiment and finite element simulation, while a value for the coefficient of friction of 0.5 exhibited the largest difference in the deformed shape.

In Snow, et al. (2001), additional finite element analyses were performed to further investigate the character and magnitude of the deformed shape of the canister. To duplicate the canister size used in Snow, et al. (1999), a 457-mm [18-in] diameter, 1,445-mm [57-in]-long canister was selected. Test canisters were obtained by cutting the undamaged ends of the full-scale test canisters used in Snow, et al. (2000).

Based on these tests, a friction parameter Snow, et al. (2001) introduced was established to account for all effects that may take place at the point of impact (e.g., heat dissipation, material property differences). The results presented show that the mode of deformation of the impact surface depends on the coefficient of friction chosen. As the angle measured from off center increases, the coefficient of friction must increase to model the same deformation as observed in the experiments. The end result is that the friction coefficient appears to be dependent on the impact angle.

Figure 4-1 shows the friction parameter required to match the observed deformation of the test canister for the 20° test case. The impact orientation was approximately 21° off vertical. As shown, as the friction parameter is decreased, the finite element deformation begins to match that of the test canister. Figure 4-2 shows the proposed friction parameter as a function of impact angle. Note that as the impact angle approaches 90° off center, the friction parameter approaches unity. For any angle greater than 70°, the friction parameter can take any value. On the other hand, as the impact angle approaches zero, the friction parameter also approaches zero (Figure 4-2) (i.e., the friction parameter can take any value). These results presented in Snow, et al. (2001) were considered preliminary.

4.3 Material Strain-Rate Effects

A key requirement in the finite element analysis is accurate stress–strain data, which is necessary to model failure of the material. Because the problem of canister drop is a dynamic (i.e., high strain-rate) problem, the strain-rate dependence of the material behavior is especially important. While stress–strain data from static testing is readily available, testing at a number of strain rates is required for accurately modeling the dynamic response. In addition, because the inelastic deformations may be large, the finite element analysis requires measuring the material response in terms of true stress and strain.

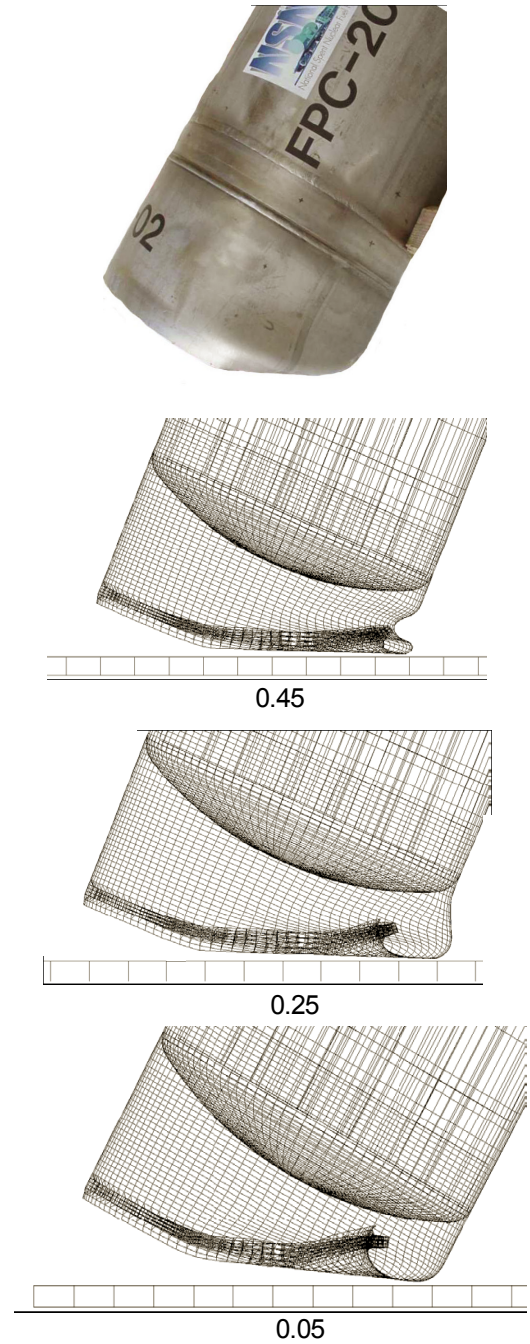

Figure 4-1. Effect of Coefficient of Friction on Deformation Behavior (Snow, et al., 2001, Used With Permission of the American Society of Mechanical Engineers International, Copyright 2001)

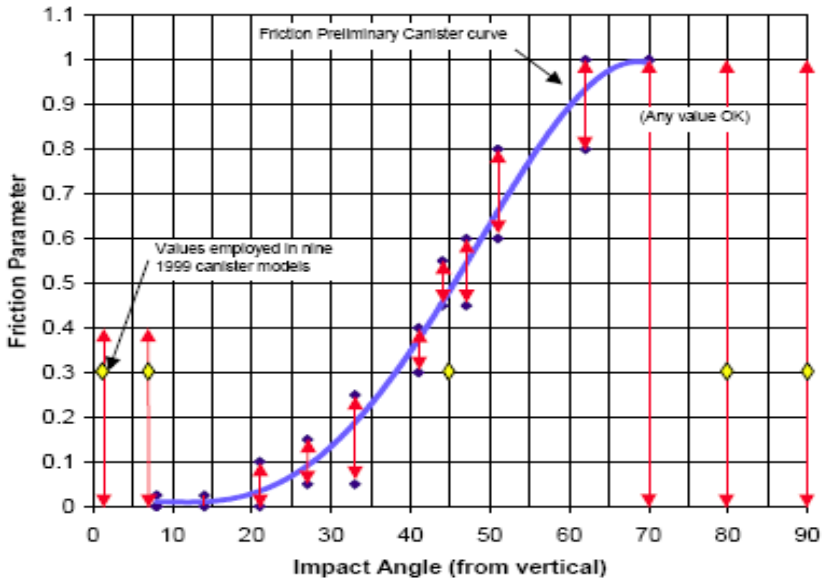

Figure 4-2. Friction Parameter Versus Impact Angle (Snow, et al., 2001, Used With Permission of the American Society of Mechanical Engineers International, Copyright 2001)

In support of the drop analysis simulations, Idaho National Laboratory undertook a test program to collect strain-rate-dependent data (Snow, et al., 2004; Blandford, et al., 2005; Morton, et al., 2006). As part of this effort, Idaho National Laboratory developed an impact testing machine (Snow, et al., 2004), which was used to determine the high strain-rate testing of the 304L and 316L stainless steel materials used in the DOE standardized canister.

Previously, the static true stress–strain curves were adjusted by assuming that the higher strain-rate curves could be adjusted by 10 to 20 percent and that the uniform elongation was equivalent to the amount of plastic strain (Snow, et al., 2000). Figure 4-3(a,b) shows the room temperature static engineering stress–strain response for 304L and 316L stainless steel, respectively. The designations 09T9 and 29B1 refer to the heats (mill runs) the specimens were manufactured from. Figure 4-3(a,b) has true strains at the onset of necking of 0.418 and 0.398, respectively.

Two strain rates of 25/second and 50/second were chosen for this investigation. These high strain-rate curves were determined using the deformation energy (i.e., the energy required to deform a material to a target strain level) of the true stress–strain curve as compared to the amount of energy dissipated from the actual high strain-rate test (Blandford, et al., 2005). A critical assumption in this approach was that the shape of the high strain rate and static true stress–strain curves are similar. Based on a literature review, Blandford, et al. (2005) stated that the elevated strain-rate tests generally have a similar shape. As a result, the high strain-rate curve can be obtained by using either a factored (multiplication of each point by a

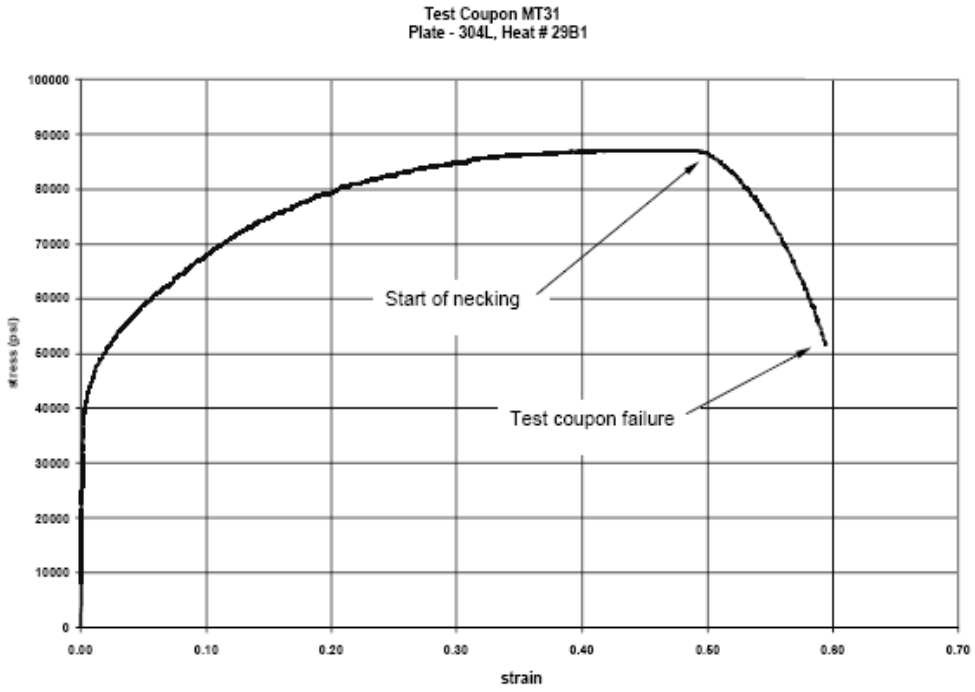

(a)

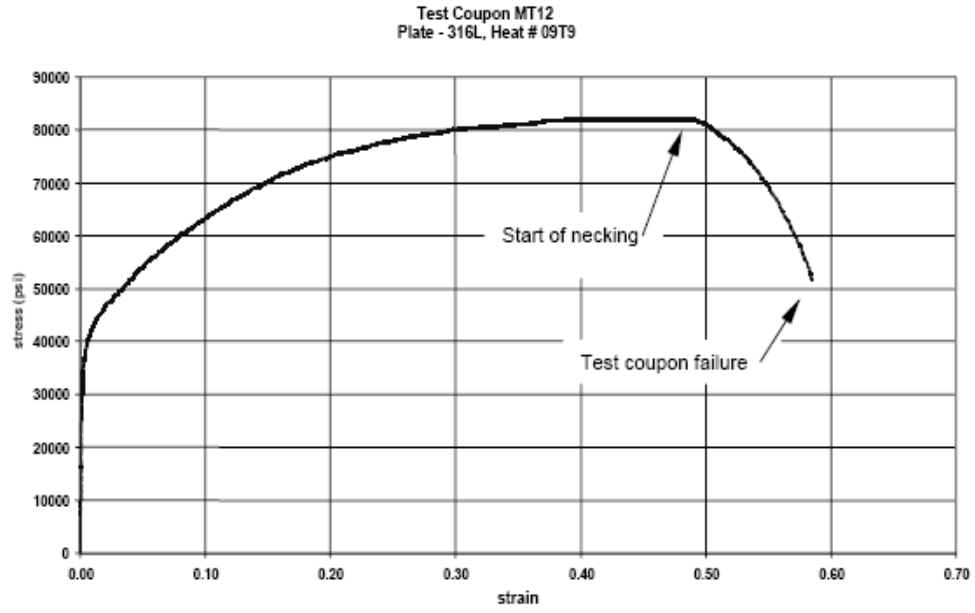

(b)

Figure 4-3. Static Engineering Stress–Strain Curves for 304L and 316L Stainless Steel (Blandford, et al., 2005, Used With Permission of the American Society of Mechanical Engineers, Copyright 2005)

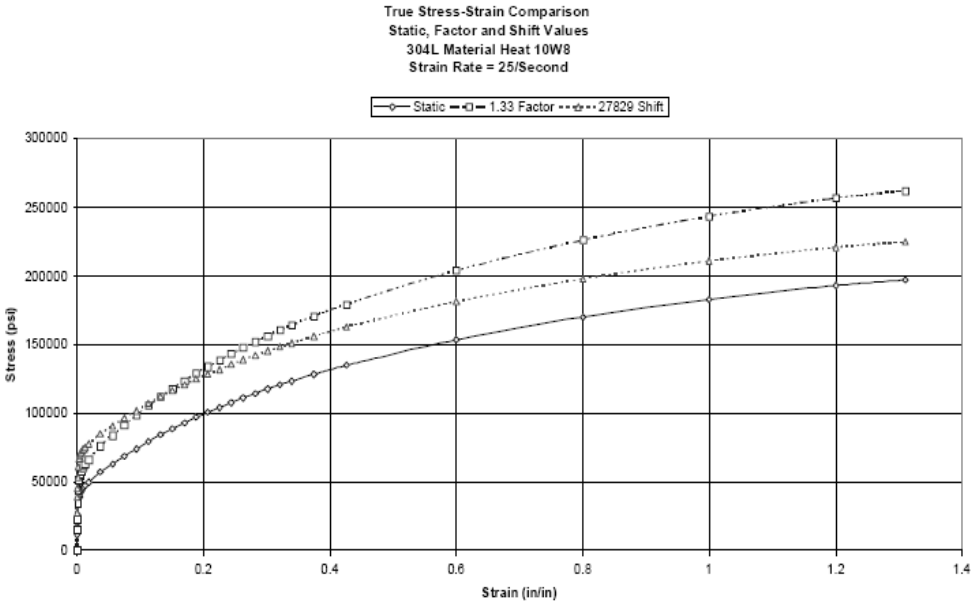

(a)

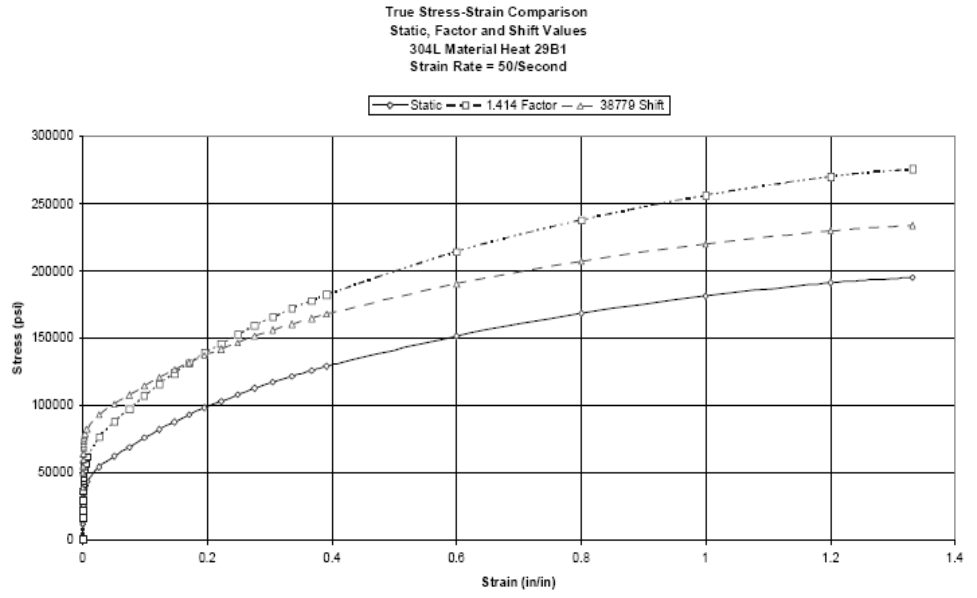

(b)

Figure 4-4. True Stress–True Strain for (a) 25/Second and (b) 50/Second Tests for 304L Stainless Steel (Blandford, et al., 2005, Used With Permission of the American Society of Mechanical Engineers, Copyright 2005)

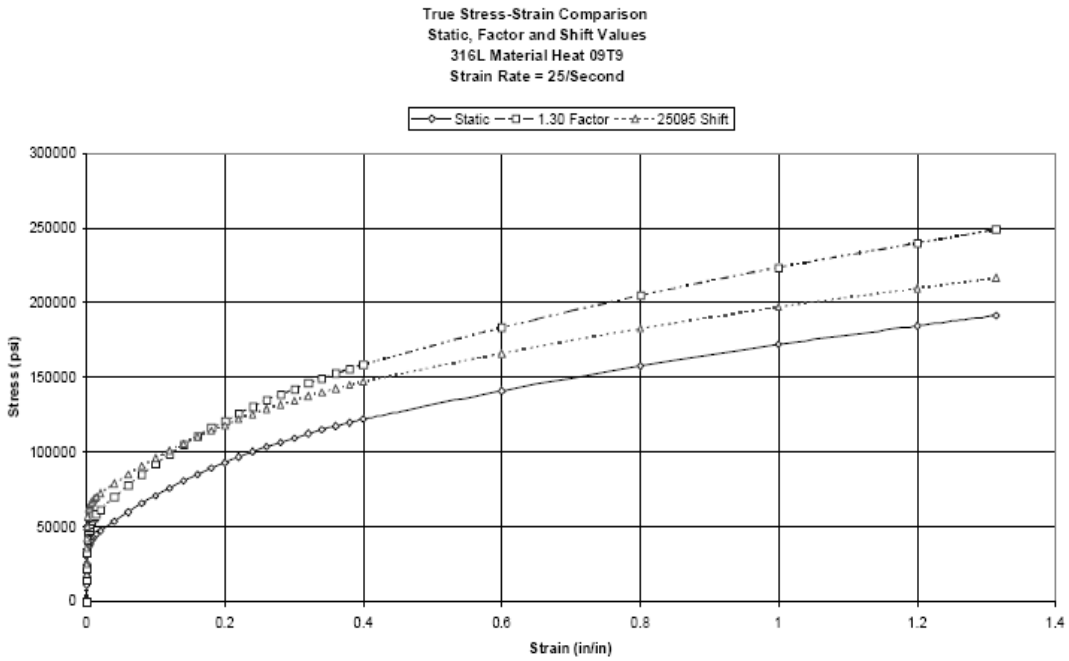

Figure 4-5. True Stress–True Strain for 316L Stainless Steel at 25/Second (Blandford, et al., 2005, Used With Permission of the American Society of Mechanical Engineers, Copyright 2005)

constant) or shifted (addition of a constant to each point) method. The factored and shifted methods produced the curves shown in Figures 4-4(a,b) and 4-5. Preliminary data showed that there is a 25-percent increase in material strength for a strain rate of 25/second and a 30-percent increase in material strength at a strain rate of 50/second for the 304L stainless steel material (Blandford, et al., 2005) over the static true stress–strain curves.

Figure 4-6 compares 304L and 316L stainless steel for a strain rate of 25/second. The difference between the two curves is approximately 5 percent (Blandford, et al., 2005). Unfortunately, it is difficult to ascertain whether these results are actual material behavior or this apparent difference may have been affected by the fact that each specimen came from different mill runs (Blandford, et al., 2005).

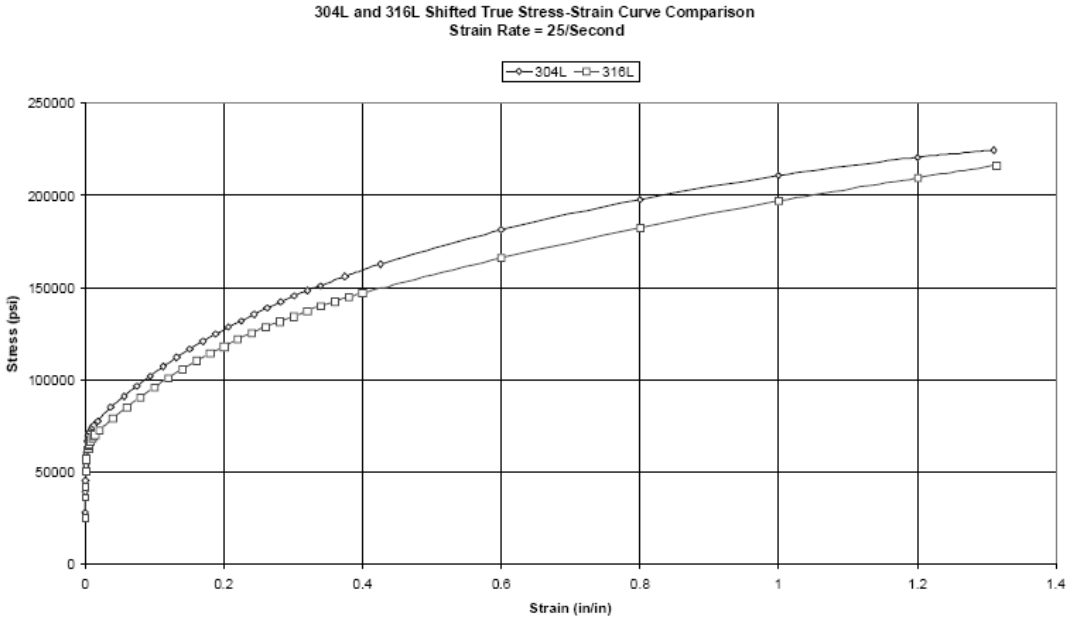

Figure 4-6. True Stress–True Strain Comparison for 304L and 316L Stainless Steel at a Strain Rate of 25/Second (Blandford, et al., 2005, Used With Permission of the American Society of Mechanical Engineers, Copyright 2005)

5 STRUCTURAL EVALUATION OF IDAHO SPENT FUEL PROJECT CANISTERS

As presented in Chapter 3, the National Spent Nuclear Fuel Program began developing and testing standardized spent nuclear fuel canisters in 1999, with 457- and 610-mm [18- and 24-in] standardized designs being proposed at that time (Morton, et al., 1999; Snow, et al., 1999). Subsequently, full-scale testing was performed on the 457-mm [18-in] standardized canisters to evaluate their structural robustness when subject to a drop (Snow, et al., 2000). Testing results showed that the canister design performed as expected with the canister body maintaining its structural integrity with respect to containment. Full-scale testing demonstrated that the canisters would remain leak-free when subjected to a helium test. At that time, the selection of the 457-mm [18-in] canister was based on the idea that it would be the only one used at DOE sites. This chapter discusses modified spent fuel canisters and presents results from preliminary finite element analyses of 457- and 610-mm [18- and 24-in]-diameter Idaho Spent Fuel Project canisters (Snow and Morton, 2003). These standardized canisters were first used at the Idaho Spent Fuel Project storage facility designed and built by the Foster Wheeler Environmental Corporation. All of these canisters have modifications that make them distinct from the standardized canister, and these modified canister designs will be referred to as the Idaho Spent Fuel Project canisters.

5.1 The Idaho Spent Fuel Project Canister

In 2002, the Foster Wheeler Environmental Corporation selected both 457- and 610-mm [18-and 24-in]-diameter canisters for use at the Idaho Spent Fuel Project facility. Seven configurations were proposed: four for the 457-mm [18-in]-diameter canister and three for the 610-mm [24-in]-diameter canister. The 457-mm [18-in]-diameter canister had the following configurations: a canister length of 4.6 m [15 ft] with three different internal component arrangements and a canister length of 3.05 m [10 ft] with one internal component arrangement. The 610-mm [24-in]-diameter canister configurations had a length of 4.6 m [15 ft] with three internal component arrangements.

The most notable design changes to Idaho Spent Fuel Project canisters when compared to the standardized canisters are (i) machining is required to match the thickness of the head and canister body as opposed to the standardized canister, which uses thinner wall thicknesses; (ii) there is a retaining ring that is welded in place to hold the interior impact plates as opposed to the standardized canister, which only used the internal components to hold them in place; (iii) the standardized canister uses an internal sleeve to prevent sharp internal components from contacting the canister body (which could result in localized stresses and strains) and to provide extra protection in drop events (the Idaho Spent Fuel Project canister does not have an internal sleeve); and (iv) the canisters have a single vent plug on the top head, whereas the standardized canisters had a small threaded plug on the top or bottom of each head (Snow and Morton, 2003).

5.2 Fabrication Details and Finite Element Models

For the 457-mm [18-in] canister design, (i) the body and skirts are made of 9.53-mm [0.375-in] stainless steel (SA–312 type 316L SST); (ii) the canister heads are standard American Society of Mechanical Engineers flanged and dished with a 51-mm [2-in] flange having a 15.9-mm [0.625-in] thickness of SA–240 type 316L SST stainless steel, which is machined to match the body thickness once the skirts are attached; and (iii) interior impact plates have a 51-mm [2-in] thickness of SA–240 type 316L stainless steel, a flat interior side, and a concave side, which matches the dished head that is held in place by a retaining ring welded in place (Figure 5-1) (Snow and Morton, 2003). For the 610-mm [24-in] canister design, (i) the body and skirts are made of 12.7-mm [0.5-in]-thick SA–312 type 316L SST stainless steel; (ii) the canister heads are American Society of Mechanical Engineers standard flanged and dished with a 51-mm [2-in] flange of 19.1-mm [7-in] thickness of SA–240 type 316L SST stainless steel; and (iii) there are interior impact plates with a 51-mm [2-in] thickness of SA–240 type 316L SST stainless steel with a welded retaining ring having similar geometry as the 457-mm [18-in] canister (Snow and Morton, 2003).

Finite element models having different weights, lengths, and internal configurations were constructed for the 457- and 610-mm [18- and 24-in]-diameter canisters. The model of a 457-mm [18-in] diameter, 4.6-m [15-ft]-long canister was created with the internal component weights adjusted such that the total canister weight was 2,721 kg [6,000 lb] (maximum design weight)—the same weight as the 457-mm [18-in]-diameter standardized canister. The canister model was then analyzed for a simulated drop height of 9 m [30 ft] at orientations matching those used in the full-scale tests of the standardized canister. With equal weights and orientations, direct comparisons between the standardized and Idaho Spent Fuel Project canister can be made. For completeness, one additional 457-mm [18-in] canister was also modeled having a total weight of 1,855 kg [4,090 lb], which corresponds to the actual maximum Idaho Spent Fuel Project canister weight. A finite element model representing a 610-mm [24-in] diameter, 4.6-m [15-ft]-long canister was made with a weight of 4,535 kg [10,000 lb] (maximum design weight) and 3,755 kg [8,280 lb] (lowest canister weight) (Snow and Morton, 2003). For this configuration, a drop height of 9 m [30 ft] was used, with similar orientations as used for the 457-mm [18-in]-diameter canister.

5.3 Finite Element Analysis Results

The accuracy of the finite element analyses in duplicating the deformation behavior of full-scale tests of the standardized canister has been previously established (Snow, et al., 1999); thus, finite element analyses were performed to evaluate the structural behavior of the Idaho Spent Fuel Project canisters. Analysis output in the form of maximum equivalent plastic true strains were examined and compared to those obtained from the finite element analysis of the standardized canisters. The results from these finite element analyses are summarized in this section.

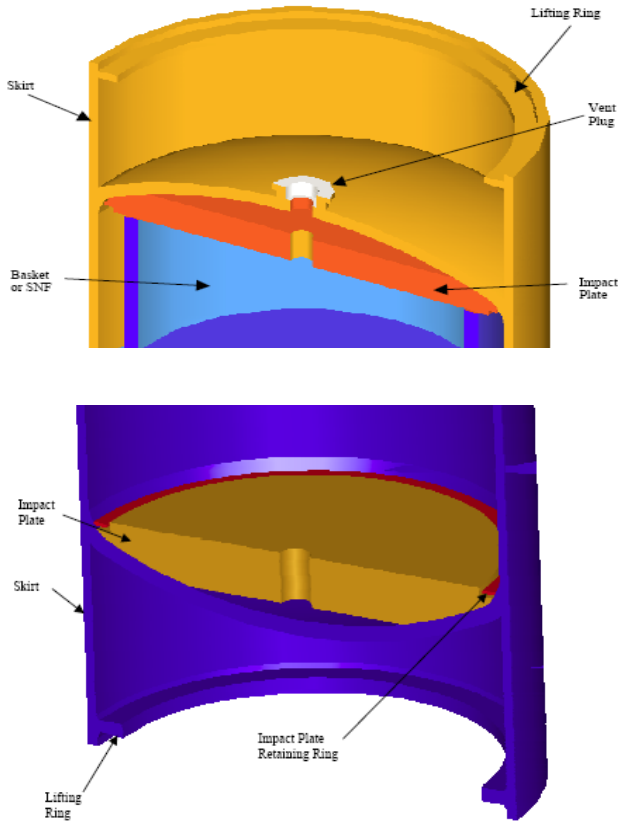

Figure 5-1. Idaho Spent Fuel Project Canister Details (Snow and Morton, 2003)

5.3.1 The 457-mm [18-in] Idaho Spent Fuel Project Canister

Because the retaining ring is welded to the canister body (Figure 5-1), straining in the canister head is expected in the case of a vertical drop. However, note that the Idaho Spent Fuel Project canister has a dish and flange head thickness larger than that of the standardized canister; therefore, these maximum plastic strains are predicted to be low (Snow and Morton, 2003). In the Idaho Spent Fuel Project canisters, the internal components consist of baskets, which are made of thick plates and tubes [e.g., simulated Shippingport Reflector Tubes (recall Figure 3-1, Section 3)]. Because these components do not have sharp edges, an internal sleeve is not needed. Note, however, that the internals making contact with the canister wall caused straining, although these strains were not the largest the canister experienced (Snow and Morton, 2003).

Table 5-1 presents the maximum equivalent plastic true strains for the 2,721 kg [6,000 lb], 457-mm [18-in]-diameter canister at a drop height of 9 m [30 ft]. The values in brackets are strains obtained from the finite element analysis of the standardized DOE spent nuclear fuel canister by Snow, et al. (1999).

Table 5-1. Maximum Equivalent Plastic True Strains for 457-mm [18-in]-Diameter, 4.6-mm [15-ft]-Long, 2,721 kg [6,000 lb] Idaho Spent Fuel Project Canisters*

Drop Height Feet	Angle From Vertical (Degrees)	Maximum Equivalent Plastic True Strain (%)														
		Lower Head			Lower Skirt			Upper Head			Upper Skirt			Body		
		out†	mid†	in†	out†	mid†	in†	out†	mid†	in†	out†	mid†	in†	out†	mid†	in†
30	½	3 [7]	1 [3]	2 [6]	61 [91]	21 [17]	53 [75]	5	0	5	—‖	—‖	—‖	—‖	—‖	—‖
30	6	0.7 [9]#	0.1 [3]	0.3 [10]	88 [107]	23 [21]	58 [94]	0.5	0	0.5	—	—	—	—	—	—
30	45	22 [33]	10 [9]	16 [36]	59 [52]	31 [33]	106 [84]	—	—	—	—	—	—	2	1	1
30‡ (33)	80	33 (34)¶	17 (17)	29 (30)	31 (33)	18 (19)	25 (26)	48 (48) [57]	24 (24) [19]	25 (25) [42]	15 (15) [24]	9 (9) [20]	9 (9) [19]	6 (7)	2 (2)	5 (6)
30§ (34)	90	31 (32)	18 (19)	18 (19)	11 (12)	6 (6)	7 (7)	30 (32) [40]	17 (18) [15]	21 (23) [26]	7 (8) [10]	4 (4) [10}	5 (5) [10]	5 (6)	2 (2)	4 (4)

Table 5-1. Maximum Equivalent Plastic True Strains for 457-mm [18-in]-Diameter, 4.6-mm [15-ft]-Long, 2,721 kg [6,000 lb] Idaho Spent Fuel Project Canisters* (continued)

Drop Height Feet	Angle From Vertical (Degrees)	Maximum Equivalent Plastic True Strain (%)														
		Lower Head			Lower Skirt			Upper Head			Upper Skirt			Body		
		out†	mid†	in†	out†	mid†	in†	out†	mid†	in†	out†	mid†	in†	out†	mid†	in†
23	0	1	0.2	1	35	18	52	5	0	5	—	—	—	—	—	—
repository		{10}**	{3}	{6}	{40}	{16}	{48}									
2§	80	2	1	2	9	5	4	20	11	8	5	2	3	4	1	4
(2.25)		(3)	(1)	(3)	(9)	(5)	(4)	(20)	(12)	(8)	(6)	(3)	(3)	(4)	(1)	(4)
repository					{6}	{5}	{9}	{24}	{11}	{13}						

*Snow, S.D. and D.K. Morton. "Analytical Evaluation of the Idaho Spent Fuel Project Canister for Accidental Drop Events." EDF–NSFNF–027. Rev. 0. New York City, New York: ASME. 2003.
†out = outside surface of component, mid = middle surface of component, in = inside surface of component.
‡This model experienced about 9% artificial energy. Artificial energy is drop energy used to prevent finite element numerical instabilities.
‖—Denotes that strains in these components are either zero or insignificant/not of interest.
§These models experienced about 13% artificial energy.
¶The results shown in parentheses are for a higher drop that accounts for this lost drop energy. All other models experienced an artificial energy below 5%, which is considered acceptable as is.
#Numbers reported in square brackets [ ] are those that were listed in Table 25 in Morton, et al., 2006.
**Numbers reported in braces { } are those that were listed in the 2003 standardized canister analysis, in Blandford, R.K. "Structural Response Evaluation of the 24-Inch Diameter DOE Standardized Spent Nuclear Fuel Canister." EDF–NSNF–026. Idaho Falls, Idaho: Idaho National Engineering and Environmental Laboratory. Table 7. 2003.

The values in Table 5-1 enclosed by parentheses are the strain values after the finite element explicit solution is rerun using a slightly higher drop height necessary to reduce artificial strain energy. The artificial energy is associated with additional stiffness used to control numerical instabilities such as hour glassing of the elements (Blandford, 2003; ABAQUS, Inc., 2006). All comparisons are made using the values in parentheses.

For the 0.5 and 6° off-vertical drop orientations, the 457-mm [18-in] Idaho Spent Fuel Project canister experienced lower strains in the lower head as well as the skirt compared to those of the 457-mm [18-in] standardized container. Snow and Morton (2003) did note the impact plate bending the welded retaining ring caused some straining in the upper head. These upper head strains were not present in the standardized canister, because it does not have the welded impact plate retaining ring. The 5 percent upper head strains for the 0.5° drop are comparable to those of the lower head and decrease for the 6° orientation. The upper head strains for the 45° orientation are small enough not to be reported (Snow and Morton, 2003). For the lower head of the Idaho Spent Fuel Project canister, the plastic strains are less than those of the standardized canister. This is because the heads of the Idaho Spent Fuel Project canister are thicker than the heads of the standardized canister. However, there was a 1 percent increase in plastic strain at the midsurface for the 45° off-vertical canister orientation. For the 80 and 90° orientations, the upper head strains are higher than the lower head strains. For the case of 80° off-vertical, the skirts have become less effective in absorbing the impact energy; therefore, the upper head will maintain a vertical velocity such that the upper head slaps down with the greatest energy (Snow and Morton, 2003; Snow, et al., 1999). For the case of 80° off-vertical, there was an increase of 5 percent equivalent plastic true strain at the midsurface of the upper head. For the 90° off vertical orientation, there was an increase of 3 percent plastic strain in the midsurface of the upper head. This result was considered significant because it exceeds the predicted strain from the corresponding analysis of the standardized canister by Snow, et al. (2000). The 80° off vertical orientation does produce the largest plastic strains in the containment components and is considered the controlling case. In general, the strains in the skirt component are not considered, because the skirts' function is to absorb the impact energy.

Table 5-2 lists the maximum equivalent plastic true strains of the 1,855-kg [4,090-lb] Idaho Spent Fuel Project canister (maximum actual canister weight) for the 6 and 80° off-vertical drop orientations. The maximum plastic strains in the lower head were the same or lower than those listed in Table 5-1 for the 2,721-kg [6,000-lb] Idaho Spent Fuel Project canister. On the other hand, the upper head maximum strains were slightly higher, although the increase was not more than 3 percent for the 2,721-kg [6,000-lb] canister. Snow and Morton (2003) attempt to explain this by noting that an impact analysis is highly nonlinear; the structural response is affected by factors such as drop height, canister weight, and impact angle; and more energy may be absorbed for a given drop scenario resulting in different maximum strains.

5.3.2 The 610-mm [24-in] Idaho Spent Fuel Project Canister

The Idaho Spent Fuel Project 610-mm [24-in]-diameter, 4.6-m [15-ft]-long canister was analyzed for 5 different orientations: vertical, the center of gravity located in line with the impact corner

Table 5-2. Maximum Equivalent Plastic True Strains in Foster Wheeler 457-mm [18-in]-Diameter, 4.6-m [15-ft]-Long Canisters, 1,860 kg [4,090 lb] Maximum Actual Weight*

Drop Height [Feet]	Angle From Vertical (Degrees)	Maximum Equivalent Plastic True Strain (%)														
		Lower Head			Lower Skirt			Upper Head			Upper Skirt			Body		
		out†	mid†	in†	out†	mid†	in†	out†	mid†	in†	out†	mid†	in†	out†	mid†	in†
30	6	0.4	0	0.2	57	19	51	0.8	0	0.8	—‡	—‡	—‡	—‡	—‡	—‡
30§ (33)	80	33 (35)	17 (17)	27 (28)	29 (31)	17 (18)	24 (24)	51 (50)	25 (24)	25 (24)	17 (15)	11 (9)	19 (9)	8 (8)	2 (2)	7 (6)

*Snow, S.D. and D.K. Morton. "Analytical Evaluation of the Idaho Spent Fuel Project Canister for Accidental Drop Events." EDF–NSFNF–027. Rev. 0. New York City, New York: ASME. 2003.

†out = outside surface of component, mid = middle surface of component, in = inside surface of component.

‡—Denotes that strains in these components are either zero or insignificant/not of interest.

§This model experienced a 9% artificial energy. Artificial energy is drop energy used to prevent finite element numerical instabilities. The results shown in parentheses are for a higher drop that accounts for this lost drop energy. All other models experienced an artificial energy that was below 5%, which is considered acceptable as is.

(7°), and 45, 70, and 90° off vertical at a drop height of 9 m [30 ft]. For all of these orientations, the canister was modeled with a maximum design weight of 4,535 kg [10,000 lb]. The results in the form of the maximum equivalent plastic true strains are shown in Table 5-3.

The 7 and 70° off-vertical orientations were also analyzed for a minimum load weight of 3,755 kg [8,280 lb] (Table 5-4). For the 0 and 7° orientations, the Idaho Spent Fuel Project canister produces strain in the upper head with a maximum strain of 5 percent at the outer surface. These upper head strains are generally due to the presence of the welded retaining ring. Also note for the 7 and 70° off vertical, the lower head (where the primary impact takes place) strains are lower than the corresponding strains in the standardized canister. For the 45° off-vertical orientation, the lower head midplane (10 percent) and inner surface (22 percent) strains are larger than those of the standardized canister. For the 70° off-vertical orientation in the lower head, there is an increase of 13 percent (outside surface), 1 percent (midsurface), and 7 percent (inside surface) plastic strains. In addition, the upper head has increased surface strains: 9 percent (outside) and 4 percent (midsurface). These values are considered significant in that they are larger than those of the standardized canister (Snow and Morton, 2003). The 90° off-vertical (horizontal) drop resulted in a 4-percent increase in strain on the outside surface of the lower head and a 3-percent increase at the midsurface of the lower head. Strains in the upper head are comparable. However, the 70° off-vertical orientation is the most critical due to the slapdown effect, and this orientation also produces significant plastic strains in containment boundary (denoted as “body” in Table 5-3). Note that in all previous cases, any increase in maximum strain in the skirt is not considered, because the purpose of the skirt is to plastically deform and absorb the impact energy; the containment pressure boundary of the canister is not affected.

Table 5-4 lists the maximum equivalent plastic true strains of the 3,755-kg [8,280-lb] Idaho Spent Fuel Project canister (maximum actual canister weight) for the 7 and 70° off-vertical drop orientations. The maximum plastic strains in all canister components (i.e., lower and upper heads and body) are the same or lower than those listed in Table 5-3 for the 4,535 kg [10,000 lb] Idaho Spent Fuel Project canister.

5.4 Full-Scale Tests of 610-mm [24-in]-Diameter Modified Canisters

Based upon the preliminary finite element analyses of Snow and Morton (2003), full-scale testing of 610-mm [24-in]-diameter canisters was performed (Snow, et al., 2005) at Sandia National Laboratories. The Sandia test facility contained a 51-mm [2-in]-thick steel plate bolted to a reinforced concrete block that had an approximate weight of 209,523 kg [462,000 lb] and was considered to be an unyielding surface. The tests consisted of two 610-mm [24-in]-diameter, 4.6-m [15-ft]-long Idaho Spent Fuel Project canisters. These modified spent fuel canisters were dropped from a height of 9 m [30 ft] onto the unyielding surface with orientations of 45 and 70° off vertical such that slapdown would occur. The test weight of each canister was approximately 4,535 kg [10,000 lb]. The canister internal components represent an actual design of an Idaho Spent Fuel Project canister that would contain a Shippingport reflector rod. The internal components consist of a 610-mm [24-in]-long and 508-mm [20-in]-diameter internal

Table 5-3. Maximum Equivalent Plastic True Strains in Foster Wheeler 610-mm [24-in]-Diameter, 4.6-m [15-ft]-Long Canisters, 4,545 kg [10,000 lb] Maximum Design Weight*

Drop Height [Feet]	Angle From Vertical (Degrees)	Maximum Equivalent Plastic True Strain (%)														
		Lower Head			Lower Skirt			Upper Head			Upper Skirt			Body		
		out†	mid†	in†	out†	mid†	in†	out†	mid†	in†	out†	mid†	in†	out†	mid†	in†
30	—	3 {6}‡	0.3 {0.6}	2 {4}	41 {45}	18 {16}	56 {54}	5	0.4	2	—§	—	—	—	—	—
30	7	0.2 {0.7}	0 {0.1}	0.1 {0.6}	86 {76}	19 {31}	56 {60}	2	0	2	—	—	—	—	—	—
30	45	18 {18}	10 {9}	22 {15}	57 {95}	30 {33}	106 {117}	1	0	1	—	—	—	3	5	8
30 (34)‖	70	47 (49) {36}	18 (18) {17}	41 (42) {35}	51 (52) {74}	31 (30) {41}	68 (67) {58}	58 (66) {57}	25 (27) {23}	27 (29) {48}	20 (21) {30}	11 (13) {15}	12 (13) {15}	10 (10)	4 (5)	9 (10)
30	90	38 {34}	19 {16}	17 {22}	11 {7}	6 {3}	7 {5}	36	18	16	12	5	8	8	2	6
23 repository	0	3 {6}	0.2 {0.5}	2 {4}	38 {44}	16 {14}	53 {53}	4	0.4	3	—	—	—	—	—	—
2 repository	70	5 {16}	3 {6}	2 {12}	8 {24}	4 {23}	5 {23}	25 {23}	14 {15}	10 {16}	6 {22}	2 {21}	4 {21}	33	1	3

*Snow, S.D. and D.K. Morton. "Analytical Evaluation of the Idaho Spent Fuel Project Canister for Accidental Drop Events." EDF–NSFNF–027. Rev. 0. New York City, New York: ASME. 2003.

†out = outside surface of component, mid = middle surface of component, in = inside surface of component.

‡Numbers reported in braces { } are those that were listed in the 2003 standardized canister analysis, Table 6 in Blandford, R.K. "Structural Response Evaluation of the 24-Inch Diameter DOE Standardized Spent Nuclear Fuel Canister." EDF–NSNF–026. Idaho Falls, Idaho: Idaho National Engineering and Environmental Laboratory. 2003.

§—Denotes that strains in these components are either zero or insignificant/not of interest.

‖This model experienced a 14% artificial energy. Artificial energy is drop energy used to prevent finite element numerical instabilities. The results shown in parentheses are for a higher drop that accounts for this lost drop energy. All other models experienced an artificial energy that was below 5%, which is considered acceptable as is.

Table 5-4. Maximum Equivalent Plastic True Strains in Foster Wheeler 610-mm [24-in]-Diameter, 4.6-m [15-ft]-Long Canisters, 3,755 kg (8,280 lb) Maximum Actual Weight*

Drop Deed [Feet]	Angle From Vertical (Degrees)	Maximum Equivalent Plastic True Strain (%)														
		Lower Head			Lower Skirt			Upper Head			Upper Skirt			Body		
		out†	mid†	in†	out†	mid†	in†	out†	mid†	in†	out†	mid†	in†	out†	mid†	in†
30	7	0.1	0	0.1	59	18	57	1	0	1	—‡	—‡	—‡	—‡	—‡	—‡
30§ (33)	70	45 (46)	18 (18)	40 (41)	49 (51)	30 (30)	67 (67)	57 (59)	25 (25)	27 (28)	20 (19)	11 (12)	13 (13)	9 (10)	4 (5)	9 (9)

*Snow, S.D. and D.K. Morton. "Analytical Evaluation of the Idaho Spent Fuel Project Canister for Accidental Drop Events." EDF–NSFNF–027. Rev. 0. New York City, New York: ASME. 2003.

† out = outside surface of component, mid = middle surface of component, in = inside surface of component.

‡—Denotes that strains in these components are either zero or insignificant/not of interest.

§This model experienced a 11% artificial energy. Artificial energy is drop energy used to prevent finite element numerical instabilities. The results shown in parentheses are for a higher drop that accounts for this lost drop energy. All other models experienced an artificial energy that was below 5%, which is considered acceptable as is.

bottom spacer made from Schedule 60 pipe with a 25.4-mm [1-in]-thick plate welded to the top and bottom. A typical spoked-wheel basket was constructed from Schedule 100 pipe and a 0.5-inch plate. The basket was filled with 210 pieces of #8 rebar each having a length of 2,946 mm [116 in], and the shield plug was made from a 146-mm [5.75-in]-thick, 581-mm [22.875-in]-diameter bar.

As was the case for the 457-mm [18-in] standardized canister (Chapter 3), the 610-mm [24-in] canister's plastic deformation occurred primarily in the skirt, as intended, for both cases—45 and 70° off vertical. Figure 5-2 shows the deformation for the 45° case. Note that the corresponding finite element results accurately model the canister's deformed shape. Snow, et al. (2005) presented very limited strain data obtained from the finite element analysis. A maximum equivalent plastic surface true strain of 26.4 percent and 9.3-percent strain at the midsurface occurred in the head of the canister. Neither of these strains was greater than 48 percent maximum equivalent plastic true strain, which was a very conservative value set by Snow, et al. (2000) (Section 3.5.1). Results for the 70° off-vertical case exhibited less deformation in the skirt due to the increased off-vertical impact angle. Because the canister orientation was closer to horizontal, minor deformations occurred over the length of the canister body (Snow, et al., 2005). The maximum equivalent plastic surface true strain from the finite element analysis was 51.9 percent with a midsurface true strain of 14.9 percent in the canister head. In both cases, because the midsurface strain is less than the 48 percent failure strain (true strain), no failure would occur through the thickness; therefore, rupture of the containment boundary is not predicted (Snow, et al., 2005).

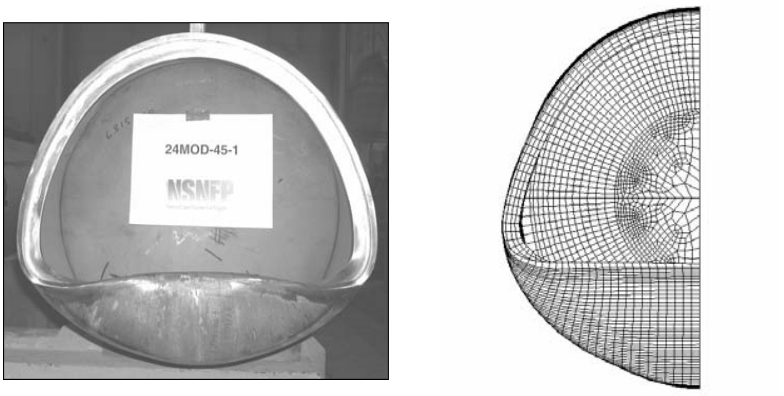

Figure 5-2. Modified Spent Nuclear Fuel Canister, 610-mm [24-in] Impact Angle of 45° (Snow, et al., 2005, Used With Permission of the American Society of Mechanical Engineers, Copyright 2005)

6 STRUCTURAL EVALUATION OF A MULTI-CANISTER OVERPACK

Multi-canister overpacks were developed as part of the Hanford Spent Nuclear Fuel Project. The multi-canister overpacks facilitate the removal, processing, and storage of deteriorating spent nuclear fuel currently stored in the Hanford site's K-East and K-West Basins. Their purpose was to contain, confine, and maintain spent nuclear fuel (Goldmann, 2000a). The multi-canister overpack is a vessel with internal components that maintain structural integrity while providing criticality control and spent nuclear fuel drying capability (Goldmann, 2000a,b; Garvin, 2001). In the following sections, the specific design of the multi-canister overpack, associated finite element analysis, and comparison with full-scale tests are discussed.

6.1 The Multi-Canister Overpack

The multi-canister overpack is a 304L stainless steel cylindrical vessel approximately 610 mm [24 in] in diameter and 4,216 mm [166 in] long, and the shell is fabricated from 12.7-mm [0.5-in]-thick stainless steel material. The bottom is forged from stainless steel with a diameter of 610 mm [24 in] and a thickness of 51 mm [2 in] {except at the center, which is 28.7 mm [1.13 in] thick}; this allows water to flow to the central process tube for removal. The bottom is welded to the vessel body to provide a permanent sealed closure. The multi-canister overpack is loaded through its top end, which is covered by a shield plug with four access ports and a locking ring. A cover plate is then welded on the top to seal the multi-canister overpack (Figure 6-1). The multi-canister overpack vessel must satisfy American Society of Mechanical Engineers Boiler and Pressure Vessel Code, Section III, Subsection NB (Garvin, 2001). The multi-canister overpack is designed so a total of five or six fuel baskets can be stacked inside. The spent fuel is placed in the baskets while underwater in the K-Basins. The baskets are filled with fuel and scrap pieces and then loaded into the multi-canister overpack. After the baskets are loaded into the multi-canister overpack, the shield plug with the central process tube is placed into the open end of the multi-canister overpack, shielding workers when the transfer cask, containing the multi-canister overpack, is lifted from the pool. The cask and the multi-canister overpacks are then taken to the dewatering and drying operations. During these operations, the fuel will not be removed from the protection of the multi-canister overpack. Covers for the process ports may be installed or removed as needed per operating procedures (Garvin, 2001; Goldmann, 2000a). The dry weight of each multi-canister overpack is 8,281 kg [18,260 lb] with six Mark 1A baskets and 9,106 kg [20,080 lb] with five Mark IV baskets (Snow, 2003; Garvin, 2001). Each basket configuration is detailed in Figure 6-2.

6.2 Finite Element Analysis and Full-Scale Tests

Rains (1999) uses finite element analysis to study the scenario in which the multi-canister overpack concentrically drops from a multi-canister overpack handling machine into the shipping cask. The multi-canister overpack is dropped from a height of 2.5 m [8.2 ft], concentrically enters the cask, and drops an additional 4 m [12.83 ft] to the cask bottom. Because of the tight fit between the canister and the cask, an air cushion effect develops and the velocity of the multi-canister overpack decreases. In addition to this cushioning effect, the shipping cask itself is supported by an impact absorber. Hollenbeck and Tu (1999) consider eccentric drops of the multi-canister overpack in which it impacts the edge of the storage tube

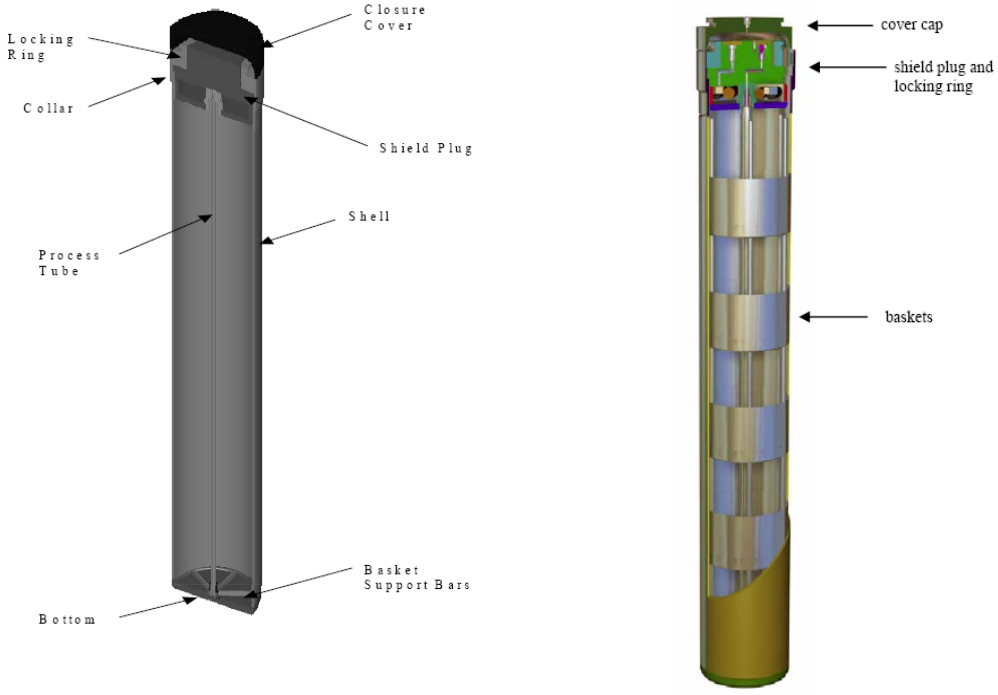

(a) **(b)**

Figure 6-1. Typical Multi-Canister Overpack [(a)Snow, et al., 2005, Used With Permission of the American Society of Mechanical Engineers, Copyright 2005; (b) Morton, et al., 2006, Used With Permission of the American Nuclear Society, Copyright 2006]

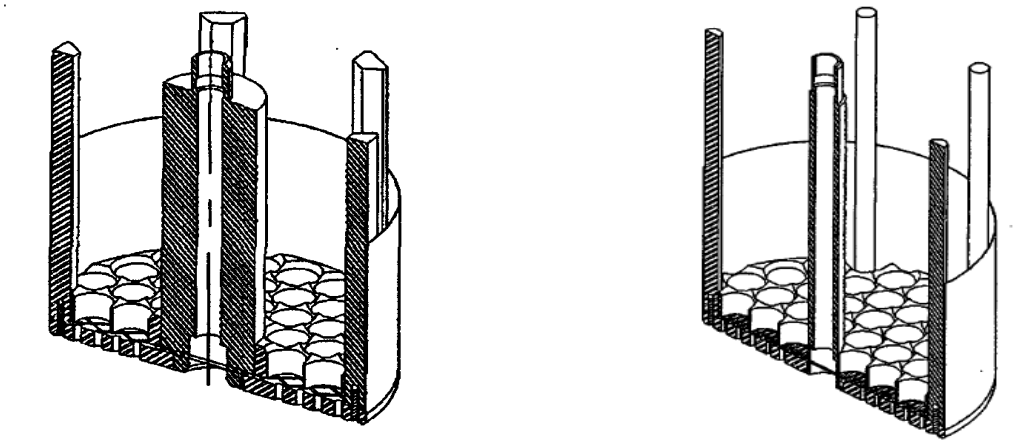

Mark 1A **Mark IV**

Figure 6-2. Mark 1A and Mark IV Multi-Canister Overpack Internal Basket Configurations (Garvin, 2001)

case. Material failure is calculated from a triaxiality factor (Garvin, 2001), which utilizes uniaxial tensile failure data to be generalized to multiaxial stress and strain states.

The concentric drop results Rains (1999) presented show that the drop into the cask produces very large impact reactions on the multi-canister overpack and internals. Plastic strains occur in the bottom of the multi-canister overpack sides, the bottom two baskets' support plates, the outside support posts, and the center support post. These plastic strains are due to a large amount of energy that is absorbed by the multi-canister overpack internals during impact. The maximum equivalent plastic true strain in the bottom of the multi-canister overpack is 2.0 percent. This is below the calculated effective failure strain of 15 percent, which is based on the multiaxial stress state (using the triaxiality factor) and strain rate (Rains, 1999). In the weld where the multi-canister overpack walls and bottom of the canister meet, equivalent plastic strains are approximately 2.1 percent, which is below the calculated effective failure strain of 12.5 percent for the weld material. Therefore, breaching of the multi-canister overpack containment boundary due to through-wall cracking is not expected (Rains, 1999).

For the case of an eccentric drop of the multi-canister overpack onto a standard storage tube (Hollenbeck and Tu, 1999), the maximum equivalent plastic true strain in compression (negative triaxiality factor) is approximately 40 to 45 percent, which occurs on the bottom of the multi-canister overpack near the point of impact. Because compressive failure strain for the base metal is 80 percent, no through-wall cracking is predicted. The maximum predicted equivalent plastic true strain at the multi-canister overpack lower weld is approximately 2 percent, which is below the weld metal failure strain of 10 percent. Note that the maximum tensile principal strain is in a radial direction, which would only lead to possible spalling or flaking of the outer surface rather than through-wall cracking (Hollenbeck and Tu, 1999).

Finite element analyses of 7-m [23-ft] and 0.61-m [2-ft] drop events, as specified in the Waste Acceptance System Requirements Document (DOE, 2002), are discussed in Snow (2004, 2003). The Waste Acceptance System Requirements Document only requires a vertical orientation for the 7-m [23-ft] drop event; however, Snow (2003) believed it would be prudent to also include orientations of 1 and 3° off vertical. The 0.61-m [2-ft] drop was analyzed for the most critical orientation as determined by previous analyses of the standardized canisters.

With regard to a failure criteria, Snow (2003) selected a value of 47 percent as the minimum elongation value considering all of the materials used in the canister (see Table 6-1). Similarly, the minimum fracture strain was taken as 118 percent. The use of these values by Snow (2003) should be considered a very conservative approach.

For the case of the 7-m [23-ft] drop, Table 6-2 shows the equivalent plastic true strains for the drop orientations of vertical and 1 and 3° off-vertical. For a vertical drop (0°), the equivalent plastic strain is 9 percent at the inside surface of the multi-canister overpack bottom, caused by the baskets bearing on the multi-canister overpack bottom, and the largest plastic strain in the

Table 6-1. Multi-Canister Overpack Component and Basket Materials*						
Component	**Yield Strength (σ_y, psi)**	**Ultimate Strength (σ_u, psi)**	**Elongation (%)**	**Area Reduction**	**Average Yield Strength ($\sigma_{y\ ave}$, psi)**	**True Fracture Strain ($\epsilon_{p\ true}$)**
Multi-Canister Overpack Components						
Main Shell SA–240/ SA–312 (304/304L)	41,388 46,067 44,702	88,145 91,401 89,164	59.2 60.9 61.8	70.1 69.4 70.8	44,052	1.207 1.184 1.231
Collar SA–182 (F304/F304L)	43,200 40,700 40,200	86000 82,000 86,000	56.0 60.0 54.0	77.0 79.0 76.0	41,366	1.470 1.561 1.427
Bottom SA–182 (F304/F304L)	35,800 35,100 35,600 40,100	80,800 80,400 80,500 82,900	56.0 63.0 58.0 57.0	75.0 75.0 75.0 73.0	36,650	1.386 1.386 1.386 1.309
Cover SA–182 (F304L)	40,500 47,500	84,500 89,000	62.0 55.0	78.0 75.0	44,000	1.514 1.386
Mark 1A Basket Components						
Base Plate SA–182 (F304/F304L)	44,800 42,800 39,800	86,500 86,000 80,500	57.0 58.0 59.0	78.0 77.0 78.0	42,467	1.514 1.470 1.514
Perimeter Bar SA–479 (304/304L)	64,940 63,440	95,730 96,100	47.1 47.6	75.1 77.4	64,190	1.390 1.487
Center Post SA–479 (304/304L)	41,200 44,000 46,200	89,500 88,500 88,000	57.0 55.0 54.0	75.0 58.0 77.0	43,800	1.386 1.514 1.470
Mark IV Basket Components						
Base Plate A240 (304/304L)	33,252 35,100 34,719	79,969 85,500 83,504	62.5 60.0 62.3	74.9 78.0 73.3	34,357	1.382 1.514 1.470
Perimeter Bar SA–479 (304/304L)	39,200 48,500 55,000 42,200	91,200 95,200 94,000 89,500	54.1 55.3 48.0 48.8	74.6 77.2 74.0 72.0	46,225	1.370 1.478 1.347 1.273
Center Post A511 (304/304L)	33,649 45,282	80,239 84,788	54.8 49.6	Not Available	39,465	Insufficient Data

*Snow, S.D. "Analytical Evaluation of the MCO for Repository—Defined and Other Related Drop Events." EDF-NSNF–029. Rev. 0. New York City, New York: ASME. 2003.

Table 6-2. Maximum Equivalent Plastic True Strains in the Multi-Canister Overpack for 7 m [23 ft] Vertical and Near-Vertical Drop Events*

Multi-Canister Overpack Basket Configuration	Drop Angle From Vertical (°)	Maximum Equivalent Plastic True Strain (%)						
		Bottom at Flange		Main Shell		Collar		Lower Basket
		Outside Surface	Inside Surface	Outside Surface	Inside Surface	Outside Surface	Inside Surface	Maximum Anywhere
Mark 1A	0	4	5†	1	3	1	2	15
	1	18	7	2	13	<0.1	0.1	14
	3	34	13	13	28	0	0	14
Mark IV	0	5	5‡	1	3	1	2	99
	1	20	4	5	14	0.1	0.1	95
	3	35	14	13	29	0	0	93

*Snow, S.D. "Analytical Evaluation of the MCO for Repository—Defined and Other Related Drop Events." EDF-NSNF–029. Rev. 0. New York City, New York: ASME. 2003.
†For this model, the maximum strain of 9% in the bottom occurred under a basket support bar and was due to bearing loads.
‡For this model, the maximum strain of 8% in the bottom occurred under a basket support bar and was due to bearing loads.

other multi-canister overpack components is 4 percent or less. For the 3° off-vertical drop, the maximum plastic strain is 35 percent (Mark IV basket, outside surface of the bottom at the flange), showing that this orientation is the most critical; however, the maximum strain is still below the 47 percent minimum elongation. Therefore, the multi-canister overpack would maintain containment for all of the drop scenarios. Note, however, that the Mark IV basket has strains approaching 100 percent. The Mark IV basket, which has a slender post as compared to the Mark 1A basket, undergoes significant deformation due to bending of the center post and perimeter bars and would significantly damage the fuel (Snow, 2003). Table 6-3 shows the maximum equivalent plastic true strain for a 0.61-m [2-ft] drop at orientations of 60, 90, and 115° off vertical. The 60° orientation was previously shown to be the most critical slapdown event in terms of maximum equivalent plastic true strains in the containment boundary (Blandford, 2003). The multi-canister overpack with Mark IV baskets was also evaluated for a 115° off-vertical orientation. This orientation takes into account that the multi-canister overpack with five Mark IV fuel baskets is not symmetric with respect to its center, and therefore the effect of slapdown of the multi-canister overpack bottom needed to be addressed (Blandford, 2003).

For the case of 60° off-vertical on the bottom at which impact occurred, the maximum equivalent plastic true strain of both multi-canister overpack canisters was 22 percent for the Mark IV basket and 20 percent for the Mark 1A basket. This maximum plastic strain is compressive and is located at the bottom of the multi-canister overpack where it contacts the surface. All other plastic strains for the 60° orientation of both multi-canister overpack components are comparable. Note that the plastic strain in the baskets themselves is 14 percent and 8 percent for the Mark IV and Mark 1A baskets, respectively. The higher compressive strains for the Mark IV basket is due to the fact the center post is smaller than the Mark 1A basket center post. Comparing the plastic strains of the Mark IV multi-canister overpack for the 60 and 115° orientations, the maximum plastic strain (22 percent) corresponds to the case of 60° and is located at the canister bottom. However, notice that the multi-canister

Table 6-3. Maximum Equivalent Plastic True Strains in the Multi-Canister Overpack for 0.61 m [2 ft] Worst Orientation Drops*

		Maximum Equivalent Plastic True Strain (%)				
		Mark 1A		Mark IV		
Component†	Surface	60% Off-Vertical Drop	90° Off-Vertical Drop	60% Off-Vertical Drop	90° Off-Vertical Drop	115° Off-Vertical Drop
Flange	outside	11	6	11	7	6
Bottom	inside	6	4	7	4	5
	outside	4	1	4	<1	1
	inside	6	7	6	7	11
Bottom	outside	20	10	22	10	15
Impact Area‡						
Main Shell	outside	4	3	4	2	10
	inside	7	10	6	6	15
Collar	outside	9	4	6	4	3
	inside	12	6	11	6	20
Cover	outside	5	2	5	2	14
	inside	4	<1	4	<1	0
Baskets§	(max.)	8	1	14	12	20

*Snow, S.D. "Analytical Evaluation of the MCO for Repository—Defined and Other Related Drop Events." EDF-NSNF–029. Rev. 0. New York City, New York: ASME. 2003.
†Components not listed in this table experienced zero or low plastic strains.
‡This was the side of the multi-canister overpack bottom where the impact occurred, which resulted in significant compressive strains.
§Peak strains in the Mark 1A baskets occurred in the basket walls or the top of the center post. Peak strains in the Mark IV baskets occurred in the base of the center post.

overpack top components (i.e., collar, cover) and the main shell have plastic strains larger than those of the 60° off-vertical drop orientation. This is consistent because the top head makes first contact with the impact surface. However, the 60° orientation has the point of first contact at the bottom of canister, which leads to larger plastic strains in the bottom flange and impact area.

Snow (2003) compares the 610-mm [24-in]-diameter standardized canister and the multi-canister overpack because both canisters have the same diameter and a nominal wall thickness of 12.7 mm [0.5 in]. The standardized canister is 4.6 m [15 ft] long, and the multi-canister overpack is approximately 4.3 m [14 ft] long. However, the standardized canister has an energy-absorbing skirt with flanged and dished heads, while the multi-canister overpack has a thick, flat bottom and is approximately twice as heavy as the standardized canister. Table 6-4 shows the maximum equivalent plastic true strains for both canisters [data for the standardized canister is from Blandford (2003)]. Note that the plastic strains are comparable for the two drop events. If the critical case of 7° off-vertical for the standardized canister is compared to the 3° off-vertical multi-canister overpack full-scale tests, the

Table 6-4. Maximum Equivalent Plastic True Strain Comparison—Multi-Canister Overpack Versus 610-mm [24-in] Standardized DOE Spent Nuclear Fuel Canister*					
	Maximum Equivalent Plastic True Strain in 610-mm [24-in] Canister Containment Boundary			Maximum Equivalent Plastic True Strain in Multi-Canister Overpack Containment Boundary	
Drop Event	Outside	Middle	Inside	Outside	Inside
23-Foot Vertical Drop	6	0.6	4	5	5
2-Foot Worst Orientation Drop	23	15	16	22	11
*Snow, S.D. "Analytical Evaluation of the MCO for Repository—Defined and Other Related Drop Events." EDF-NSNF–029. Rev. 0. New York City, New York: ASME. 2003.					

multi-canister overpack has 34- or 35-percent strain (Table 6-2) in the containment boundary, while the standardized canister has less than 1-percent strain [i.e., 0.7 percent given in Table 5-1 (Blandford, 2003)]. This shows once again that the skirt of the standardized canister absorbs a significant amount of energy and protects the containment boundary. Nevertheless, the predicted plastic strains in the multi-canister overpack are below the minimum elongation strain of 47 percent and minimum fracture strain of 118 percent.

Similar finite element analyses investigate the puncture resistance of the multi-canister overpack subject to a 0.61- or 1-m [24- or 40-in] drop onto a 152-mm [6-in]-diameter rigid post (Snow, 2004). The multi-canister overpack with a Mark IV basket was chosen for the study because it has the largest design weight {9,107 kg [20,080 lb]}, and the Mark IV basket, with its smaller center support post and perimeter bars, has less stiffness to prevent puncture of the main shell. The performance of this multi-canister overpack should envelope (bound) all other multi-canister overpack canister configurations (Snow, 2004).

Two finite element models were analyzed: (i) the rigid post makes contact with the multi-canister overpack at a point halfway between two basket base plates (which will be referred to as center post) and (ii) the rigid post makes contact at approximately 25.4 mm [1 in] from the basket base plate (which will be referred to as offset post). Figure 6-3 shows the location of the post with respect to the geometry of the multi-canister overpack. Table 6-5 shows the maximum equivalent plastic true strains for all four of the finite element analyses. For the offset post analyses, the outside, midsurface (thickness), and inside maximum equivalent plastic true strains are at the same location through the thickness, while for the centered post analysis, the maximum strains did not occur at the same location through the thickness (Snow, 2004).

Recall that in Snow (2003), the minimum elongation strain was 47 percent and the minimum fracture strain level was 118 percent, considering the material properties of all the canister component properties. For the puncture analyses, Snow (2004) assumes that only the shell experiences significant strains. Therefore, from Table 6-1, the minimum elongation is 59 percent and the minimum failure strain is 118 percent.

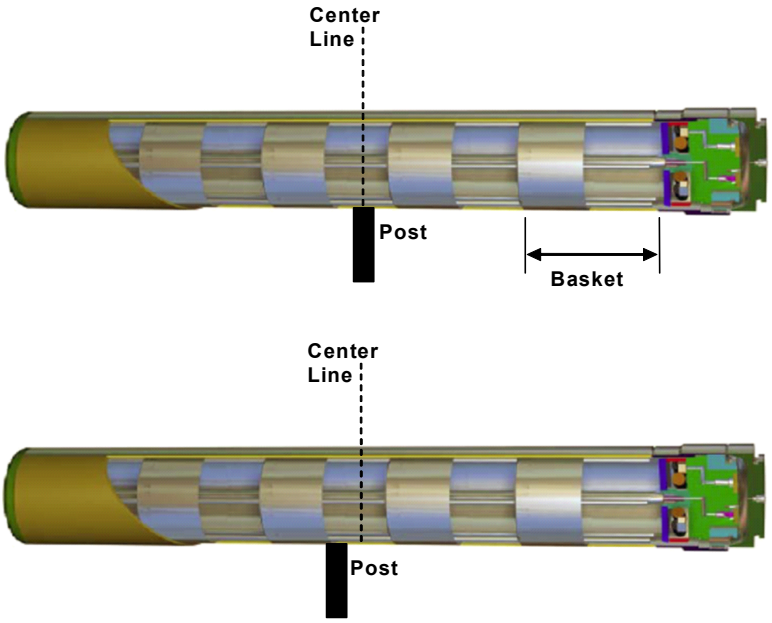

Figure 6-3. Multi-Canister Overpack Impact Post Locations (Morton, et al., 2006, Used with Permission of the Nuclear Society, Copyright 2006)

Table 6-5. Maximum Equivalent Plastic True Strains in the Multi-Canister Overpack Mark IV Main Shell for the Rigid Post Impact Events*

Rigid Post Impact Height and Post Position	Maximum Equivalent Plastic True Strain (%) in the Multi-Canister Main Shell		
	Outside Surface	Midsurface	Inside Surface
24-in† Centered Rigid Post	8	6	9
24-in† Offset Rigid Post	47	45	43
40-in‡ Centered Rigid Post	20	9	12
40-in‡ Offset Rigid Post	63	60	56

*Snow, S.D. "Analytical Evaluation of the Multi-canister Overpack for Puncture Drop Events." EDF–NSNF–039. Rev. 0. New York City, New York: ASME. 2004.
†Adjusted to 28-in to account for artificial energy losses (see Section 5.3.1).
‡Adjusted to 48-in to account for artificial energy losses (see Section 5.3.1).

From Table 6-5, the maximum equivalent plastic true strains from the centered post for both drop heights are low {i.e., 9- and 12-percent strain for the 0.61- and 1-m [24- and 40-in] drops, respectively}. These values indicate no rupture of the containment boundary is likely to occur. On the other hand, the offset analyses have significant strains for both drop heights. Specifically, the 610-mm [24-in] drop onto the offset post had maximum plastic true strains of 47, 45, and 43 percent for the outside surface, midsurface, and inside surface, respectively.

Because these values are below the minimum elongation of 59 percent, the 610-mm [24-in]-offset drop does not result in a breach of the containment boundary. For the analysis of the 1-m [40-in]-offset drop, the largest maximum equivalent plastic true strains are produced. Specifically, strain values of 63, 60, and 56 percent occur at the outside surface, midsurface, and inner surface, respectively.

Because the midsurface strain is just above the minimum elongation of 59 percent, a through crack and rupture of the containment boundary is likely to occur (Snow, 2004). Figure 6-4 shows the results for the 1,016-mm [40-in] drop height. In Figure 6-4(a), the deformation is symmetric about the center post analysis, and because the deformation occurs between two rigid plates of the basket, the post is restrained uniformly by the canister containment boundary.

On the other hand, for the offset post analysis [Figure 6-4(b)], there is significantly higher (more severe) deformation (strains) to the left of the post. The rigid plate to the left of the post (at the bottom of the basket) restrains the deformation, resulting in a large amount of localized, asymmetric plastic strain. Limited full-scale testing of a multi-canister overpack was undertaken in 2004 (Snow, et al., 2005; Morton, et al., 2006). Two multi-canister overpacks were fabricated, with each representing a typical Hanford multi-canister overpack and having the dimensions as given in Section 6.1. To account for strain-rate dependence of the stainless steel, the static true stress–strain curve was increased by 20 percent (see Section 4.3 for further discussion). For the finite element analysis, the multi-canister overpack had 4 baskets containing a 508-mm [20-in]-diameter, 660-mm [26-in]-long bar with a center hole to fit around the center post of the basket. The fifth (bottom) basket contained 54 carbon steel bars 63.5 mm [2.5 in] in diameter to represent individual pieces of spent nuclear fuel. The tests consisted of one multi-canister overpack dropped from a height of 7 m [23 ft] in a vertical orientation, while the second multi-canister overpack was dropped from a height of 0.61 m [2 ft] with an initial angle of 60° off-vertical (previously established as a critical orientation for slapdown to occur).

The first full-scale drop test {7 m [23 ft]} resulted in small deformations at the canister end {i.e., less than 6.35 mm [0.25 in] (Snow, et al., 2005)}. However, the majority of the deformation was in the internal components, with the impact energy absorbed by the fuel baskets, causing significant plastic deformation in the Mark IV bottom basket [Figure 6-5(a)]. Note that the tear in the multi-canister overpack basket was made for postdrop inspection and was not due to the drop (Snow, et al., 2005). The maximum equivalent plastic true strains measured from the finite element analysis occurred at the bottom of the multi-canister overpack with a maximum surface strain of 3.5 percent and a midsurface strain of 2.9 percent. These small strains indicate there would be no breach of the multi-canister overpack containment boundary. However, as noted in the full-scale test results, a significant amount of deformation occurs in the bottom basket, as shown in Figure 6-5(b). For the multi-canister overpack dropped from a height of 0.61 m [2 ft] at

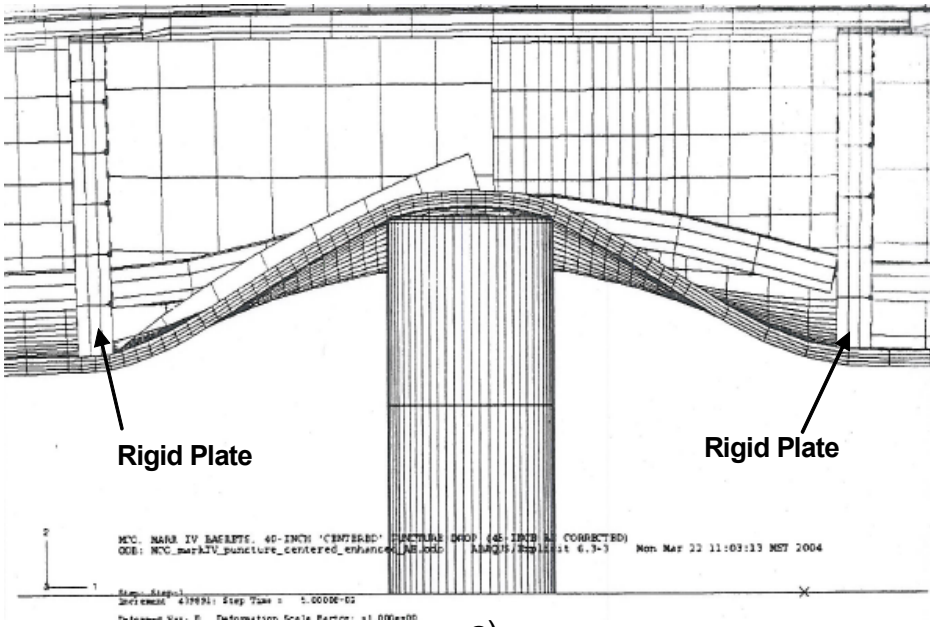

a)

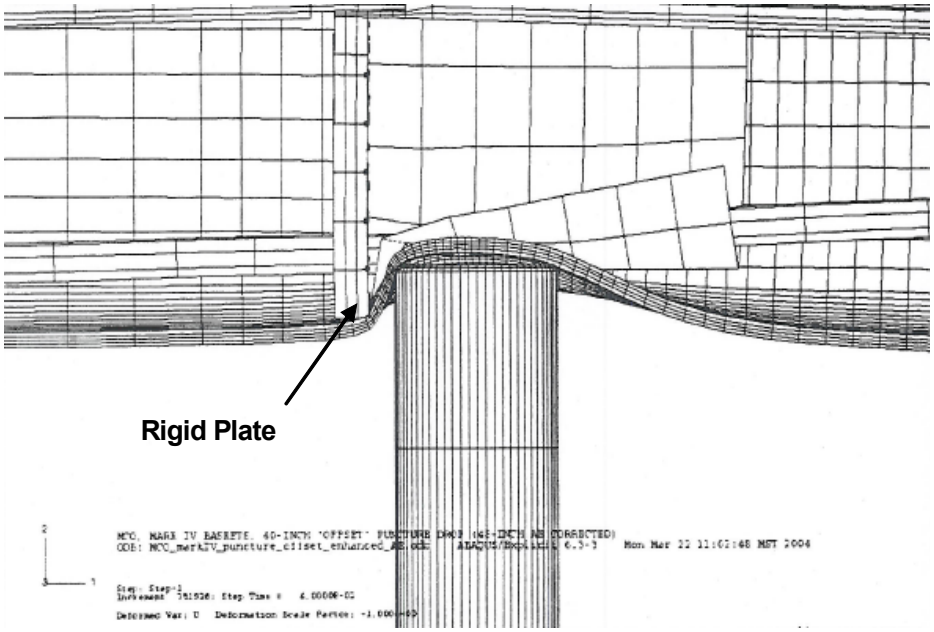

b)

Figure 6-4. (a) Center Post Strike, (b) Offset Post Strike on Multi-Canister Overpack (Snow, 2004)

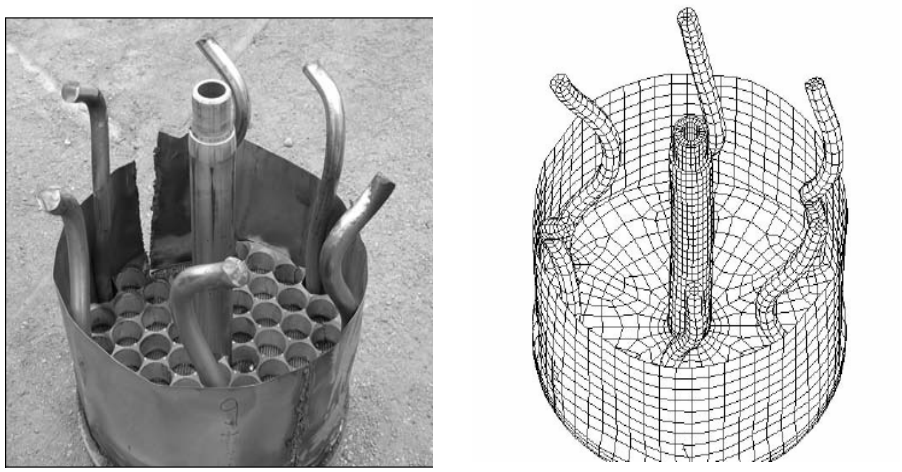

(a) (b)

Figure 6-5. Postdrop, Damaged Multi-Canister Mark IV Fuel Basket for (a) Full-Scale Test, (b) Finite Element Analysis (Snow, et al., 2005, Used With Permission of the American Society of Mechanical Engineers, Copyright 2005)

an angle of 60° off-vertical, there was minimal deformation. This limited height results in a small amount of impact energy, and as a result, only minor scuffing and flattening occurred along the bottom edge at the location of first impact. Due to the near-horizontal orientation, the top of the multi-canister overpack also contacted the surface, yet no noticeable deformations occurred (Snow, et al., 2005). Both of the multi-canister overpacks were helium leak tested and were determined to be leaktight.

7 STUDIES OF HIGH-LEVEL WASTE CANISTER DESIGNS

In the mid-1970s, Pacific Northwest Laboratories initiated a series of full-scale impact drop tests on canisters that contained high-level waste glass. The testing had two objectives: (i) to demonstrate that an impact due to an accidental drop would not breach the canister and possibly release the glass and (ii) to determine whether there was a breach such that the amount of respirable size (<10 μm diameter) glass particles released would be less than the amount allowed in the shipping cask (Peterson, et al., 1985). The drop tests demonstrated the structural integrity of components (e.g., the canister body, welds, fill nozzle) when subjected to impact from an accidental drop. The drop height of these tests varied from 1 to 2.6 m [40 to 104 in] at a number of orientations. The following sections discuss full-scale testing of actual canister designs and numerical modeling of purposed canister designs.

7.1 Impact Testing of High-Level Waste Canisters

In 1983, full-scale tests were performed at Pacific Northwest Laboratory on representative Savannah River Laboratory high-level waste canisters. For these drop tests, two separate canisters were fabricated from 304L stainless steel and one canister was fabricated from Grade 2 Titanium (Peterson, et al., 1985). Figure 7-1 shows typical canister dimensions. For these tests, the canister had a 610-mm [24-in] diameter and a length of 3 m [10 ft]. The canister was tested for both bottom and top drop orientations with the point of impact directly in line with the canister's center of gravity. The top and bottom drops were from a height of 9 m [30 ft], while the side drop was from a height of 1 m [40 in] onto a 152-mm [6-in]-diameter cylinder. The average filled weight of the canister was approximately 2,130 kg [4,740 lb].

Figure 7-2 shows the canister orientation for the top drop event. The titanium canister was dropped onto its bottom edge and produced asymmetric deformation as shown in Figure 7-3. The asymmetry was due to the point of impact being in line with the center of gravity; thus, the cylinder was not perfectly vertical. No rupture of the canister body was observed. For the top drop of the canister, the collapse of the nozzle also resulted in asymmetric deformation (Figure 7-4). Note that there is severe deformation of the canister top (nozzle), and a tear in the titanium body is observed. Peterson, et al. (1985) reasoned that the failure may be because titanium has less ductility than stainless steel, but they were not able to conclude the exact cause of the tear and suggested further testing. Strain circles were placed on the canister prior to the test. The strains near this location were approximately 14 percent, which was below the elongation to failure of 17 percent. However, the failure mode appeared to be tearing of the material and not tensile failure. Direct measurements of the strain circles near the nozzle were not possible due to the severe deformation of the canister top.

Figure 7-5 shows the deformation of the top end of one of the stainless steel canisters. Note that the deformation is rather symmetric because there is no failure at the nozzle. Figure 7-6 shows the bottom canister deformation resulting from the bottom end drop test. Note again that the asymmetry of the deformation is the result of the point of impact being directly in line with the center of gravity of the canister (i.e., the canister is not in a perfectly vertical orientation). Strains measured from the test specimens showed tensile strains on the order of 12 to 14 percent. Figure 7-7 shows the stainless steel canister after the side impact with no rupture of

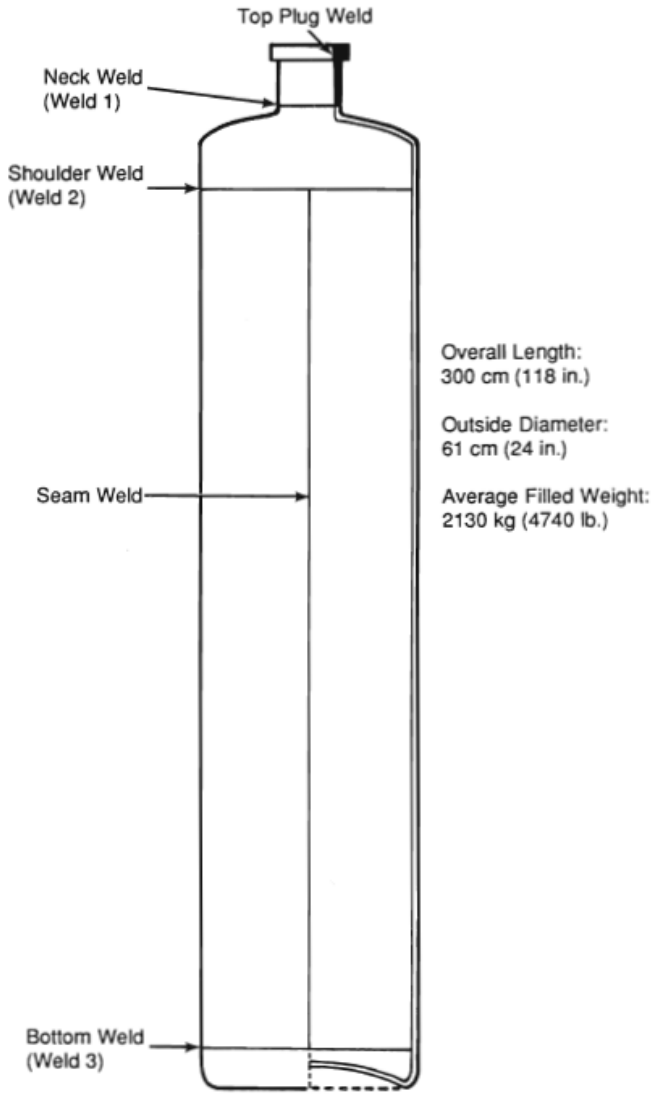

Figure 7-1. High-Level Waste Canister with Fabrication Details (Olson and Alzheimer, 1989)

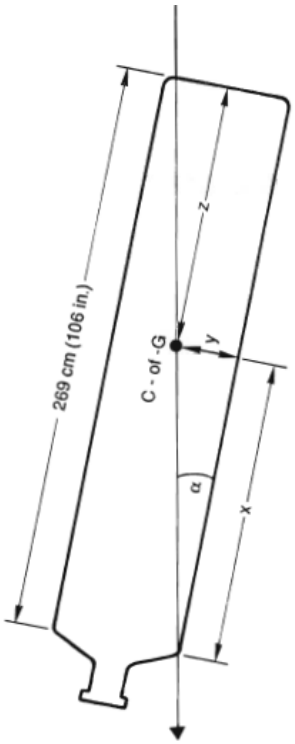

Figure 7-2. Canister Orientation for Center of Gravity Aligning With Corner Shoulder of High-Level Waste Canister (Olson and Alzheimer, 1989)

Figure 7-3. Asymmetric Deformation of Titanium Canister Bottom. Bottom Drop Event From a Height of 9 m [30 ft] (Peterson, et al., 1985)

Figure 7-4. Asymmetric Deformation of Titanium Canister Showing Rupture at the Nozzle. Top Drop Event From a Height of 9 m [30 ft] (Peterson, et al., 1985)

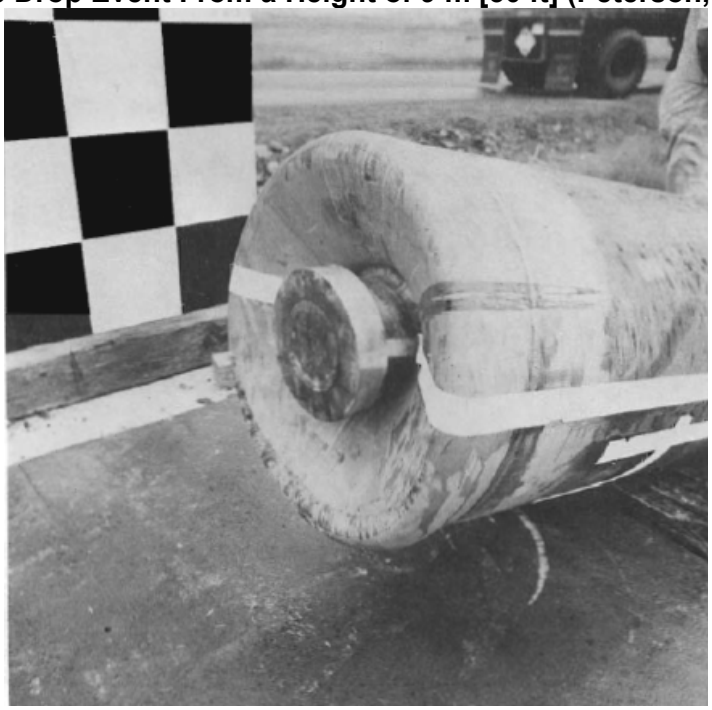

Figure 7-5. Symmetric Deformation of Stainless Steel Canister Nozzle Deformation. Top Drop Event From a Height of 9 m [30 ft] (Peterson, et al., 1985)

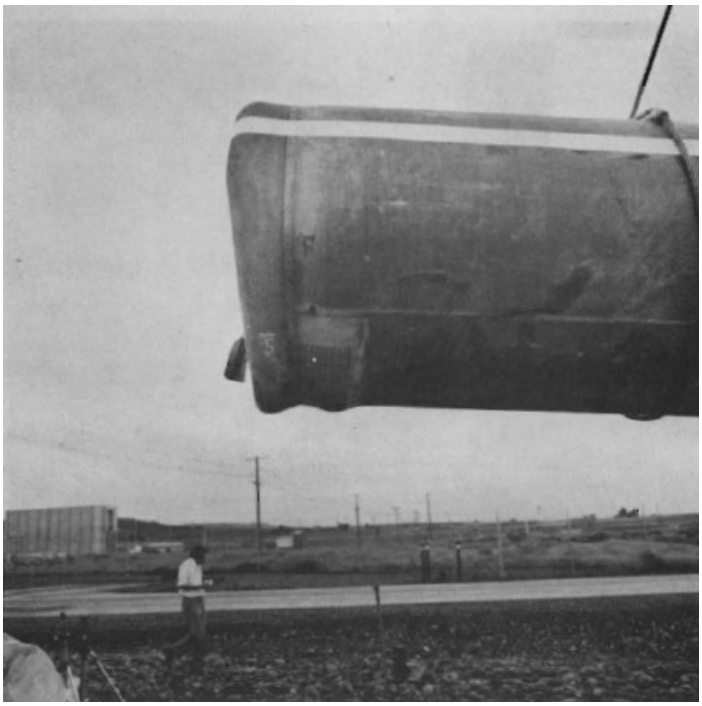

Figure 7-6. Asymmetric Deformation of Stainless Steel Canister Bottom. Bottom Drop Event From a Height of 9 m [30 ft] (Peterson, et al., 1985)

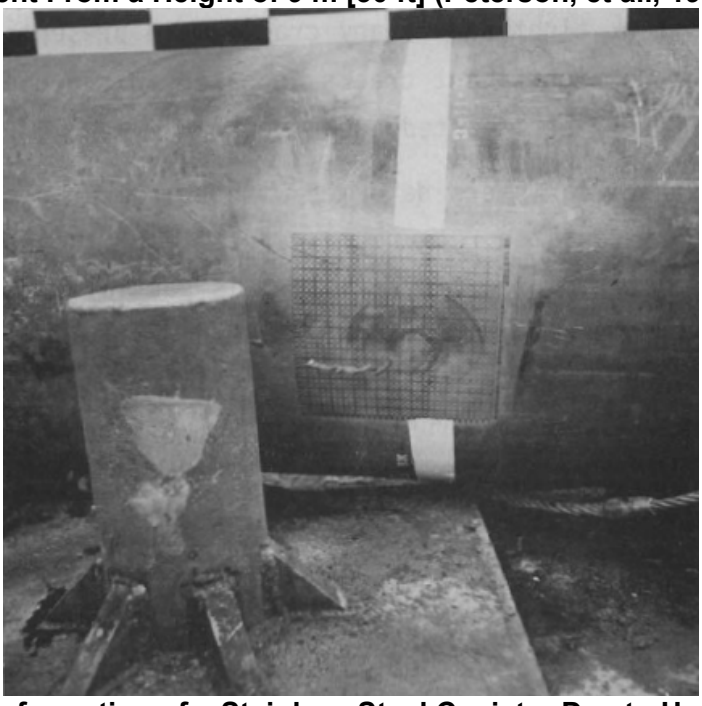

Figure 7-7. Side Deformation of a Stainless Steel Canister Due to Horizontal Drop Onto a 0.15-m [6-in] Cylinder. Drop Height is 1 m [40 in] (Peterson, et al., 1985)

the canister body observed. Helium leak testing and dye penetrant testing of the welds showed that the canisters were able to maintain their structural integrity (Peterson, et al., 1985).

In 1989, a series of full-scale impact tests was performed on Defense Waste Processing Facility canisters to show the canisters would not breach when subject to a 7-m [23-ft] drop onto an unyielding surface (Olson and Alzheimer, 1989). The test containers were filled at the Savannah River Laboratory with simulated waste glass to approximately 85 percent of their capacity with a total weight of approximately 2,150 kg [4,740 lb]. Each canister was 3 m [10 ft] long with a diameter of 610 mm [24 in]. The impact surface was a 216-mm [8.5-in]-thick steel plate placed on a 1.8-m [5.8-ft] reinforced concrete slab, which provided an essentially unyielding surface. Test orientations were similar to those described previously.

A small amount of deformation was observed for the vertically oriented (0° off center) bottom drop test. There also was observable rebound of approximately 750 mm [30 in] after first striking the impact surface. The amount of deformation was expected to be small because of the waste glass inside the canisters. Strain measurements were on the order of 2 percent or less. The height of the canisters on average decreased by 0.3 percent {i.e., 7.5 to 10 mm [0.3 to 0.4 in]}, and the average diameter increased by 2.5 percent {i.e., 10 to 15 mm [0.4 to 0.6 in]} in the area close to the bottom of the canister (Olson and Alzheimer, 1989).

A second orientation was chosen in which the center of gravity was in line with the shoulder of the canister [i.e., where the canister body meets the curved top just above the shoulder (Weld 2, Figures 7-1 and 7-2)]. All of the canisters exhibited a significant amount of deformation to the canister top flange/nozzle (Figure 7-8) (Olson and Alzheimer, 1989). For this case, approximately 150 mm [6 in] of rebound after first impact was observed. This markedly smaller amount of rebound is to be expected because there was significant plastic deformation of the canister top. As in the previous study, strain circles were used to measure the amount of strain produced by the impact. The largest measured strain for the top drop test was 52 percent, which occurred perpendicular to the weld where the top meets the canister body (see Figure 7-1, Weld 2); however, the strains in this location were compressive. Olson and Alzheimer (1989) state that tensile strains would be produced on the inside of the canister, but they would be lower in magnitude. Any preexisting flaws of the weld on the inside of the canister could open, but they would not propagate through the thickness because of the compressive strains on the outside surface. With respect to the changes in canister dimensions, there was a decrease in height of 5 percent {i.e., 140 to 164 mm [5.5 to 6.5 in]}, which was mainly due to the nozzle being pushed back into the canister top, and a 1-percent increase in diameter from 17 to 24 mm [0.4 to 0.6 in]. All of the canisters remained leaktight as measured by the standard helium test. Dye penetrant testing of the welds also showed no cracks developed in the welds. Thus, all canisters showed no indication of breach.

In 1994, Pacific Northwest Laboratory similarly tested five containers from the West Valley Demonstration Project to store high-level waste glass (Whittington, et al., 1995). The canisters were approximately 3 m [118 in] long and 610 mm [24 in] in diameter. Each canister, in a vertical orientation, was dropped from a height of 7 m [23 ft] onto an unyielding impact surface constructed at the Pacific Northwest Laboratory test facilities.

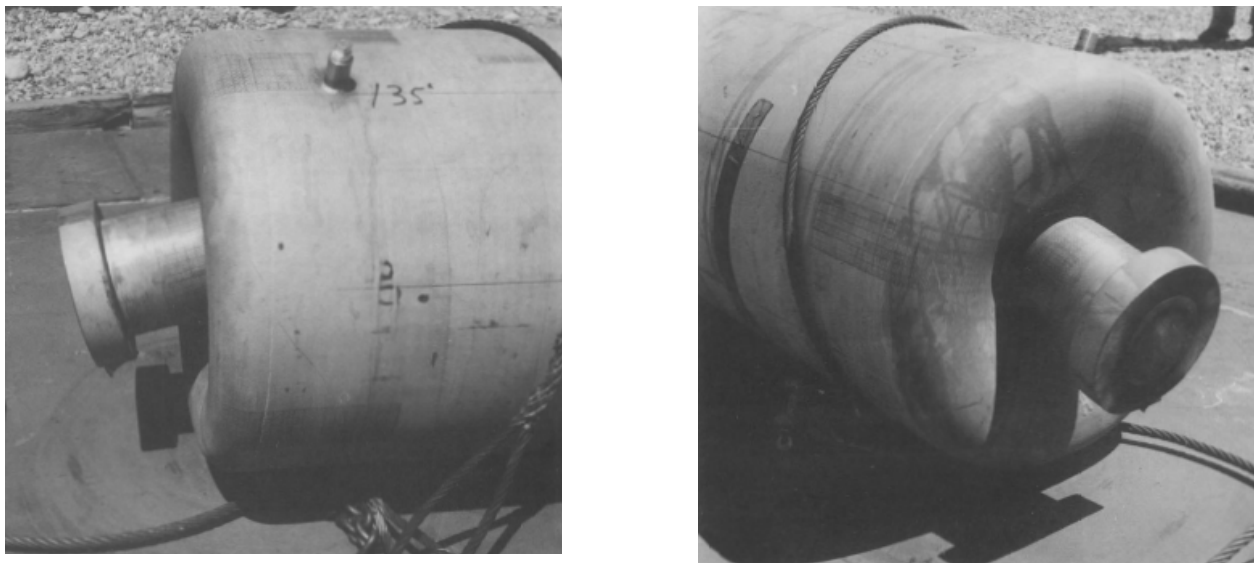

Figure 7-8. End Deformation of Stainless Steel Test Canister Subjected to a Top Drop With Center of Gravity in Line With Canister Shoulder (Olson and Alzheimer, 1989)

When each of the canisters were drop tested, three remained upright, while two canisters experienced slapdown. Each canister rebounded from the impact surface by 152 to 203 mm [6 to 8 in]. All of the canisters showed a minimum amount of deformation after impact with an increase in diameter located approximately 305 mm [12 in] from the bottom head (Whittington, et al., 1995). Each canister was marked with strain circles to measure the amount of strain at regions that were expected to produce the maximum amount of deformation along a line that extended from the bottom to a distance of 254 mm [10 in] above the bottom. The strain circles measured strains of 1 to 3 percent. At a distance above 254 mm [10 in], the strains were somewhat constant and smaller than those measured at the lower side wall of the canister (Whittington, et al., 1995). Most of the axial strains were compressive, as expected, with some tensile strains present due to bending of the canister. The axial strains measured were in the range of 5 percent compressive and 3 percent tensile. The strains measured in the hoop direction were tensile with a maximum hoop strain of 7 percent. These strains were well below the 56 percent failure strain of 304L stainless steel.

The amount of canister deformation was quantified by measuring the change in diameter and height and was used to judge the straightness of the canisters. This is necessary because the damaged canister was required to fit into a 635-mm [25-in]-diameter cylindrical cavity without forcing. For all of the canisters, there was a small amount of increase in diameter on the order of 12.7 mm [0.5 in] (2 percent) at the bottom head. The change in the height of the canister was decreased by approximately 12 mm [0.47 in] (0.4 percent) on average. With these small changes in canister dimension, the canisters were able to fit into the outside sleeve. Helium leak testing was performed on each of the canisters, and the canisters were considered leaktight (Whittington, et al., 1995).

7.2 A Numerical Study of Conceptual High-Level Waste Canisters

This section presents a number of conceptual canister designs described in Hill, et al. (2004). These canisters are used to dispose of calcine, a vitrified (particulate) form of high-level waste. All of the work presented in this section is purely conceptual and, therefore, studied solely using finite element models of the proposed canisters. The validity and accuracy of using the finite element method to estimate the deformation behavior of standardized canisters has been discussed in previous sections. Four types of canister designs will be discussed: (i) 610 mm [24 in]; (ii) 1,676 mm [66 in]; (iii) 1,676-mm [66-in] donut; and (iv) 1,676-mm [66-in] flat bottom.

The 610-mm [24-in] high-level waste canister model is quite similar to the 610-mm [24-in]-diameter DOE standardized spent nuclear fuel canister design, although there are a few design elements that would be different [i.e., the top head is modified for loading the calcine waste, and there would be no internal impact plates (located at each end)]. The 610-mm [24-in]-diameter canister has a wall thickness of 12.7 mm [0.5 in] or 9.525 mm [0.375 in] for these conceptual designs. This canister would also have a length of 4,572 mm [180 in] consistent with the standardized spent nuclear fuel canister.

The design of the 1,676-mm [66-in]-diameter canister has the same structural modifications as the 610-mm [24-in] canister. The wall thicknesses to be analyzed are 9.5, 12.7, 19.1, 25.4, and 35 mm [0.375, 0.50, 0.75, 1.00, and 1.375 in], and the 1,676-mm [66-in]-diameter canister length is 5,334 mm [210 in] (Hill, et al., 2004). The so-called donut design (Figure 7-9) is similar to the 1,676-mm [66-in] option, except the canister has a cylindrical opening at the center with an approximate inside diameter of 470 mm [18.5 in]. This cylindrical opening would allow the codisposal of a DOE standardized spent fuel canister. Each of these three canisters would have a 686-mm [27-in] skirt around each end.

Unlike the previous three canisters, the proposed 1,676-mm [66-in] flat bottom design (Figure 7-10) would not have a skirt on each head of the canister and has a design similar to the Navy Long Spent Fuel Canister (Hill, et al., 2004). The 1,676-mm [66-in] flat bottom canister has a wall thickness of 25.4, 19.05, 12.1, and 9.5 mm [1.0, 0.75, 0.5, and 0.375 in], and the top and bottom heads have 381-mm [15.0-in] and 89-mm [3.5-in]-thick plates, respectively. The overall length of the canister is 5,334 mm [210 in].

As in the standardized spent nuclear fuel canister designs, the material chosen for these conceptual canisters is 316L stainless steel. To account for the high strain rates, the dynamic true stress–strain curve is obtained by increasing the original true stress–strain curve values by 20 percent.

The proposed canisters were subjected to a number of drop simulations using the finite element code ABAQUS/Explicit. Specific details of each canister's finite element model are described in Hill, et al. (2004). A number of drop orientations were analyzed similar to those used in the finite element analysis of the nine standardized spent fuel canisters discussed in Chapter 3. Some of the parameters used in this study to evaluate the proposed designs were maximum

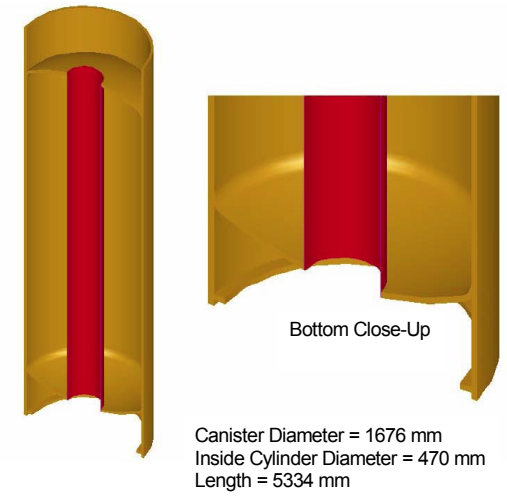

Figure 7-9. 1,676-mm [66-in] Donut Canister (Hill, et al., 2004, Used With Permission of WM Symposia, Inc., Copyright 2005) [25.4 mm = 1 in]

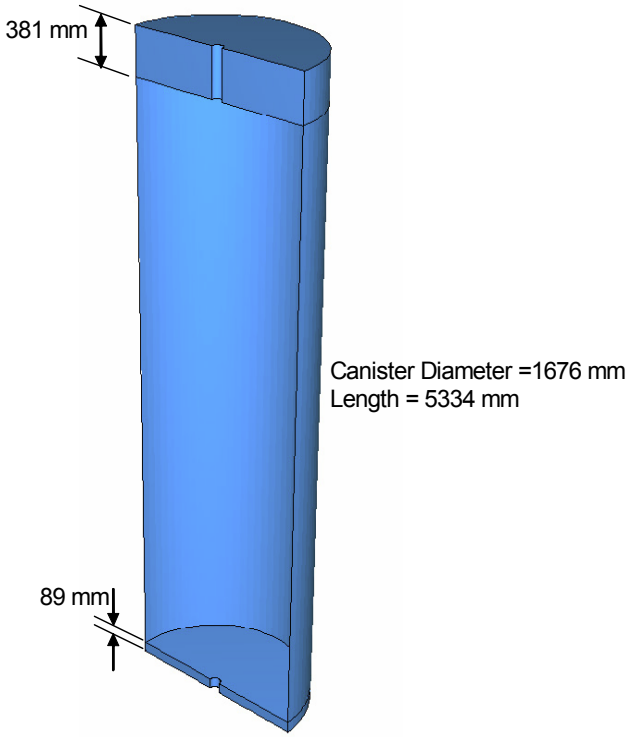

Figure 7-10. 1,676-mm [66-in] Flat Bottom Canister (Hill, et al., 2004, Used With Permission of WM Symposia, Inc., Copyright 2004) [25.4 mm = 1 in]

allowable design pressure, maximum plastic strain, and maximum deformation. The maximum plastic strain and the amount of deformation will be discussed next.

Table 7-1 shows the maximum equivalent plastic true strain. Rupture is said to occur if the midplane strain exceeds 60 to 80 percent, which is based upon the correlation of the finite element analyses with the full-scale testing of Snow, et al. (1999). Note that for all cases, the midplane strain is below the rupture strain. The 1,676-mm [66-in] canister and the 1,676-mm [66-in] donut canister have the lowest strains of all the designs. These canisters have the flange at each end of the canister. The 1,676-mm [66-in] flat bottom canister has a maximum containment pressure boundary strain of 72 percent (true strain) at the surface, but because the head plates are so thick, the canister does not incur a significant amount of deformation (Hill, et al., 2004).

Figure 7-11 shows the representative deformations of a canister resulting from a corner impact (i.e., its center of gravity is directly over the contact corner). Note that the deformation is limited to the skirt, and the amount of deformation depends on the wall thickness. The deformation acceptability is summarized in Table 7-2. The determination of whether the canister deformation is acceptable was based strictly on the judgment of Hill, et al. (2004).

The final conclusion was that the 610- or 1,676-mm [24- or 66-in] canisters (with the dished head and skirt) had comparable deformations. The 610-mm [24-in] canister would provide ease of handling, while the 1,676-mm [66-in] canister would result in fewer canisters required for waste disposal.

Table 7-1. Surface and Midplane Plastic True Strains*

Model	Maximum Equivalent Plastic True Strain (%)	
	Surface	Midplane
610-mm [24-in] Canister	65	32
1,676-mm [66-in] Canister	50	22
1,676-mm [66-in] Donut Canister	48	22
1,676-mm [66-in] Flat Bottom	72	27

*Hill, T.J., T.E. Rahl, D.K. Morton, K.C. Coughlan, J.T. Beck, and M.W. Patterson. "Canister Design for Direct Disposal of HLW Calcine Produced at the Idaho National Engineering and Environmental Laboratory." Waste Management 2004 Conference, Tucson, Arizona, February 29. Table VIII. Tucson, Arizona: Waste Management Symposium, Inc. 2004. Used With Permission of WM Symposia, Inc., Copyright 2004.

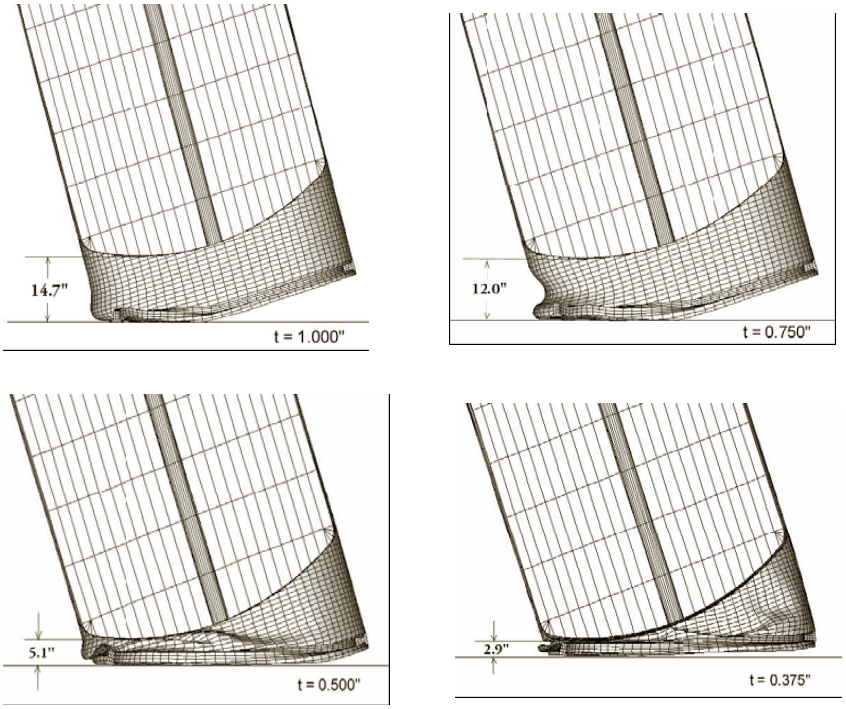

Figure 7-11. Corner Drop for Different Skirt Thickness (Hill, et al., 2004, Used With Permission of WM Symposia, Inc., Copyright 2004) [25.4 mm = 1 in]

Table 7-2. Summary of Observed and Predicted Acceptability of Deformation*			
		Max Deformation	
Model	**Thickness Variation**	**Acceptable**	**Not Acceptable**
610-mm [24-in] Canister	$t_{wall} = t_{head}$ = 12.7 mm [0.500 in]	X	
	$t_{wall} = t_{head}$ = 9.5 mm [0.375 in]	X	
1,676-mm [66-in] Canister	$t_{wall} = t_{head}$ = 35 mm [1.375 in]	X	
	$t_{wall} = t_{head}$ = 25.4 mm [1.000 in]	X	
	$t_{wall} = t_{head}$ = 19 mm [0.750 in]	X	
	$t_{wall} = t_{head}$ =12.7 mm [0.500 in]		X
	$t_{wall} = t_{head}$ = 9.5 mm [0.375 in]		X
1,676-mm [66-in] Donut Canister	$t_{wall} = t_{head}$ = 35 mm [1.375 in]	X	
	$t_{wall} = t_{head}$ = 25.4 mm [1.000 in]	X	
	$t_{wall} = t_{head}$ = 19 mm [0.750 in]	X	
	$t_{wall} = t_{head}$ =12.7 mm [0.500 in]		
	$t_{wall} = t_{head}$ = 9.5 mm [0.375 in]		X
1,676-mm [66-in] Flat Bottom	t_{wall} = 25.4 mm [1.0 in] $t_{bottom\ head}$ = 89 mm [3.50 in]	X	
	t_{wall} =19 mm [0.75 in] $t_{bottom\ head}$ = 89 mm [3.5 in]	Marginal	Marginal
	t_{wall} = 12.7 mm [0.50 in] $t_{bottom\ head}$ = 89 mm [3.5 in]		X
	t_{wall} = 9.5 mm [0.375 in] $t_{bottom\ head}$ = 89 mm [3.5 in]		X

*Hill, T.J., T.E. Rahl, D.K. Morton, K.C. Coughlan, J.T. Beck, and M.W. Patterson. "Canister Design for Direct Disposal of HLW Calcine Produced at the Idaho National Engineering and Environmental Laboratory." Waste Management 2004 Conference, Tucson, Arizona, February 29, 2004. Tucson, Arizona: Waste Management Symposium, Inc. 2004.

8 CANISTER FABRICATION AND WELDING

In the previous chapters, various canister types (i.e., standardized, multi-canister overpack, and high-level waste) in the literature were reviewed to determine whether the canisters were able to withstand dynamic loads in the form of drop events. These canisters were evaluated in terms of maximum equivalent plastic true strains and their ability to pass a leak test. Utilizing longitudinally welded 316L stainless steel pipe provided limited experimental testing of the welds. By satisfying the American Society of Mechanical Engineers Boiler and Pressure Vessel Code, Section III, fabrication requirements, this should produce a canister without any significant flaws. However, a flaw may be introduced because the materials may become embrittled during welding. As part of the evaluation of the canister subject to dynamic loads (i.e., a drop event), the fracture toughness of the welds is important. One method used to measure toughness is the Charpy V-Notch impact energy test. The following sections will discuss the mechanical and impact properties of the welds.

8.1 DOE Standardized Spent Nuclear Fuel Canister

The fabrication and welding process is described in DOE/SNF/REP–011 for the DOE standardized spent nuclear fuel canister (DOE, 1999a,b). The DOE spent nuclear fuel canisters may be made of SA–312 type 316L stainless steel for the shell and SA–240 type 316L for all other parts, including the heads, labels, and lifting rings. The optional plugs may be SA–479 type 316L stainless steel. All stainless steel materials may be annealed and pickled. A pressure boundary wall thickness reduction of 1.27 mm [0.050 in] has been established as the corrosion and erosion value to be used for canister design purposes. This value reflects the full design lifetime of 100 years. It is assumed that once the DOE spent nuclear fuel canister is placed inside the waste package, insignificant corrosion or erosion will occur for the next 50-year interval (DOE, 1999a).

Both the inner and outer surfaces of the canisters may have a finished condition for acceptable nondestructive examinations. The size of any burrs, sharp edges, and weld edges may be controlled. The interior surfaces may be smooth enough to allow easy loading of any DOE spent nuclear fuel or internals so as to not damage the spent nuclear fuel. During accidental drop events, high stress and strain values may be expected in local regions of the DOE spent nuclear fuel canisters where internal structures contact the canister shell pressure boundary. Internal structures (including baskets, spacers, sleeves, dividers, cans, welds) and fuel elements may contain sharp, stiff elements that could puncture the canister containment.

The DOE spent nuclear fuel canisters may be designed, fabricated, and examined per the requirements of the American Society of Mechanical Engineers Boiler and Pressure Vessel Code, Section III, Division 3, Subsections WA and WB, 1997 Edition (or the most current edition NRC approves, provided the specific code changes) for the loads and environments identified in this design specification. Certain changes to Section III, Division 3, need to be made for the DOE spent nuclear fuel canisters to be fabricated as N-stamped vessels, including (i) allowing field operations, (ii) allowing the actual N-stamping before the spent nuclear fuel is loaded into the DOE spent nuclear fuel canisters, (iii) allowing the use of ultrasonic examination for the final closure weld, and (iv) testing for helium leaks in lieu of pressure test requirements, after loading

the spent nuclear fuel and final closure welding, and allowing helium leak testing in lieu of pressure testing for low design pressure vessels.

Due to the presence of the spent nuclear fuel after loading, the DOE spent nuclear fuel canisters may not be required to satisfy pressure test requirements of Section III, Division 3, after loading, final seal, and welding. The final canister weld may implement a welding procedure that can be qualified to yield leaktight welds. A leaktight weld may be considered equal to or better than the required leak rate necessary to satisfy the applicable 10 CFR Parts 71 and 72 requirements.

Morton and Snow (2000) indicate that all possible situations were adjusted to inflict the most damage to the test canister welds during their drop tests. The test canisters contained a number of weld joints that did not receive any postweld heat treatment. Although a seamless pipe can be used, the pipe used to fabricate the test canister bodies and skirts was longitudinally welded pipe. By using this type of pipe, the weld joint would be the logical first location to check if a problem were to develop.

A combination of manual tungsten inert gas and manual pulse metal arc (wire feed) welding techniques may be used. All of the pressure boundary welds existing before loading the test canisters with internals may be volumetrically examined using radiography testing and liquid penetrant examinations. Ultrasonic testing methods may be used to perform volumetric examinations of the final closure welds. After the drop tests are completed, the same two welds may be reexamined using both ultrasonic testing and radiography testing.

Schuster, et al. (2000) indicate that base metal flaws such as laminations (e.g., caused by multiple weld passes) may cause the breach of a dropped canister. An undetected flaw of sufficient size in specific locations with a particular orientation could lead to a canister breach.

Based on the American Society of Mechanical Engineers Code, construction, examination requirements, and operational experience, a maximum undetected cracklike flaw size of more than 1 mm [0.04 in] is the weld flaw criteria for which canister drop survivability is judged (Smith, 2003).

The designer and fabricator of the DOE spent nuclear fuel canisters may establish, maintain, and execute a quality assurance program based on the criteria necessary to satisfy the American Society of Mechanical Engineers Boiler and Pressure Vessel Code, Division 3 construction criteria, 10 CFR Part 71 (Subpart H), and Part 72 (Subpart G) quality assurance requirements.

8.2 Multi-Canister Overpack Design

Goldmann (2000a) describes the multi-canister overpack designs, and related detailed design information is further given in Garvin (2001) and Goldmann (2000b). The multi-canister overpack shell may be fabricated from type 304/304L stainless steel. All components welded to the multi-canister overpack shell may be made of austenitic stainless steels compatible for welding to 304L stainless steel. A mechanically attached shield plug and any components thereof may be made from either 304L, 304N B&S, or B&SA. All materials may be American Society of Mechanical Engineers/American Standard Testing and Materials certified. A

provision may be made to preclude metal-to-metal galling in threaded multi-canister overpack components.

All multi-canister overpack fabrication pressure boundary welds may be made in accordance with American Society of Mechanical Engineers Code, Section III, requirements. All welds may be sufficiently smooth to enable easy decontamination. Butt welds may be ground flush to within 0.76 mm [0.03 in] of base metal. Weld joint designs may avoid potential contamination traps to the greatest extent practicable. All multi-canister overpack pressure boundary welds and welds bearing the weight of the fully loaded multi-canister overpack may be designed for and pass nondestructive examination per American Society of Mechanical Engineers Code, Section III, Division I, requirements.

Materials corrosion in terms of thickness reduction should be considered in drop event analyses. Some potential corrosion modes include passive general corrosion, localized corrosion, galvanic corrosion, stress corrosion cracking, and hydrogen embrittlement. However, no quantitative penetration depth is given that can be potentially used in a drop event analysis.

Quality assurance requirements from the Project Hanford Office of Civilian Radioactive Waste Management Quality Assurance Program Plan may be applied to applicable fabrication, inspection, testing, handling, cleaning, shipping, and storage. The Quality Assurance Program Plan requires that Office of Civilian Radioactive Waste Management related spent nuclear fuel project activities comply with DOE/RW–0333P, Quality Assurance Requirements and Description for the Civilian Radioactive Waste Management Program (Quality Assurance Requirements and Description). Retrofit of the multi-canister overpack design to comply with the Office of Civilian Radioactive Waste Management is not required.

8.3 High-Level Waste Glass Canister

High-level waste glass canisters have been planned to be produced from West Valley Demonstration Project, Defense Waste Process Facilities, Hanford Waste Vitrification Plant, or Idaho Chemical Processing Plant. Ahn (1999) summarizes design specifications and processing guidance. The majority of the high-level waste glass canisters are made of 304L stainless steel. Gas tungsten arc welding and upset resistance welding are used. Details are similar to other canister processes.

8.4 NRC Interim Staff Guidance

NRC issued Interim Staff Guidance on alternatives to the American Society of Mechanical Engineers Code (NRC, 2000) and on materials evaluation (NRC, 2001). These interim staff guidances address storage and transportation (10 CFR Parts 71 and 72).

ISG–10, Revision 1, Code Section III, may be used as an acceptable standard for the design and fabrication of a canister. Because a canister is not a pressure vessel, American Society of Mechanical Engineers Code, Section III, cannot be implemented without allowing some alternatives to its requirements. Specific alternatives may be used on a case-by-case basis for those requirements that are not applicable or practical to implement for the canister. The proposed alternatives may provide an acceptable level of quality and safety. Compliance with

the specified requirements of American Society of Mechanical Engineers Code, Section III, may result in hardship or unusual difficulty without a compensating increase in the level of quality and safety.

The materials evaluation chapter, ISG–15, ensures quality and uniformity in reviews performed. There are two nationally recognized codes that address welding: American Society of Mechanical Engineers and AWS D1.1. The American Society of Mechanical Engineers Code governs welded pressure vessels, from domestic water heaters to nuclear reactors. The AWS D1.1 Structural Welding Code is the applicable code for welding structural steel, such as the steel used for bridges and steel-framed skyscrapers. The various construction codes differ in their requirements for materials and welding procedures because each code is specialized with a particular application in mind. Standard weld and nondestructive examination symbols may be found in AWS A2.4. Except for welded closure lids, all welds of the confinement shell need to be full penetration welds. The nondestructive examination for these confinement welds is volumetric.

For designs employing lid materials and welds, either volumetric or multipass liquid penetrant testing inspection methods are acceptable. For either ultrasonic testing or liquid penetrant examination, the minimum detectable flaw size may be demonstrated to be less than the critical flaw size. The critical flaw size may be calculated in accordance with American Society of Mechanical Engineers XI methodology; however, net section stress may be governing for austenitic stainless steels and may not violate American Society of Mechanical Engineers Code, Section III, requirements. Flaws in austenitic stainless steels are expected to exceed the thickness of one weld bead. If using ultrasonic testing, the ultrasonic testing acceptance criteria are the same as those of NB–5332 for preservice examination. In accordance with code practice for supplementing volumetric examinations with a surface examination, a ultrasonic testing examination may be performed in conjunction with a root pass and cover pass liquid penetrant testing examination. If liquid penetrant testing is specified (i.e., no volumetric inspection), a stress reduction factor of 0.8 must be applied to the weld design.

8.5 Mechanical and Impact Properties of Welds

In the impact (i.e., drop) analysis/modeling of the 316L stainless steel canister, mechanical properties are important as input parameters. It is likely that 316L is used in the design of a currently considered canister (e.g., DOE, 2006). Therefore, data for 316L and its analogs are summarized here. The mechanical properties include yield strength, tensile strength, ductility, fracture toughness, and Charpy V-Notch impact energy. These mechanical properties vary depending on temperature, strain rate, fabrication, and welding. Recently, Dunn, et al. (2003) summarized relevant mechanical property data of 316L stainless steel or its analogs for various material and test conditions. Dunn, et al. (2003) discusses a few important parameter values associated with fabrication and welding for potential use in reviewing the assessment of the integrity of the 316L stainless steel canister under drop conditions:

> “The effects of fabrication processes on the mechanical properties of austenitic stainless steels are receiving considerable attention as a result of the use of these materials in nuclear power plants. Multiple studies have investigated the yield strength, tensile strength, and ductility of austenitic stainless steel base metals and welds. Although a marginal loss of ductility is observed for welded

materials, welded austenitic stainless steels remain quite ductile. Fracture toughness measurements have been conducted to investigate the effects of crack orientation, cold work, inclusion content, temperature, weld metal composition, and welding method.

"Although heat-to-heat variations are large, the fracture toughness of austenitic stainless steel base metals and welds is generally high owing to their relatively low strength, strain hardening, and high ductility. Nevertheless, the fracture toughness of wrought austenitic stainless steel is dependent on the inclusion content, cold work, and crack orientation. A minor amount of cold work can result in a substantial decrease in fracture toughness. Inclusions have the greatest impact on cracks oriented along the rolling direction and parallel to the surface of wrought plate. Welds in austenitic stainless steels also have high fracture toughness, but the toughness value is dependent on the welding processes. Welds produced with methods that result in a minimal increase in the inclusion content, such as gas tungsten-arc welding and gas metal-arc welding retain fracture toughness similar to that of the wrought base material. Welding methods that result in a substantial increase in inclusion content such as submerged-arc welding, reduce the fracture toughness of the weld. Nevertheless, the fracture toughness of welded stainless steels is generally sufficiently high to preclude fracture-dominated failure."

In the impact analysis/modeling, the use of Charpy V-Notch impact energy may be more important. Dunn, et al. (2003) attempted to correlate the fracture toughness to the Charpy V-Notch impact energy. For example, the fracture toughness of ferritic pressure vessel steels with yield strength of more than 690 MPa (100 ksi) can be related to the Charpy V-Notch impact energy through an empirical relationship

$$[K_{IC}/\sigma_{YS}]^2 = 5.0\,[CVN/\sigma_{YS} - 0.05] \qquad (8\text{-}1)$$

where K_{IC} is fracture toughness, σ_{YS} is yield strength, and CVN is Charpy V-Notch impact energy. Detailed correlation in 316L welded stainless steel is not established. However, the Charpy V-Notch impact energy of welded 316L stainless steel is available in the literature, as shown in Figure 8-1.

8.6 Preclosure Safety Analysis

The primary function of the canister (e.g., DOE, 2006) would be the containment of radionuclides during preclosure operations. Currently, the canister is considered to be important to safety in the Preclosure Safety Analysis during preclosure operations (NRC and DOE, 2006a,b). However, under canister drop conditions from various

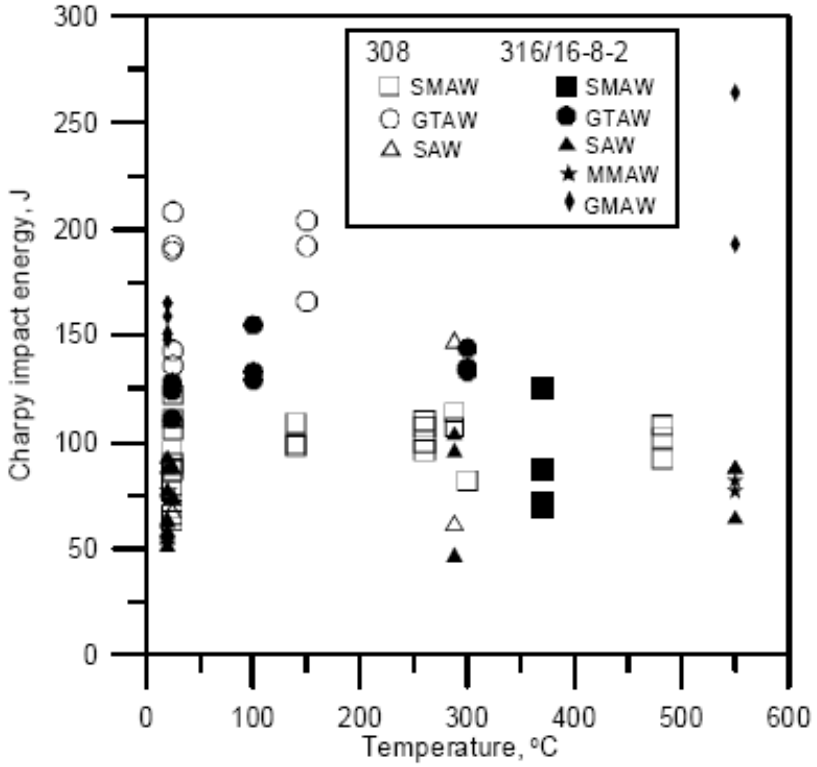

Figure 8-1. Charpy V-Notch Impact Energy for Austenitic Stainless Steel Welds (Gavenda, et al., 1996) [°F = 9/5 °C + 32, 1 Ft-lb = Joule/1.35] (SMAW = Shielded Metal-Arc Weld; GTAW = gas; Tungsten = Arc Weld; SAW = Submerged Arc Weld; GMAW = Gas Metal-Arc Weld; MMAW = Manual Metal-Arc Weld)

accidents, the possibility that the canister may fail must be considered. The failed canister could release radionuclides. The dose to the worker and the public from the radionuclide release needs to meet the performance objectives in 10 CFR Part 63.111 (a). The consequence analysis of radionuclide release from the failed canister needs the radionuclide source term. In the Preclosure Safety Analysis, the source term for a given event sequence depends on release fraction and leak path factor, among several others (Kamas, et al., 2006). Release fraction is the fraction of each radionuclide released from the inventory. Leak path factor is the product of various factors involved in the subsequent mitigation of radionuclide release and dispersion from the release fraction (e.g., failed canister mitigation factor, building discharge fraction, and HEPA filter mitigation factor).

The failed canister mitigation factor was determined primarily by how much canister surface area would be exposed upon the canister failure. The surface area opening will in turn depend on the impact energy. For example, Sprung, et al. (2000) indicate a radionuclide particulate leak path factor of 0.02 for a impact speed of 96.5 meters per hour [60 miles per hour] pressurized to 5 atmospheres (506.6 kPa). In the drop case, this impact speed is determined primarily by the drop height. Alternatively, the drop height or the impact speed gives the impact energy onto the canister.

The Charpy V-Notch impact energy shown in Table 8-1 suggests how the open surface area of the canister could be estimated upon impact. The American Standard Testing and Materials accepted Charpy V-Notch specimen has a normal size of $1 \times 1 \times 5.5$ cm [$0.4 \times 0.4 \times 2.2$ in] (American Standard Testing and Materials, 2007) with a 0.2-cm [0.08-in] notch. Assuming the total impact energy is used to create the surface area of the notched ligament, a correlation of the impact energy input and the open surface area can be estimated. For example, 100 J of Charpy V-Notch impact energy may create a fraction of ~0.03 of the surface area. The specific impact energy in this case would be higher than normally expected from the canister drop test at a 7-m [23-ft] height. This type of estimate can be normally used for ductile materials such as 316L stainless steel. The background information for the estimate of the specific impact energy for a canister might be obtained from Sprung, et al. (2000), and Kamas, et al. (2006) presented some exercise results. Recently, DOE conservatively assessed the particulate leak path factor of radionuclides as 0.1 (Dexheimer, et al., 2006).

Table 8-1. Effect of Inclusions and Specimen Orientation on Yield Strength, Tensile Strength, and Ductility*

	Type 316L Heat A Inclusion Number: 41			Type 316L Heat B Inclusion Number: 85		
Orientation	Yield Strength MPa [ksi]	Tensile Strength MPa [ksi]	Elongation Percent	Yield Strength MPa [ksi]	Tensile Strength MPa [ksi]	Elongation Percent
S-L	293 [42.5]	571 [82.8]	73	281 [40.8]	445 [64.5]	15
T-L	303 [43.9]	597 [86.6]	73	279 [40.5]	558 [80.9]	74
L-T	310 [44.9]	591 [85.7]	76	279 [40.5]	561 [81.4]	78

*Dunn, D.S., Y.-M. Pan, D. Daruwalla, and A. Csontos. "The Effects of Fabrication Processes on the Mechanical Properties of Waste Packages—Progress Report." San Antonio, Texas: CNWRA. 2003.

9 SUMMARY

This report compiles literature evaluating the structural behavior of DOE spent nuclear fuel, Idaho Spent Fuel Project canisters, multi-canister overpack, and high-level waste canisters.

In several of these studies, finite element analyses were initially used to determine a preliminary canister design that would preserve the canister containment boundary (i.e., no breach). DOE performed small- and full-scale drop tests of proposed standardized canister designs to verify and validate the finite element analyses; accuracy was evaluated by comparing deformations of the test canister and those of the finite element model. Once the preliminary design was selected, two full-scale tests on 457- and 610-mm [18- and 24-in] canisters were performed. Finite element analyses of both drop tests were once again validated by comparison with the full-scale tests. Based upon these full-scale tests and corresponding finite element analyses, DOE chose the standardized canister design with the notable design feature of a flanged and dished head with a skirt welded around each end.

Based upon the previous small- and limited-full-scale tests, DOE performed a broader set of nine full-scale drop tests on the proposed standardized spent fuel canister. One test objective was to verify that the skirt attached to each end absorbed the impact energy, as designed. Each full-scale test measured the amount of canister deformation and whether or not the containment boundary was affected. Visual inspection and pressure tests were used to determine whether the containment boundary was intact. Finite element analysis of each drop test was performed, and DOE observed very good agreement, in terms of deformation, between the test and analysis. Surface and midsurface (thickness) maximum equivalent plastic true strains obtained from the finite element analyses also verified no breach of the containment boundary. For a drop height of 9 m [30 ft], a maximum equivalent plastic surface true strain of 57 percent occurred in the canister upper head, a maximum midplane (thickness) strain of 19 percent occurred, and a maximum inside surface strain of 42 percent occurred for the canister orientation with the largest slapdown effect. The important quantity was the maximum midplane strain (19 percent), which controls breach. These strains were below the DOE-selected conservative ultimate strain value of 48 percent.

The Idaho Project Spent Nuclear Fuel canister was based upon the standardized spent nuclear fuel canisters with modifications limited to fabrication details (i.e., wall thickness, welding of the dished head and skirt). The basic canister design is unchanged—particularly the welded skirt at each end of the canister. After establishing the accuracy of finite element analyses to simulate drop tests, drop events similar to those used in the standardized canister were performed. Deformations and maximum equivalent plastic true strains obtained from these analyses were evaluated to verify that the canister would not breach. Midsurface strains were especially important because they indicated whether any surface damage would propagate through the containment boundary and result in a breach. For the drop event of 80° off-vertical, the upper head (due to slapdown) had 48, 24, and 25 percent maximum surface, midsurface, and inner surface strains (true strain), respectively. In all cases, the maximum equivalent plastic true strains of the containment pressure boundary were below the failure strain.

The standardized canister and the multi-canister overpack were compared because both canisters have the same diameter, nominal wall thickness, and approximately the same

length. However, the standardized canister has an energy-absorbing skirt with flanged and dished heads, while the multi-canister overpack has a thick, flat bottom and is approximately twice as heavy as the standardized canister. For the 7-m [23-ft] repository drop, the plastic strains are comparable for the two canisters. The multi-canister overpack had strains of 5 percent at both the outside and inside surfaces. The standardized canister had outside and inside surface strains of 6 and 4 percent, respectively. However, the critical case of 7° off vertical of the standardized canister was compared to the 3° off vertical multi-canister overpack orientation; the multi-canister overpack had 34- or 35-percent strain in the containment boundary, while the standardized canister had less than 1-percent strain. This shows once again that the skirt of the standardized canister absorbs a significant amount of energy and protects the containment boundary. Nevertheless, the predicted plastic strains in the multi-canister overpack are below the minimum elongation strain of 47 percent and minimum fracture strain of 118 percent.

High-level waste canisters were evaluated for their structural behavior when subjected to a drop event. Pacific Northwest Laboratories performed full-scale impact tests on canisters that contained high-level waste glass. The tests consisted of a vertical bottom drop where the bottom contacts the surface and a vertical top drop where the corner of the top shoulder and fill nozzle contacts the impact surface. Both tests were oriented such that the center of gravity of the canister was over the point of impact. The test canisters were constructed of titanium or stainless steel. The bottom drop of the titanium and stainless steel canisters showed asymmetric deformation of the canister bottom with no failure. However, for the case of the top drop, the titanium canister had a visible failure that appeared to be due to tearing around the fill nozzle. A similar test at the same orientation for the stainless steel canister did not have the tearing failure. The difference in ductility between titanium and stainless steel may have attributed to the failure.

Finite element studies of proposed canister designs for disposal of high-level waste were evaluated. The 610- and 1,676-mm [24- and 66-in] dished bottom canisters have an energy-absorbing skirt attached to the bottom, and one 1,676-mm [66-in] canister had a flat bottom. The canisters with the skirt had maximum surface strains of 65 to 48 percent for the 610-mm [24-in] and 1,676-mm [66-in] dished bottom, respectively. These strains are below the 60- to 80-percent maximum strain. One design in particular—the 1,676-mm [66-in] diameter, flat bottom canister—appears to be somewhat similar to the proposed transportation, aging, and disposal canister. Current specifications proposed for the transportation, aging, and disposal canister are a flat bottom; a diameter of approximately 1,676 mm [66 in]; and a length of 5.5 m [18 ft] as specified in the Revision B of the Preliminary Transportation, Aging, and Disposal Canister System Performance Specification. The 1,676-mm [66-in] flat bottom canister (with no skirt) had a maximum surface true strain of 72 percent, which is in between the 60 to 80 percent maximum strain. Midsurface strains for all canisters averaged 30 percent, which is well below failure; therefore, no surface cracks would propagate through the thickness.

The analyses described here have demonstrated that the various canister types can withstand dynamic loads due to drop events of 9 m [30 ft] or below. These canisters were evaluated in terms of changes in geometry, maximum equivalent plastic true strains, and their ability to pass a leak test. The standardized canister, for example, utilized longitudinally welded 316L stainless steel pipe as opposed to seamless pipe,

and there are welds where the skirt joins the canister body. Using this type of pipe provided very limited experimental testing of the welds. The mechanical properties of the welds and the factors that may affect the weld were discussed. The fracture toughness of welds was discussed, including one method used to measure toughness: the Charpy V-Notch impact energy, which may provide estimates of the weld open surface area.

Extensive results and discussion with regard to full-scale testing and finite element simulations of canister drop events has been documented. This review indicates that finite element analysis can accurately analyze canister behavior for other loading scenarios such that full-scale testing may not be required. Knowledge gained from the full-scale testing and the corresponding finite element analyses of the canisters in this review should prove useful when evaluating the proposed transportation, aging, and disposal canisters for the potential Yucca Mountain Repository.

10 REFERENCES

ABAQUS Inc. "ABAQUS User's Manual." Version 6.6. Providence, Rhode Island: ABAQUS, Inc. 2006.

Ahn, T. "Compendium of HLW Solidification Process." ML 033450471. Washington, DC: Office of Civilian Radioactive Waste Management. 1999.

American Society of Mechanical Engineers International. "ASME International Boiler and Pressure Vessel Code." New York City, New York: ASME. 2001.

American Standard Testing and Materials. "Standard Test Methods for Notched Bar Impact Testing of Metallic Materials." ASTM E 23–06. West Conshohocken, Pennsylvania: ASTM International. 2007.

Blandford, R.K. "Structural Response Evaluation of the 24-Inch Diameter DOE Standardized Spent Nuclear Fuel Canister." EDF–NSNF–026. Idaho Falls, Idaho: Idaho National Engineering and Environmental Laboratory. 2003.

Blandford, R.K., D.K. Morton, T.E. Rahl, and S.D. Snow. "Impact Testing of Stainless Steel Materials." PVP2005–71133. American Society of Mechanical Engineers Pressure Vessels and Piping Conference, Denver, Colorado. New York City, New York: ASME. 2005.

———. "Preventing Failure in Spent Nuclear Fuel Canisters." *ASM International, Practical Failure Analysis*. Vol. 3, No. 4. 2003.

Dexheimer, D., J. Schulz, and S.-S. Tsai. "Preclosure Source Terms and Consequence Methodology." NRC/DOE Technical Exchange and Management Meeting on Preclosure Topics. Las Vegas, Nevada: Bechtel SAIC Company, LLC. 2006.

DOE. DOE/RW–0585, "Preliminary Transportation, Aging, and Disposal Canister System Performance Specification Revision B." Washington, DC: Office of Civilian Radioactive Waste Management. 2006.

———. DOE/RW–0351, "Civilian Radioactive Management System Waste Acceptance System Requirements Document." Rev. 4. Washington, DC: Office of Civilian Radioactive Waste Management. 2002.

———. DOE/SNF/REP–011, "Preliminary Design Specification of Department of Energy Standardized Spent Nuclear Fuel Canisters, Vol. I Design Specification." Rev. 3. Washington, DC: DOE. 1999a.

———. DOE/SNF/REP–011, "Preliminary Design Specification of Department of Energy Standardized Spent Nuclear Fuel Canisters, Vol. II Rational Document." Rev. 3. Washington, DC: DOE. 1999b.

———. DOE/RW-0432, “Conceptual Design for a Waste-Management System That Uses Multi-purpose Canisters.” Washington, DC: Office of Civilian Radioactive Waste Management. 1994a.

———. DOE/RW–0445, “Multi-Purpose Canister System Evaluation, A Systems Engineering Approach.” Washington, DC: Office of Civilian Radioactive Waste Management. 1994b.

Dunn, D.S., Y.-M. Pan, D. Daruwalla, and A. Csontos. “The Effects of Fabrication Processes on the Mechanical Properties of Waste Packages—Progress Report.” San Antonio, Texas: CNWRA. 2003.

Garvin, L.J. “Multi-Canister Overpack Topical Report.” HNF–SD–SNF–SARR–005. Rev. 3. Richland, Washington: Fluor Harford. 2001.

Gavenda, D.J., W.F. Michaud, T.M. Galvin, W.F. Burke, and O.K. Chopra. NUREG/CR–6428, “Effects of Thermal Aging on Fracture Toughness and Charpy-Impact Strength of Stainless Steel Pipe Welds.” Washington, DC: NRC. pp. 333–349. 1996.

Glass, R.E., J.R. Friley, H. Obata, T. Nakae, M. Itoh, and P. Rasmusson. “Structural Code Benchmarking: Impact Response Resulting From the Regulatory Nine-Meter Drop.” SAN–84–2042C. Livermore, California: Sandia National Laboratory. 1984.

Goldmann, L.H. “Performance Specification for the Spent Nuclear Fuel Multi-Canister Overpack.” HNF–S–0426. Rev. 6. Richland, Washington: Fluor Hanford. 2000a.

———. “Multi-Canister Overpack Design Report.” HNF–SD–SNF–DR–003, Rev. 3. Richland, Washington: Fluor Hanford. 2000b.

Hill, T.J., T.E. Rahl, D.K. Morton, K.C. Coughlan, J.T. Beck, and M.W. Patterson. “Canister Design for Direct Disposal of HLW Calcine Produced at the Idaho National Engineering and Environmental Laboratory.” Waste Management 2004 Conference, Tucson, Arizona, February 29, 2004. Tucson, Arizona: Waste Management Symposium, Inc. 2004.

Hollenbeck, R.G. and K.C. Tu. “Analysis For Eccentric Multi-Canister Overpack Drops at the Canister Storage Building.” Contract 80460210 1800. Richland, Washington: Fluor Daniel Northwest, Inc. 1999.

Holmes, P.A. “A High Integrity Can Design for Degraded Nuclear Fuel.” ASME Pressure Vessels and Piping Conference, Boston, Massachusetts. PVP Vol. 390. New York City, New York: ASME. 1999.

International Atomic Energy Agency. “Multi-purpose Container Technologies For Spent Fuel Management.” IAEA–TECDOC–1192. Vienna, Austria: International Atomic Energy Agency. 2000.

Kamas, S., T. Ahn, and M. Bailey. "Pre-closure Safety Analysis: Sensitivity Studies and Preliminary Dose Results." Proceedings of the 11th International High-Level Radioactive Waste Management Conference (IHLRWM), Las Vegas, Nevada, April 30–May 4, 2006. LaGrange Park, Illinois: American Nuclear Society. pp. 1,096–1,100. 2006.

Knecht, D.A. "White Paper on Multi-Purpose Canister (MPC) for DOE-Owned Spent Nuclear Fuel." Idaho Falls, Idaho: Westinghouse Idaho Nuclear Company, Inc. 1994.

Lopez, D.A. and D.G. Abbott. "Feasibility Study for a DOE Research and Production Fuel Multi-Purpose Canister." EGG–WM–11011. Idaho Falls, Idaho: Idaho National Engineering Laboratory. 1994.

Morton, D.K. and S.D. Snow. "FY1999 Drop Testing Report For The Standardized 18-inch DOE SNF Canister." EDF–NSNF–007. Rev. 2. Idaho Falls, Idaho: Idaho National Engineering and Environmental Laboratory. 2000.

Morton, D.K., S.D. Snow, T.E. Rahl, R.K. Blandford, and T.J. Hill. "Can Canister Containment Be Maintained After Accidental Drop Events?" International High-Level Radioactive Waste Management Conference, Las Vegas, Nevada, April 30–May 4, 2006. LaGrange Park, Illinois: American Nuclear Society. 2006.

Morton, D.K., S.D. Snow, T.E. Rahl, T.J. Hill, and R.P. Morissette. "Recent Progress on the Standardized DOE Spent Fuel Canister." American Society of Mechanical Engineers Pressure Vessels and Piping Conference, Vancouver, British Columbia, Canada. PVP Vol. 449. New York City, New York: ASME. pp. 49–54. 2002.

Morton, D.K., S.D. Snow, T.E. Rahl, and A.G. Ware. "Containment and Analysis Capability Insights Gained from Drop Testing Representative Spent Nuclear Fuel Containers." 16th International Conference on Structural Mechanics in Reactor Technology. Washington, DC: Structural Mechanics in Reactor Technology. 2001.

Morton, D.K., S.D. Snow, T.E. Rahl, A.G. Ware, and N.L. Smith. "Highlights Associated With the Development of the Standardized DOE SNF Canister." ANS 2000 Annual Meeting, San Diego, California. Proceedings of the Embedded Topical Meeting on DOE Spent Nuclear Fuel and Fissile Material Management. LaGrange Park, Illinois: American Nuclear Society. pp. 334–338. 2000.

Morton, D.K., A.G. Ware, T.E. Rahl, S.D. Snow, and N.L. Smith. "Development of the Standardized DOE Spent Nuclear Fuel Canister Design and Preliminary Design Specification." American Society of Mechanical Engineers Pressure Vessels and Piping Conference, Boston, Massachusetts. PVP Vol. 390. New York City, New York: American Society of Mechanical Engineers. pp. 15–20. 1999.

NRC. "Spent Fuel Project Office, Interim Staff Guidance 15: Materials Evaluation." Rev. 1. Washington, DC: NRC. 2001.

———. “Spent Fuel Project Office, Interim Staff Guidance 10: Alternatives to the ASME Code.” Rev. 1. Washington, DC: NRC. 2000.

NRC and DOE. “Technical Exchange and Management Meeting on Design Changes Approved Through DOE’s Critical Decision—1 (CD-1) Process.” Las Vegas, Nevada: NRC and DOE. 2006a.

———. “Technical Exchange and Management Meeting of Preclosure Topics.” Las Vegas, Nevada: NRC and DOE. 2006b.

Olson, K.M. and J.M. Alzheimer. “Defense Waste Processing Facility Canister Impact Testing.” Contract DE–AC06–76RLO. Richland, Washington: Pacific Northwest Laboratories. 1989.

Peterson, M.E., J.M. Alzheimer, and S.C. Slate. “Impact Testing of Simulated High-Level Waste Glass Canisters.” Contract DE–AC–06–76RLO. Richland, Washington: Pacific Northwest Laboratory. 1985.

Rains, D.J. “Analysis for Spent Nuclear Fuel Multi-Canister Overpack Drop Into the Cask From the Multi-Canister Overpack-Handling Machine With Air Cushion.” DOE Contract DE–AC06–96RL13200. Richland, Washington: Fluor Daniel Northwest, Inc. 1999.

Schuster, G.J., S.R. Doctor, A.F. Pardini, and S.L. Crawford. NUREG/CR–6471, “Characterization of Flaws in U.S. Reactor Pressure Vessels. Validation of Flaw Density and Distribution in the Weld Metal of the PVRUF Vessel.” Vol. 2. Washington, DC: NRC. August 2000.

Smith, D. “Weld Flaw Evaluation and NDE Process Comparison Results for HLW Packaging Manufacturing Program.” TDR–EBS–ND–000007. Rev. 1. Las Vegas, Nevada: Bechtel SAIC Company, LLC. 2003.

Snow, S.D. “Analytical Evaluation of the Multi-canister Overpack for Puncture Drop Events.” EDF–NSNF–039. Rev. 0. New York City, New York: ASME. 2004.

———. “Analytical Evaluation of the MCO for Repository—Defined and Other Related Drop Events.” EDF–NSNF–029. Rev. 0. New York City, New York: AMSE. 2003.

Snow, S.D. and D.K. Morton. “Analytical Evaluation of the Idaho Spent Fuel Project Canister for Accidental Drop Events.” EDF–NSFNF–027. Rev. 0. New York City, New York: ASME. 2003.

Snow, S.D., D.K. Morton, T.E. Rahl, R.K. Blandford, and T.J. Hill. “Drop Testing of DOE Spent Nuclear Fuel Canisters.” Proceedings of the ASME Pressure Vessels and Piping Conference, Denver, Colorado. PVP2005–71134. New York City, New York: ASME. 2005.

Snow, S.D., D.K. Morton. T.E. Rahl, R.K. Blandford, and T.J. Hill. “Preliminary Elevated Strain Rate Material Testing To Support Accidental Drop Analysis of Radioactive Material Containers.”

Transportation, Storage, and Disposal of Radioactive Materials, San Diego, California. PVP Vol. 483. New York City, New York: ASME. pp. 197–201. 2004.

Snow, S.D., D.K. Morton, T.E. Rahl, and A.G. Ware. "Preliminary Drop Testing Results To Validate An Analysis Methodology for Accidental Drop Events of Containers for Radioactive Materials." Proceedings of Transportation, Storage, and Disposal of Radioactive Materials, Atlanta, Georgia. PVP Vol. 425. New York City, New York: ASME. pp. 63–68. 2001.

Snow, S.D., D.K. Morton, T.E. Rahl, A.G. Ware, and N.L. Smith. "Analytical Evaluation of Drop Tests Performed on Nine 18-inch Diameter Standardized DOE Spent Nuclear Fuel Canisters." ASME. PVP–2000. INEEL/CON–99–01072. Idaho Falls, Idaho: Idaho National Laboratory. 2000.

Snow, S.D., D.K. Morton, A.G. Ware, T.E. Rahl, and N.L. Smith. "Analytical Evaluation of Preliminary Drop Tests Performed To Develop a Robust Design for the Standardized DOE Spent Nuclear Fuel Canister." Proceedings of the American Society of Mechanical Engineers Transportation, Storage, and Disposal of Radioactive Materials, American Society of Mechanical Engineers, Boston, Massachusetts. PVP Vol. 390. New York City, New York: ASME. pp. 69–80. 1999.

Spears, R.E. "Elastic/Plastic Drop Analysis Using Finite Element Techniques." 1999 American Society of Mechanical Engineers Pressure Vessels and Piping Conference, Boston, Massachusetts. PVP Vol. 390. New York City, New York: ASME. pp. 57–67. 1999.

Sprung, J.L., D.J. Ammerman, N.L. Breivik, R.J. Dukart, F.L. Kanipe, J.A. Koski, G.S. Mills, K.S. Neuhauser, H.D. Radloff, R.F. Weiner, and H.R. Yoshimura. NUREG/CR–6672, "Reexamination of Spent Fuel Shipment Risk Estimates, Sandia National Laboratory." Vol. 1. Washington, DC: NRC. 2000.

Völzke, H., G. Wieser, U. Zencker, L. Qiao, and V. Ballheimer. "German Competent Authority Guidance in FE Methods Applications to Package Design Assessment." 14th International Symposium on the Packaging and Transportation of Radioactive Materials (PATRAM 2004). Berlin, Germany: Bundesanstalt für Material Forschung Und-prüfung. 2004.

Whittington, K.F., J.M. Alzheimer, and C.E. Lutz. "West Valley Demonstration Project Full-Scale Canister Impact Tests." PNL–SA–25033. Richland, Washington: Pacific Northwest Laboratory. 1995.